Universidade de Lisboa

Faculdade de Farmácia

HPLC-MS analysis of Atorvastatin and its metabolites in plasma and prostate cancer tissue

Mariana de Araújo Solano

Mestrado Integrado em Ciências Farmacêuticas

2017

Universidade de Lisboa

Faculdade de Farmácia

HPLC-MS analysis of Atorvastatin and its metabolites in plasma and prostate cancer tissue

Mariana de Araújo Solano

Monografia de Mestrado Integrado em Ciências Farmacêuticas apresentada à Universidade de Lisboa através da Faculdade de Farmácia

Orientador: Professor Seppo Auriola

Co-Orientador: Professora Doutora Maria do Rosário Bronze

2017

Itä-Suomen yliopisto

Kuopio

HPLC-MS analysis of Atorvastatin and its metabolites in plasma and prostate cancer tissue

Erasmus

Advisor: Professor Seppo Auriola

Kuopio, 27th of April of 2017

Resumo

O objetivo do trabalho proposto foi desenvolver e validar um método simples e sensível para a análise e deteção da atorvastatina (ATV) e respetivos metabolitos presentes no plasma humano e no tecido (próstata), utilizando a cromatografia líquida de alta eficiência acoplada à espectrometria de massa (HPLC-MS/MS).

57 amostras de plasma e tecido provenientes de pacientes com cancro de próstata foram analisadas, todos eles a realizar tratamento com atorvastatina. A deteção de espectrometria de massa foi realizada através de ionização por electrospray (modo positivo), com monitoramento de múltiplas reações. Neste ensaio obteve-se um intervalo linear de concentrações entre 0,25-250 ng/mL e as curvas de calibração para os analitos foram igualmente lineares e aceitáveis ($R2 \geq 0.8997$). A exactidão (86.2-111.8 %), o efeito da matriz (80.6-94.71 %), a taxa de recuperação (74.7-81.8 %) foram outros parâmetros avaliados, baseados em guidelines da Agência Europeia do Medicamento (EMA).

O método validado tem vindo a ser aplicado com sucesso, com o intuito de analisar amostras de plasma humano para aplicação em estudos de farmacocinética, biodisponibilidade ou bioequivalência.

Apesar da atorvastatina ter sido detetada na próstata, ainda são necessários estudos adicionais para concluir acerca do mecanismo pelo qual o fármaco consegue atravessar o tecido e qual o seu impacto e possível benefício em doentes com cancro da próstata.

PALAVRAS-CHAVE: ATV; cancro da próstata; LC-MS/MS; farmacocinética

Abstract

The aim of the proposed work was to develop and validate a simple and sensitive method for the analysis of atorvastatin (ATV) and its metabolites in human plasma and in the tissue (prostate) using liquid chromatography-tandem mass spectrometry. 57 samples of plasma and tissue from prostate cancer patients, treated with atorvastatin, were analyzed. Mass spectrometry detection was carried out in positive electrospray ionization mode, with multiple reaction monitoring scan. The assay exhibited a linear dynamic range from 0,25-250 ng/mL and the calibration curves for the analytes were linear ($R^2 \geq 0.8997$). The accuracy (86.2-111.8%), matrix effect (80.6-94.71%), overall recovery (74.7-81.8%) were another parameters evaluated based on guidelines of the European Medicines Agency (EMA) and Food and drug Administration (FDA).

The validated method was successfully applied to analyze human plasma samples for application in pharmacokinetic, bioavailability or bioequivalence studies.

Despite ATV was detected in prostate, further studies are still required to conclude the mechanism how the drug can go into the tissue and the way it can lead to benefits in prostate cancer.

KEYWORDS: ATV; LC-MS/MS; prostate cancer; pharmacokinetic

Index

Tables index

Figures index

1. Introduction

1.1. Prostate Cancer

Cancer is a generic term for a large group of diseases characterized by the growth of abnormal cells beyond their normal boundaries that can then invade adjacent parts of the body and spread to other organs. It can affect almost any part of the body and has many anatomic and molecular subtypes with specific management strategies. Cancer is indeed the second leading cause of death globally and accounted for 8.8 million death in 2015 (1). Prostate cancer (PC) remains one of the most common cancers affecting men today.

The prostate is an exocrine gland of the male reproductive system, and exists directly under the bladder, in front of the rectum. It has approximately the size of a walnut. The urethra - a tube that goes from the bladder to the end of the penis and carries urine and semen out of the body - goes through the prostate (2).

There are thousands of tiny glands in the prostate - they all produce a fluid that forms part of the semen, which also has protective functions. The liquid is produced in the prostate gland, while the sperm is kept and produced in the testicles. During ejaculation, the prostate presses this fluid into the urethra, and it's expelled with sperm as semen (2).

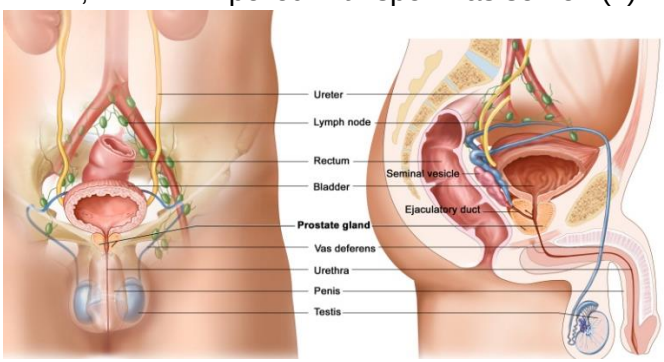

***Figure 1- Anatomy of the male reproductive and urinary systems* (2)**

PC's clinical course can be highly variable. Most of them have a slow growth rate, however, with a long latency period before manifestation of clinically significant disease (3).

More than 1.1 million cases of prostate cancer were recorded in 2012, representing around 8 % of all new cancer cases (3). More than 70% of the cases occurs in men above 65 years of age. However, the risk of clinical prostate cancer also rises abruptly after the age of 40 years (4). The worldwide PC burden is expected to grow to 499 000 new deaths and 1.7 million new cases by 2030 simply due to the growth and aging of the global population (5). According to the World Cancer Fund International, about 68 per cent of prostate cancer cases occurred in more developed countries. The highest incidence of prostate cancer is in Oceania and Northern America; and the lowest incidence in Asia and Africa.

In fact, the introduction of the serum PSA test to routine clinical practice in the mid-1980s changed totally the diagnosis of prostate cancer. This screening test can detect and confirm the presence of a large proportion of latent tumors of the prostate in men without symptoms, which has led to a notable and dramatic rise in the incidence of prostate cancer. Abnormal digital rectal examination (DRE) findings and biopsy are also used. The last one establishes the diagnosis and the first one is less sensitive: most patients diagnosed with prostate cancer have normal DRE results but abnormal PSA readings (3,6).

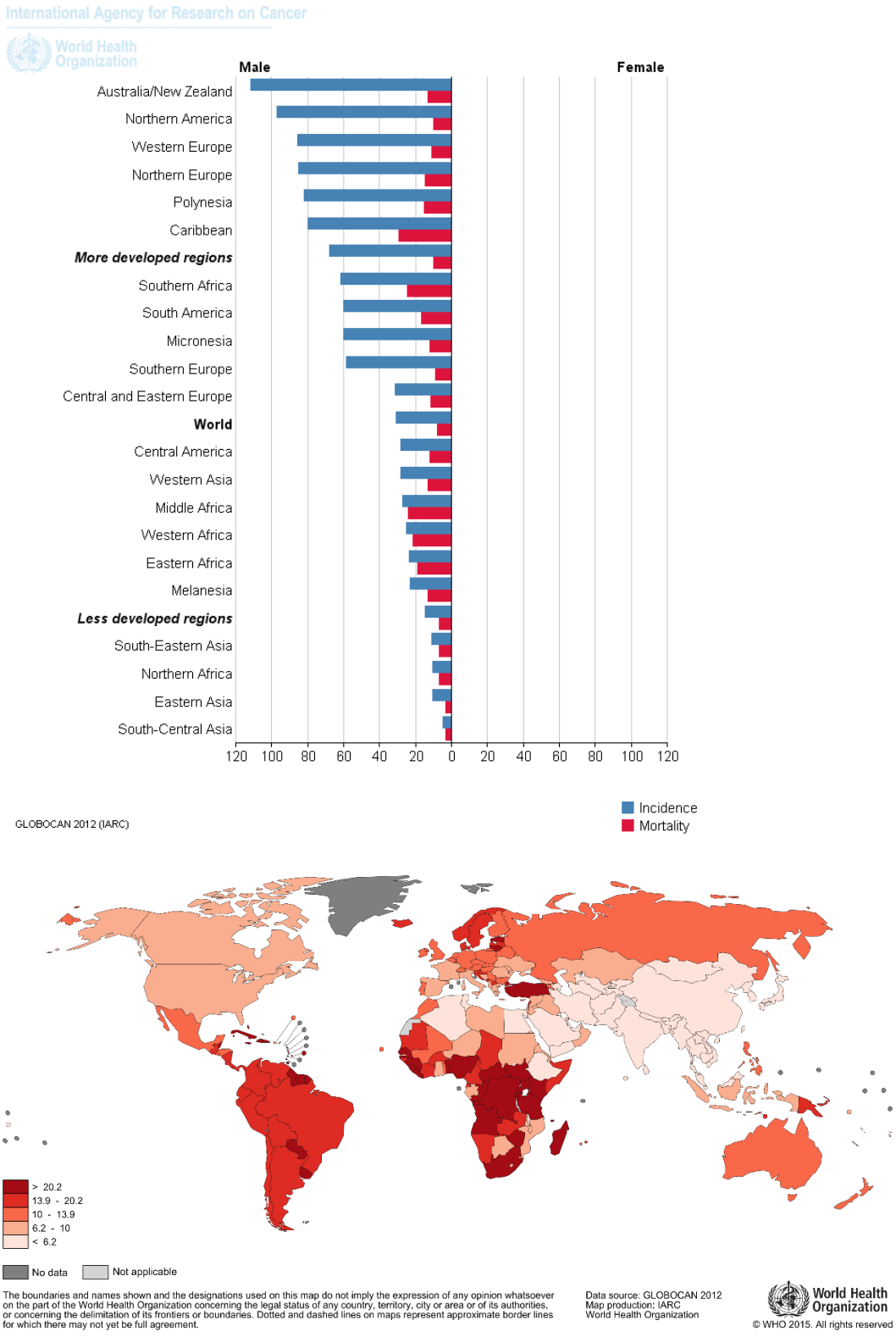

Figure 2- Incidence and mortality in the world by prostate cancer, according through World Health Organization

1.1.1. Statins and its metabolism and mechanism

Hypercholesterolemia is a risk factor for the development of atherosclerotic disease. Statins are currently the most widely used cholesterol-lowering drugs; they were originally discovered in the 1970s when Endo and Kuroda identified an inhibitor of the enzyme 3-hydroxy-3-methylglutaryl-coenzyme A (HMG-CoA) reductase, the rate-limiting enzyme of the mevalonate pathway (Figure 3), which leads to reduced cholesterol biosynthesis in the liver (7). Mevastatin. atorvastatin, lovastatin, simvastatin, pravastatin, fluvastatin, rosuvastatin and pitavastatin are the members of this class of drugs in current use, since Endo and Kuroda's discovery. Atorvastatin, fluvastatin, pitavastatin and rosuvastatin are synthetic compounds while lovastatin is naturally derived (i.e. of fungal origin, like mevastatin). Statins can also be classified as hydrophilic (atorvastatin, pravastatin, fluvastatin, rosuvastatin) or lipophilic (lovastatin, pitavastatin and simvastatin) (3) (1).

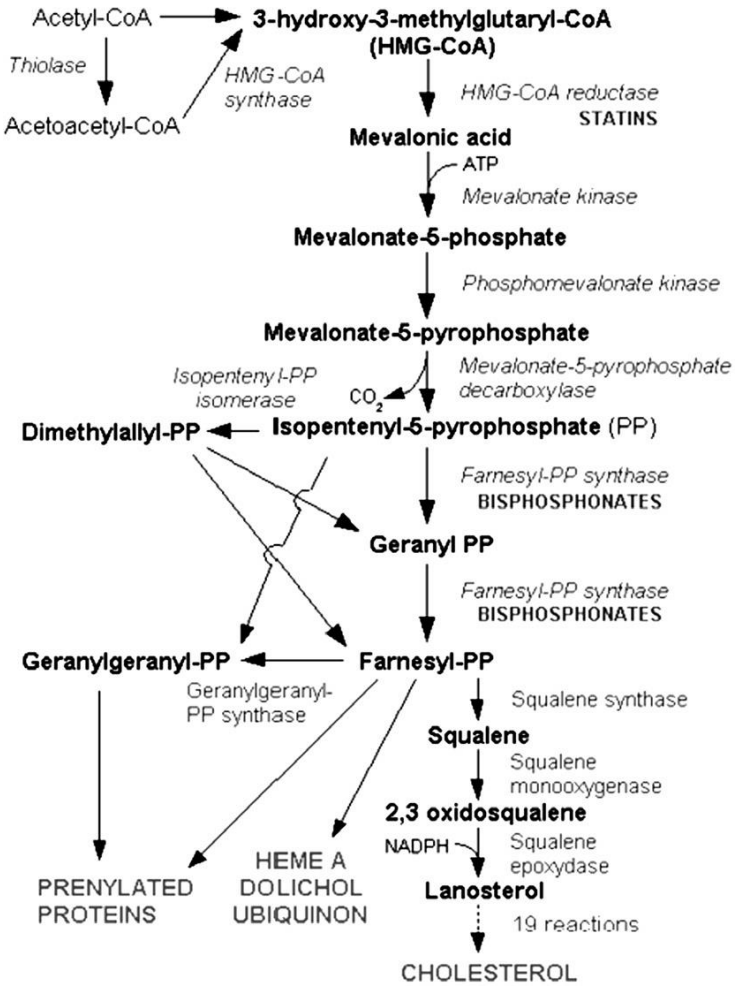

***Figure 3. Biosynthesis of cholesterol* (7)**

1.2. Atorvastatin's pharmaceutics

Atorvastatin (molecular weight 546 g/mol, pka 4.46), which belongs to the second generation of statins, is given orally as the calcium salt of the active hydroxyl acid and not as the lactone prodrug (8). The clinical dosage range for atorvastatin is 10-80 mg/day, and it is given in the acid form. Atorvastatin acid is highly soluble and permeable, and the drug is completely absorbed after oral administration. However, atorvastatin acid has an extensive first-pass metabolism in the gut wall as well as in the liver, as oral bioavailability is 14%. The volume of distribution of atorvastatin acid is 381 L, and plasma protein binding exceeds 98% (9).

Atorvastatin acid is extensively metabolized in both the gut and the liver by oxidation, lactnonisation and glucuronidation, and the metabolites are eliminated by biliary secretion and direct secretion from blood to the intestine (figure 4) (8).

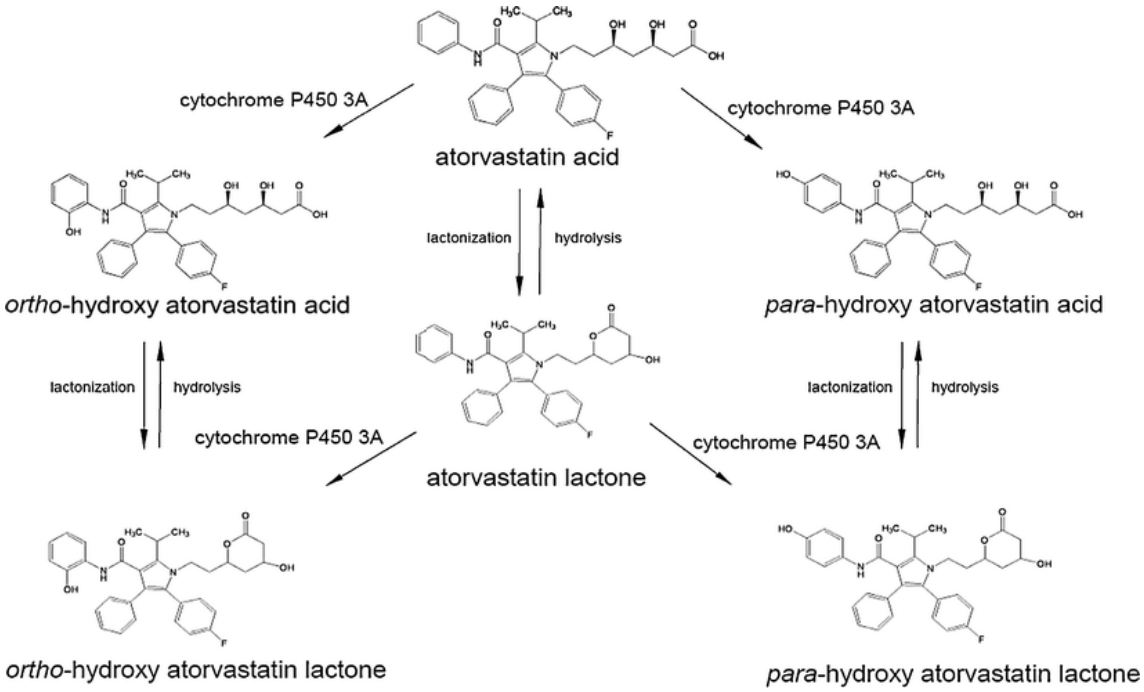

***Figure 4- Proposed metabolism pathway of atorvastatin to atorvastatin lactone, ortho-hydroxy-atorvastatin, para-hydroxy-atorvastatin, ortho-hydroxy-atorvastatin lactone, and para-hydroxy-atorvastatin lactone* (8)**

The acid form is a surface-active molecule, since it consists of a lipophilic part and a more hydrophilic part. It is believed that the surface activity of a molecule is an important physicochemical property, as it will affect its partition into biological membranes and diffusion across the membrane (10). In vivo, atorvastatin is converted to its lactone, and these two forms appear to have approximately the same area under the plasma concentration-time curve (AUC). The acid and lactone forms of drug have log D values (partition coefficient octanol/water) at pH 7.4 of 1.53 and 4.2, respectively (11). The difference in physicochemical properties between the two forms, i.e. the lactone form is more lipophilic than the acid form, has an impact on their pharmacokinetics. The solubility of the sodium salt of atorvastatin is

1.23 mg/mL at pH 6.0, which means that solubility in the intestinal lumen will not be a limiting factor in vivo (8).

1.2.1. Pharmacodynamics

Plasma levels of LDL-cholesterol are lowered by inhibition of HMG-CoA reductase, which affects endogenous cholesterol synthesis and subsequent increases the expression of the LDL receptor. This results in an upregulated catabolic rate for LDL-cholesterol (12).

In clinical studies with statins an equilibrium level is found 4-6 weeks after the initiation of the therapy. The major clinical variable, LDL-cholesterol, has a half-life of 3-4 days, which predicts that steady state should be reached between 10 and 14 days (13). The LDL-cholesterol reduction after 2 weeks of atorvastatin 10 mg once daily reached 90% if the steady-state of the major marker for pharmacological response might be due to the existence of several regulatory feed-back processes (8).In vivo, atorvastatin is metabolized by cytochrome P450 (CYP) 3A4 to two active metabolites, 2-hydroxy-atorvastatin acid and 4-hydroxy-atorvastatin acid, both of which are in equilibrium with their inactive lactone forms. It has also been reported that about 70% of the circulating inhibitory activity for HMG-CoA reductase is attributable to these active metabolites (figure 4) (14) (8).

1.2.2. Pharmacokinetics

1.2.2.1. Absorption and Bioavailability

In general, oral bioavailability of a drug is affected by factors such dissolution rate, stability issues in the lumen, transit time, intestinal permeability, and the first-pass effect (8).

The net transport (permeability) of a drug across the intestinal barrier (as well as other biological membranes) is complex and may involve multiple transport mechanisms. In general, permeability in the absorptive direction may occur by passive diffusion such as the oligopeptide transporter (MCT), organic anion-transporting polypeptide family (OATPs), organic cation transport protein(s) (OCTs) and amino acid transporters (15).

After passage across the apical enterocyte membrane, drugs may be metabolized by several enzymes. The most abundant CYP isoenzyme in the intestine is CYP3A4 (15).

The intestinal permeability of atorvastatin acid is high at the physiologically relevant intestinal luminal pH of 6.0-6.5, and predicts complete absorption (8). In the same in vitro experiment it was shown that atorvastatin was transported by P-glycoprotein. However, P-glycoprotein transport appeared to make only a minor contribution to the extent of intestinal absorption of atorvastatin. It is possible that the nonlinear increase of plasma AUC seen after increasing the oral dose from 10 mg to 80 mg might be due to saturation of P-glycoprotein-mediated efflux (16).

The absolute bioavailability (F) of atorvastatin acid, based on specific plasma measurements by GC-MS, was 14 % after 10 mg oral dose.(8).

It is apparent that the hepatic first-pass effect of atorvastatin is too small to fully explain the low bioavailability of 14%. It may be a consequence of incomplete intestinal absorption and/or extensive gut wall extraction. Based on the nonpolar nature of atorvastatin, its high solubility and high in vitro permeability, and that P-glycoprotein-mediated efflux is considered to be of minor importance, absorption is expected to be complete (17).

In clinical studies, the ratio of the plasma AUC for atorvastatin, several metabolites were found in plasma and bile. ATV acid probably undergoes complete metabolism, and the major

organ for elimination seems to be the liver, even if gut wall metabolism makes a significant contribution to the first-pass effect (18).

The plasma elimination half-life of atorvastatin acid was about 7 hours by use of a specific plasma with LC-MS/MS, whereas the plasma half-life of active HMG-CoA reductase inhibitors was 13-16 hours (19). The half-life in plasma of total radioactivity has been reported to be approximately 60 hours, indicating the presence of long-lived inactive metabolites. The total clearance of atorvastatin acid is about 625 mL/min, determined following an intravenous dose of 5 mg given as an infusion over 2 hours. This classifies atorvastatin acid as a drug with an intermediate liver extraction (20).

1.2.3. Food-drug interactions

A medium-fat breakfast decreased the rate of intestinal absorption of atorvastatin equivalents significantly, but had little impact on the amount that reached the systemic circulation (8). The C_{max} and plasma AUC values for ATV with food were 48 % and 13 % lower, respectively, than without food. The t_{max} and elimination half-life values were 5.9 and 32 hours, respectively, with food and 2.6 and 35.7 hours, respectively without food (21).

1.3. Possible mechanisms of statins in Prostate Cancer

Atorvastatin also has other effects that are independent of their cholesterol-lowering ability. In particular statins seem to impair the growth and reduce the risk of many malignancies, including colorectal, breast and skin cancers (3)(22).

Statins have also been reported to inhibit the growth of prostate cancer cells. Additionally, epidemiological studies reported a reduced risk of advanced prostate cancer in patients who were taking statins, so these drugs seem to have promise in the prevention of prostate cancer (3). The following mechanisms for this effect have been proposed, on the basis of experimental studies.

1.3.1. Cell cycle and apoptosis

Reduced activation of the small GTPases Ras and Rho is one proposed mechanism for growth inhibition (23). Besides cholesterol, the mevalonate pathway results in synthesis of the isoprenoid compounds farnesyl pyrophosphate and geranylgeranyl pyrophosphate, levels of which are also reduced by statin treatment (3).These isoprenoids, in turn, activate Ras and Rho GTPases, which are involved in regulation of the cell cycle and apoptosis.

Intracellular depletion of cholesterol is in fact a mechanism that is activated in statin-induced apoptosis, once cholesterol is abundant in intracellular lipid rafts (i.e. cholesterol-rich areas of the cell membrane) and lipid rafts regulate the phosphatidylinositol 3 kinase–protein kinase B (PI3K–Akt) signaling pathway, which has been implicated in tumor progression in many cancers (24).

1.3.2. Anti-inflammatory effects

Statins induce anti-inflammatory effects in numerous tissues. In fact, the effects of statins are probably also synergistically increased by cyclo-oxygenase (COX) 2 inhibitors. Many studies indicate that COX-2 is overexpressed in human prostate adenocarcinoma with consistently high levels observed in lymph node metastasis, suggesting that in the prostate,

COX-2 may act early in tumor promotion and progression and potentially a target for drug therapy in the management of the disease (22). Earlier studies indicate that atorvastatin and celecoxib in combination synergistically inhibited the growth and induced apoptosis in cultured prostate cancer cells more effectively than either agent alone. Clinically, however, cardiac toxicity is a concern for celecoxib with long-term use increasing the risk of cardiovascular events (25) (26).

The mechanisms by which atorvastatin and aspirin in combination strongly inhibited the growth and induced apoptosis in prostate cancer cells are still not clear (3,26).

1.3.3. Steroid sex hormones

Both androgens and estrogens—have important roles in prostate cancer development. Statins could change the balance of steroid hormones by two methods: by reducing levels of cholesterol, which is a required intermediate in steroid synthesis; or by affecting cytochrome P450, an enzyme complex involved in steroid-hormone metabolism (27).

In fact, androgen deprivation therapy (ADT) facilitates the response of prostate cancer (PC) to radiation. Androgens have been shown to induce elevated basal levels of reactive oxygen species (ROS) in PC, leading to adaptation to radiation-induced cytotoxic oxidative stress (27) (28).Thus, upon radiation these cells become less sensitive to toxic levels of ROS compared with androgen-deprived cells and so are less susceptible to treatment by radiation (28).

1.3.4. ATV in Chemotherapy with docetaxel

Docetaxel is one of the promising chemotherapeutic treatments for carcinomas. His main chemotherapeutic targets are microtubules, which cause cell-cycle arrest and apoptosis by increasing tubulin polymerization, promoting microtubule assembly, and inhibiting tubulin depolymerization (29). It has been assumed that docetaxel is able to inactivate their anti-apoptotic capacity. Earlier studies tested the anti-proliferative effects of docetaxel on PC and discovered that pre-treatment with cholesterol decreased the sensitivity of docetaxel. Treatments with agents that specifically target the biochemical synthesis of cholesterol may increase the sensitivity of docetaxel, with more potent effects on growth inhibition. Atorvastatin, has been considered to be among the safest drugs (29) (30).

1.3.5. Autophagy-associated cell death

In addition to its cholesterol-lowering effect, atorvastatin has pro-apoptotic and anti-metastatic effects on prostate cancer cells (31). Parikh *et al* hypothesized that atorvastatin may induce autophagy-associated cell death in PC cells (32). However, the biological mechanisms underlying the anti-cancer effects of atorvastatin remain to be elucidated. Autophagy is a homeostatic, catabolic process responsible for the packaging and degradation of cytoplasmic proteins and organelles. Autophagy is therefore required in order to maintain genomic stability and overall cell survival (33).

1.4. The method

Multiple studies have been reporting a development and validation of a sensitive, simple and rapid method for simultaneous quantification of ATV and its metabolites by liquid chromatography-tandem mass spectrometry (LC-MS/MS) in human whole blood (34) (35) (36).

1.4.1. Origins of Liquid Chromatography

Today, liquid chromatography, in its various forms, has become one of the most powerful tools in analytical chemistry (37).

High Performance Liquid Chromatography (HPLC) is a technique in analytical chemistry used to separate, identify, and quantify each component in a mixture. There are some advantages of HPLC´s method: analysis has no volatility issues (however the analyte must be soluble in the mobile phase); the samples used are over a wide polarity range and it´s able to analyze ionic samples (38).

The samples are prepared in a solvent system that has the same or less organic solvent than the mobile phase and volumes of 1 to 50 µL are common (39).

HPLC is usually carried out at (or around) room temperature and most HPLC detectors apart from the Mass Spectrometer are non-destructive (38) (the analyte may be recovered) and typical sensitivity is in the order of nanograms and also has the capability of producing spectra associated with sample components (37).

1.4.2. Chromatographic Separation Mechanisms

HPLC separations involve both the mobile phase (a liquid) and the stationary phase (usually materials of varying hydrophobicity chemically bonded to a solid support) (38).

The amount of water in an HPLC mobile phase will determine how strongly a hydrophobic analyte is repelled into the stationary phase, and how well it is retained. The chemical nature of the stationary phase will also govern how strongly the analyte is retained. For this reason, HPLC is a technique that is driven by the 'selectivity' achieved using two interacting phases (37,39).

1.4.3. The Liquid Chromatograph

In HPLC, several instrument and column chemistry parameters need to be optimized in order to generate a satisfactory separation (40).

Each of the following parameters need to be optimized in order to generate a chromatogram that is suitable for qualitative or quantitative purposes (scheme 1, in anexs) (37):

- Mobile phase composition
- Bonded phase chemistry
- Column and packing dimensions
- Injection volume
- Sample pre-treatment and concentration
- Mobile phase flow rate
- Column temperature
- Detector parameters

1.4.4. The Liquid Chromatographic Process

The mobile phase is continuously pumped at a fixed flow rate through the system and mixed (if required) by the pump. The injector is used to introduce a plug of sample into the mobile phase without having to stop the mobile phase flow, and without introducing air into the system (37).

The detector is then used to respond to a physicochemical property of the analyte (perhaps a UV chromophore consisting of a set of conjugated double bonds or an aromatic group). This response is digitally amplified and sent to a data system where it is recorded as the 'chromatogram' (see figure 1, in appendix) (37).

1.4.5. High Performance Liquid Chromatogram

Components (such as the injection solvent) that are not retained within the column elute at the 'dead time' or 'hold up time' t0 (37). Those compounds (analytes and sample components) that are retained elute as approximately 'Gaussian' shaped peaks later in the chromatogram. Retention times provide the qualitative aspect of the chromatogram and the retention time of a compound should be the same under identical chromatographic conditions (37). The chromatographic peak height or peak area is related to the quantity of analyte. For determination of the actual amount of the compound, the area or height is compared against standards of known concentration (38,40).

1.4.6. Modes of Chromatography

The 'mode' of chromatography is usually defined by a combination of a certain stationary phase type with a certain mobile phase type. For example, 'Normal Phase' chromatography has a non-polar mobile phase with a more polar stationary phase. Reversed phase HPLC (as the name implies) uses a system in which the mobile phase is more polar than the stationary phase (37).

The main modes of chromatography and their uses are described in Table 1- see annex.

1.4.7. Gradient Elution

After sample introduction, the ratio of these solvents is programmed to vary either continuously or in steps, resulting in enhanced separation efficiency (40).

The solvents that make up the mobile phase can be mixed in several ways, including (38):

Isocratic - the composition of the mobile phase remains constant throughout the analysis.

Binary - this is an extremely accurate and reproducible way of mixing solvents under high pressure as 2 pumps (or two pump heads on a single pump unit) are used. Binary HPLC systems generally allow mixing of only 2 solvents.

Quaternary - mixing of any combination of up to 4 mobile phase solvents is possible. This gives the user greater flexibility. Mixing is usually achieved with the use of an in-line (low pressure) gradient proportioning valve. This method of mixing is less accurate and precise than binary systems.

1.4.8. Mass Spectrometry

Allows specific compound identification, it is very sensitive and highly selective.

The mass spectrometer is an instrument designed to separate gas phase ions according to their m/z (mass to charge ratio) value (38).

Ionization is the process where electrons can be removed or added to atoms or molecules to produce ions. In LC-MS charge may also be applied to the molecule via association with other charged molecules – for example a proton (H^+). Such ions are produced in LC/MS systems by the use of strong electric fields in a vapor or condensed phase (37). The separated sample species are then sprayed into an Atmospheric Pressure Ion Source (API) where they are converted to ions in the gas phase and the majority of the eluent is pumped to waste. In API, the solvent elimination and ionization steps are combined and take place in the ion source (38).

The most common ionization methods in LC-MS include:

- Electrospray Ionization (ESI) – ionization in the condensed phase
- Atmospheric Pressure Chemical Ionization (APCI) – ionization in the gas phase
- Atmospheric Pressure Photo Ionization (APPI) – ionization in the gas phase

1.4.9. Ionization Overview

The two main modes of ionization used in API LC/MS are Electrospray Ionization (ESI) and Atmospheric Pressure Chemical Ionization (APCI) (37).

Electrospray Ionization (ESI)	**Atmospheric Pressure Chemical Ionization (APCI)**	**Atmospheric Pressure Photo Ionization (APPI)**
-uses condensed phase (liquid) charge separation and ion evaporation techniques to produce vapor phase; - Primarily analyte molecules of interest must be in the ionized form prior to spraying into the Electrospray interface (39);	- uses analyte desolvation and charge transfer reactions to produce vapor phase; - no potential is applied to the capillary but instead the liquid emerges from the capillary surrounded by a flow of inert, nebulising gas into a heated region; - The combination of nebulising gas and heat forms an aerosol that begins to rapidly evaporate (37)	- Complementary technique; -has been developed to broaden the range of analyte types; -Important for certain compounds that are not easily ionizable by ESI or APCI, for example non-polar compounds and polycyclic aromatic hydrocarbons. - the ionization process is accomplished by exposing an aerosol of sprayed droplets to photo - irradiation. A molecular radical ion is formed when

		the molecule absorbs a photon (39).

Table 1- Main modes of ionization used in API LC/MS

Both ESI and APCI are termed “soft” ionization methods. This means that in the process of producing ions there is negligible energy transferred to the ion. Therefore, the ion formed does not fragment to give lower mass ions. The resultant mass spectrum therefore consists predominantly of either [M+H]+ or [M-H]- or adduct ions such as [M+Na] + (39).

In addition to the mass analyzer, the mass spectrometer also includes an atmospheric ionization chamber, and a detector. The mass analyzer and detector systems are held within a vacuum chamber (38).

The detector is used to ‘count’ the ions emergent from the mass analyser, and may also amplify the signal generated from each ion. Widely used detector types include: electron multiplier, dynode, photodiode and multi-channel plate (39).

1.4.10. Mass analyzers

In its simplest form the process of mass analysis in LC/MS involves the separation or filtration of analyte ions or fragments of analyte ions created in the Atmospheric Pressure Ionization (API) interface or in the regions between the API interface and the high vacuum region of the mass analyzer (products of collision-induced dissociation etc.) (39).

Most popular analyzer types include Quadrupole, Time of Flight, Ion Trap and Magnetic Sector (38).

Quadrupole and Ion Trap Mass analyzers: ions are filtered using electrostatic potentials applied to the elements of the mass analyzers which are used to ‘select’ ions according to their mass to charge ratio, non-selected ions are ejected from the mass analyzer device and are not detected (37).

Time of Flight (TOF) mass analyzers: use differences in flight times of accelerated ions through an extended flight path to separate ions (38).

Magnetic Sector Mass Analyzers: use magnetic fields to conduce ions of interest towards the detector (38).

The analyte and fragment ions are plotted in terms of their mass-to-charge ratio (m/z) against the abundance of each mass to yield a mass spectrum of the analyte (37).

It should be noted that the spectra acquired with an ion trap mass analyzer has some unique capabilities, including the ability to perform multiple product ion scans with very good sensitivity (40).

1.4.11. Tandem mass spectrometry (MS/MS)

MS/MS is the combination of two or more MS experiments. The aim is either to get structural information by fragmenting the ions isolated during the first experiment, and/or to achieve better selectivity and sensitivity for quantitative analysis by selecting representative ion transitions using both the first and second analyzers (37).

MS/MS analysis can be achieved either by coupling multiple analyzers (of the same or different kind) or, with an ion trap and carrying out successive fragmentations of trapped ions (39).

2. Objectives

This study aims to implement a method for detection and identification of atorvastatin in human plasma and prostate tissue. Until now there are only studies and reports about quantification of ATV in blood by LC-MS/MS, not in the tissue. Besides that, we want to provide insight into what is currently known about the effect of atorvastatin on the development of prostate cancer and on the risk of this disease, to show the possible mechanisms of action for statins, as well as at these drugs' potential to prevent prostate cancer.

3. First Experimental

3.1. Reagents and materials

Atorvastatin	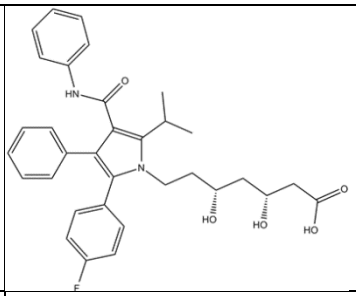
Formula	$C_{33}H_{35}FN_2O_5$
Molecular Weight	559.26 g/mol
Atorvastatin-d_5	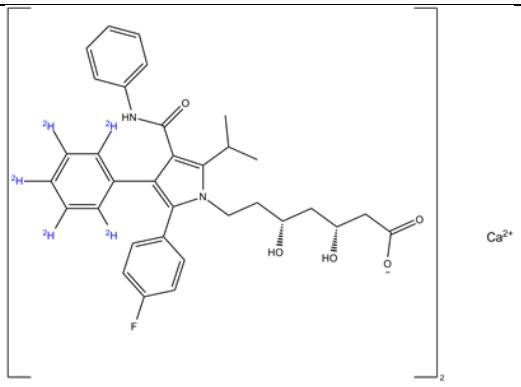
Formula	$C_{33}H_{35}D_5FN_2O_5$
Molecular Weight	564.2 g/mol
Atorvastatin-lactone	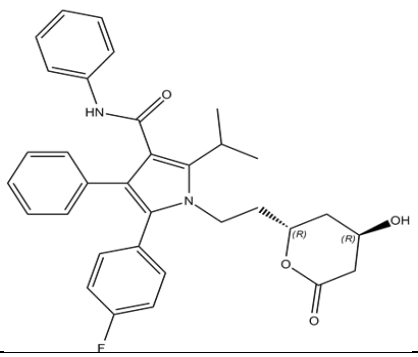

Formula	$C_{33}H_{33}FN_2O_4$
Molecular Weight	541 g/mol
2-Hydroxy Atorvastatin	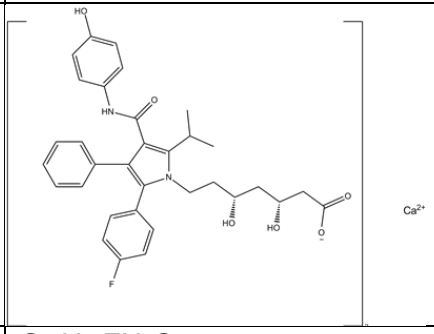
Formula	$C_{33}H_{34}FN_2O_6$
Molecular Weight	575 g/mol
Storage Conditions for all	-20 ºC and protected from light
Safety Precautions for all	Routine laboratory procedures (gloves, goggles, and face mask) are sufficient to assure personnel health and safety

Table 2: Chemical structure, formula, molecular weight, storage conditions and safety precautions for ATV and its metabolites

ATV calcium hydroxy acid and lactone metabolites (ATV-lactone) and corresponding deuterium (d_5)-labeled internal standards (IS) were purchased from *Toronto Research Chemicals* (Toronto, ON, Canada). ATV calcium salt trihydrate was purchased from *Sigma Aldrich.* The internal standard is a compound that is very similar, but not identical to the chemical species of interest. It is used for calibration by plotting the ratio of the analyte signal to the internal standard signal as a function of the analyte concentration of the standards. This is done to correct for the loss of analyte during sample preparation or sample inlet.

Acetronitrile and acetic acid (which helps to release the drug from the proteins) were purchased from *Fluka Analytical.* DMSO, from Sigma-Aldrich; Methanol from Fisher Chemical (UK) and water was purified in a MilliQ Gradient A10 purification system (Millipore, Milford, MA, USA). The tissue is from liver homogenate, in 50 mM phosph. buffer pH of 7.4.

3.2. Standards preparation

Stock drugs solutions were made by diluting each compound in DMSO, getting a concentration of 1 mg/mL. For ATV and ATV-lactone solutions, 100 μL were pipetted to a 10 mL volumetric flask, that was filled with 50% MeOH. This was the first working solution 10 μg/mL (see table 6). ATV-OH (100 μL) was only added to 1 μg/mL working solution because of the lower amount of volume of this available compound compared with the other ones. The stock internal standard solution had a concentration of 1 mg/mL in DMSO and it was diluted to final concentration of 50 ng/mL in 50% MeOH.

Dilution of IS: 100 μL of IS 1 mg/mL was added to a volumetric flask of 10 mL (final concentration- 10 μg/mL), the second one, 1 mL from the 10 μg/mL one was added to a volumetric flask of 10 mL (final concentration- 1μg/mL) and the last one, 1 mL from the second one was added to a volumetric flask of 20 mL until the final concentration of 50 ng/mL, all in MeOH.

Standard working solutions were made from stock solution drug in 50% methanol and their concentrations are 10, 5, 2.5, 1, 0.5, 0.25, 0.1, 0.05, 0.025, 0.0125 and 0.005 µg/mL.

Drug Concentration (µg/ml)	Add	Final Volume
10	100 µL of ATV and ATV-lactone of each stock solution	10 mL MeOH/H_2O (1:1, v/v)
5	5 mL of sol 10 µg /mL	10 mL MeOH/H_2O (1:1, v/v)
2.5	5 mL of sol 5 µg /mL	10 mL MeOH/H_2O (1:1, v/v)
1	100 µL ATV-OH of stock solution + 4 mL of sol 2.5 µg /mL	10 mL MeOH/H_2O (1:1, v/v)
0.5	5 mL of sol 1 µg/mL	10 mL MeOH/H_2O (1:1, v/v)
0.25	5 mL of sol 0.5 µg/mL	10 mL MeOH/H_2O (1:1, v/v)
0.1	4 mL of sol 0.25 µg/mL	10 mL MeOH/H_2O (1:1, v/v)
0,05	5 mL of sol 0.1 µg/mL	10 mL MeOH/H_2O (1:1, v/v)
0,025	5 mL of sol 0.05 µg/mL	10 mL MeOH/H_2O (1:1, v/v)
0,0125	5 mL of sol 0.025 µg/mL	10 mL MeOH/H_2O (1:1, v/v)
0,005	4 mL of sol 0.0125 µg/mL	10 mL MeOH/H_2O (1:1, v/v)

***Table 3: Working solutions of* Atorvastatin, Atorvastatin-lactone and Hydroxy-Atorvastatin**

3.3. Chromatographic equipment and conditions

The HPLC system was an Agilent 1200 Series RRLC consisting of a micro degasser, binary pump SL in low delay volume configuration (damper and mixer bypassed), high performance autosampler SL, and column thermostat SL (Agilent Technologies, Waldbronn, Germany). Zorbax SB-C18 column (2.1 x 50 mm, 2.7 µm) was used with a dedicated 0.2 µm in-line filter (Agilent Technologies). Column was maintained at 50 ºC and autosampler tray at ambient temperature. Injection volume was 2 µL. The autosampler was set to perform vial bottom sensing and sample draw from the vial bottom. Further autosampler functions in use were automatic delay volume reduction with default timing settings. Flow rate was 0.500 mL/min and gradient elution was used with 100 % water (eluent A) and 100 % methanol (eluent B). The gradient was as follows: 2.0 min: 98% A and 2% B, 2.0 to 7.0 min: 98%→0.0% A and 2%→100% B, 7.0 to 7.1 min: 0.0%→98% A and 100%→2% B, 7.1 to 9.0 min: 98% A and 2% B. Total run time from injection to injection was 9.0 min.

3.4. Mass spectrometric equipment and conditions

The mass spectrometer was an Agilent 6495 Triple Quadrupole LC/MS with electrospray ion source (Agilent Technologies, Palo Alto, CA, USA). Nitrogen was used as a drying, nebulizer, and collision gas. The following ion source conditions were employed: positive ion mode, drying gas temperature 200 ºC, drying gas flow 16 L/min, nebulizer pressure 25 psi. Instrument was tuned with the built-in autotune function using the associated tuning solution. The resulting voltage for the electron multiplier was then increased by using an instrument software function.

3.5. Measurement of full scan mass spectra and MS/MS spectra

The 1 μg/mL working solution of each analyte and internal standard was injected, without the column in the instrument to obtain the full scan MS and collision induced dissociation MS/MS mass spectra, for 10 V, 15 V, 20 V, 25 V collision energies.

Multiple reaction monitoring (MRM) was used with both quadrupoles set at unit resolution.

3.6. Calibration curve

A calibration curve and respectively concentrations, using the working solutions was elaborated. Eight calibrators were used that covered the range of 0.5-100 ng/mL for ATV and its two main metabolites. Calibration standards and QC's were made in human serum.

Drug concentration in plasma (ng/mL)	Working solution in 100 µL of human serum	IS (ATV-d5)
100	10 µL solution of 1 µg/mL	20 µL
50	10 µL solution of 0,5 µg/mL	20 µL
25	10 µL solution of 0,25 µg/mL	20 µL
10	10 µL solution of 0,1 µg/mL	20 µL
5	10 µL solution of 0,05 µg/mL	20 µL
2,5	10 µL solution of 0,025 µg/mL	20 µL
1,25	10 µL solution of 0,0125 µg/mL	20 µL
0,5	10 µL solution of 0,005 µg/mL	20 µL
0	10 µL solution of 50% MeOH	20 µL

***Table 4: Calibration curve* for Atorvastatin, Atorvastatin-lactone and Hydroxy-Atorvastatin**

It was added 400 µL of 0.1% acetic acid in acetonitrile, ice cold, to the calibration standards.

The test tubes were vortex-mixed for approximately 10 seconds and thereafter, all precipitated proteins were separated by centrifugation for 15 min at 14000xg and 4 ºC temperature. The supernatant was recovered (200 µL) and transferred into HPLC vials.

Each concentration was analyzed in duplicate, in addition to the blank and zero samples.

3.7. Validation procedure

The following steps of validation were performed based on the guidelines for bioanalytical method validation defined by the European Medicines Agency (EMA) and Food and Drug Administration (FDA).

3.7.1. Lower limit of quantification

LLOQ was defined as the lowest concentration of analyte in a sample which can be quantified reliably, with an acceptable accuracy and precision. The LLOQ is considered being the lowest

calibration standard, with an intra and inter-day coefficient of variation less than 20% and intra and inter day accuracy within 20 % of the nominal value. In addition, the analyte signal of the LLOQ sample should be at least 5 times the signal of a blank sample.

3.7.2. Carry-over

Carry-over effect was tested by injecting methanol samples after the highest concentration (100 ng/ml) and before the samples to study the matrix effect. Carry over in the blank sample following the high concentration standard should not be greater than 20% of the lower limit of quantification and 5% for the internal standard. If it appears that carry-over is unavoidable, study samples should not be randomized.

3.7.3. Accuracy and precision

The accuracy of an analytical method describes the closeness of the determined value obtained by the method to the nominal concentration of the analyte (expressed in %). The QC samples were analyzed against the calibration curve, and the obtained concentrations were compared with the nominal value.

Accuracy and precision were determined by analyzing four quality control (QC) samples in sixtuplicate for each analytical run, namely a low QC level (0.5 ng/mL) and a medium QC level (1.25 ng/mL).

Intra-day accuracy and precision were established in one single run and were reported as percent of the nominal value and did not exceed 15% for QC samples, and 20% for the LLOQ.

3.7.4. Matrix effect and overall recovery

Matrix effects were performed with just one level of QC (1.25 ng/mL) and three different solutions: one with MeOH (100 µL), drug (10 µL), IS (20 µL) and ACN (400 µL) - set A.

Set B is composed by plasma (B1) and liver tissue (B2). For each one, ACN (400 µL) was firstly added and 200 µL of the supernatant were collected. Then, the drug (10 µL of 1,25 ng/mL concentration) and 20 µL of IS were added as well as 300 µL of ACN in the end to end up with the same amount of volume than Set A.

Set	Procedure	Final Volume (µL)
A	100 µL of MeOH 50% + 10 µL of drug + 20 µL of IS+ 400 µL of CAN	530 µL
B1	100 µL of plasma + 400 µL of ACN. 200 µL of the supernatant were taken; 10 µL of drug + 20 µL of IS were added + 300 µL of CAN	530 µL
B2	100 µL of liver tissue + 400 µL of ACN. 200 µL of the supernatant were taken; 10 µL of drug + 20 µL of IS were added + 300 µL of CAN	530 µL

Table 5: Matrix effect procedure

The set C is composed by the calibration curve for the 1.25 ng/mL concentration, previously done. For this concentration level, overall recovery was obtained by comparing signals from set C to set A, the extraction yield was evaluated by comparing signals from conditions B and C, and

matrix effect was assessed by comparing signals from sets A and B. Overall recovery, extraction yield and matrix effect were calculated according to the following equations (see appendix).

$$\text{Overall recovery} = \frac{\text{peak area in set C}}{\text{peak area in set A}} \text{ x } 100$$

$$\text{Extraction yield} = \frac{\text{peak area in set C}}{\text{peak area in set B}} \text{ x } 100$$

$$\text{Matrix effect} = \frac{\text{peak area in set B}}{\text{peak area in set A}} \text{ x } 100$$

4. Results and discussion

4.1. MS and MS/MS spectra determination

At the beginning it is necessary to choose the best conditions for the detection of the compounds. Best conditions for ionization must be chosen as well as best conditions for fragmentation as in this type of work MRM is the method chosen for quantitation due to its selectivity and sensitivity.

MS products were characterized with Agilent 6495 QQQ.

The products scan of ATV, ATV-Lactone, ATV-OH and ATV-d5 were made at 10, 15, 20 and 25 V.

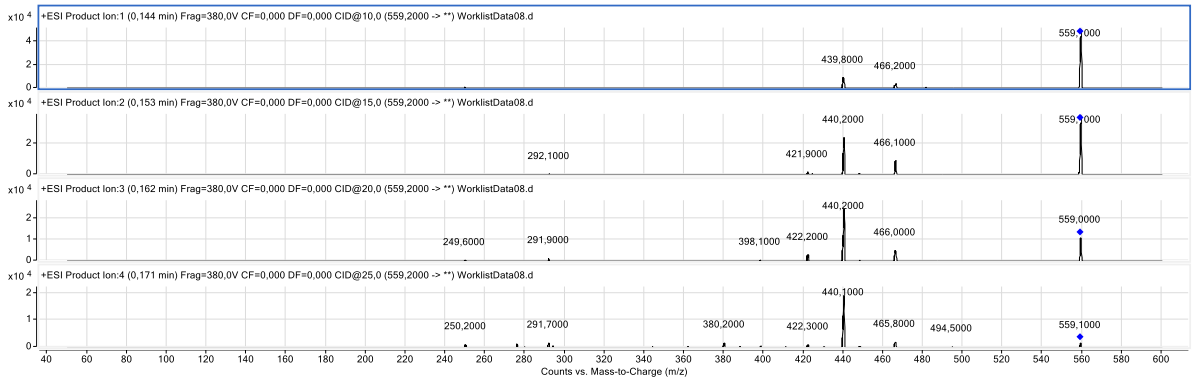

Figure 5: Product ions of Atorvastatin (m/z 559.26 →m/z 440)

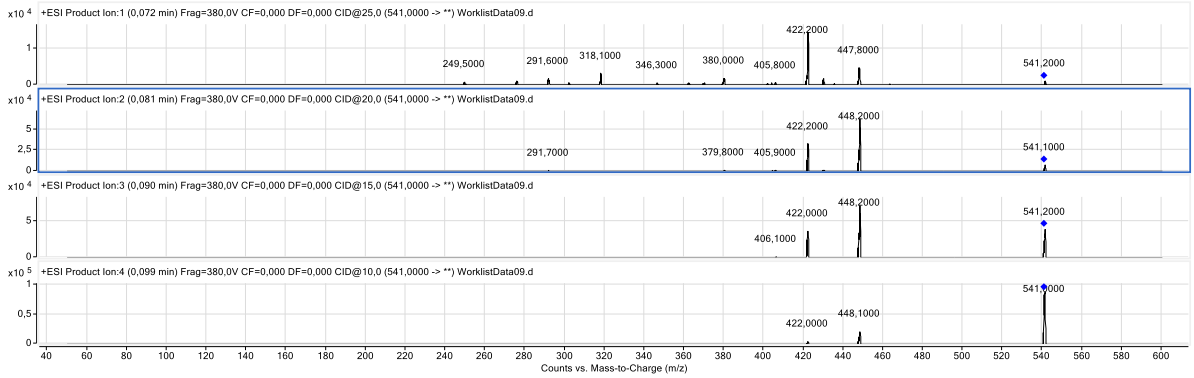

Figure 6: Product ions of Atorvastatin-Lactone (m/z 541 →m/z 448.2, m/z 541 →m/z 422.1)

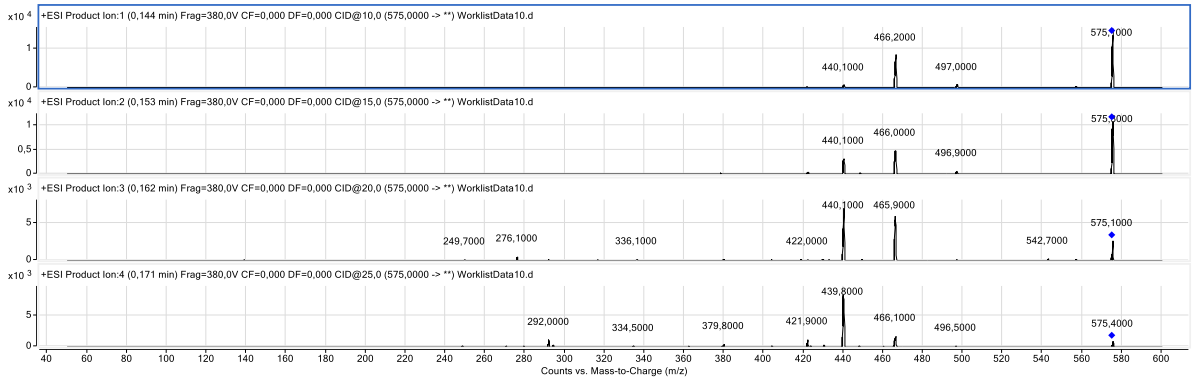

Figure 7: Product ions of Hydroxy-Atorvastatin (m/z 575 →m/z 440.1, m/z 575 →m/z 466)

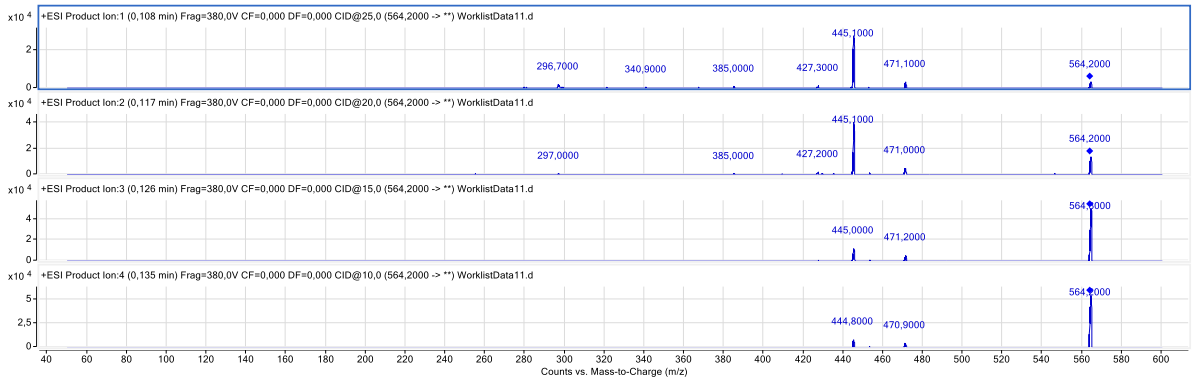

Figure 8: Product ions of Atorvastatin-d5 (m/z 564.2 →m/z 445.1)

20 V was the collision energy that produced the best results for all the compounds, once all the peaks corresponding to product ions could be seen clearly in the MS/MS mass spectra (Fig. 5, 6, 7 and 8).Therefore, the energy of 20 V was the one to be selected to this method.

4.2. Qualitative Analysis B.06.00

The following MRM's show the retention time for each analyte (atorvastatin, internal standard-ATV-d5, atorvastatin-lactone and hydroxy-atorvastatin) in blank human plasma (drug and internal standard free-figures 9,12,15), in 'zero' of calibration curve (only drug-free- figures 10,13,16) and in 0.5 ng/ml of calibration curve (figures 11,14,17), which corresponds to the LLOQ.

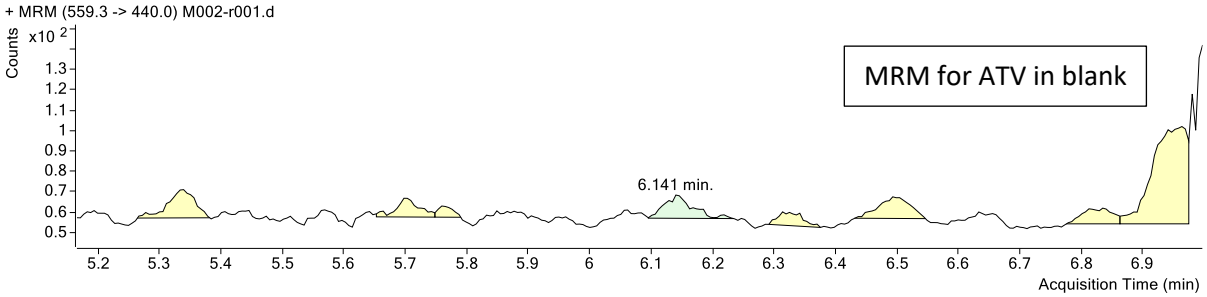

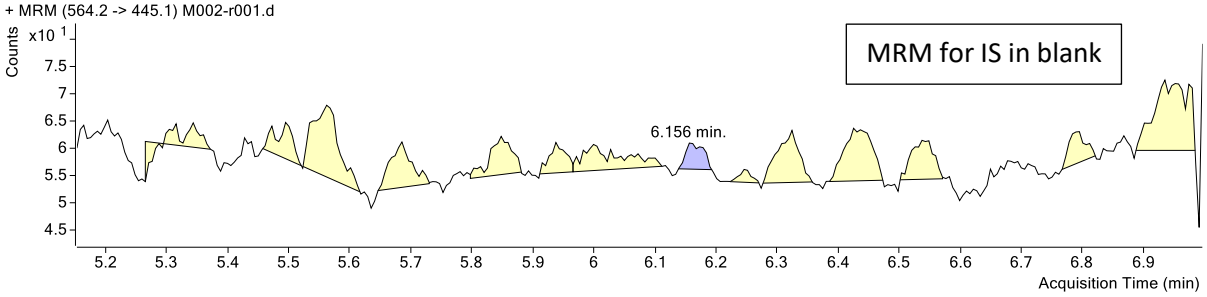

Figure 9: MRM chromatogram for Atorvastatin (upper) and Internal Standard (down) from analysis of blank human plasma (drug and IS free)

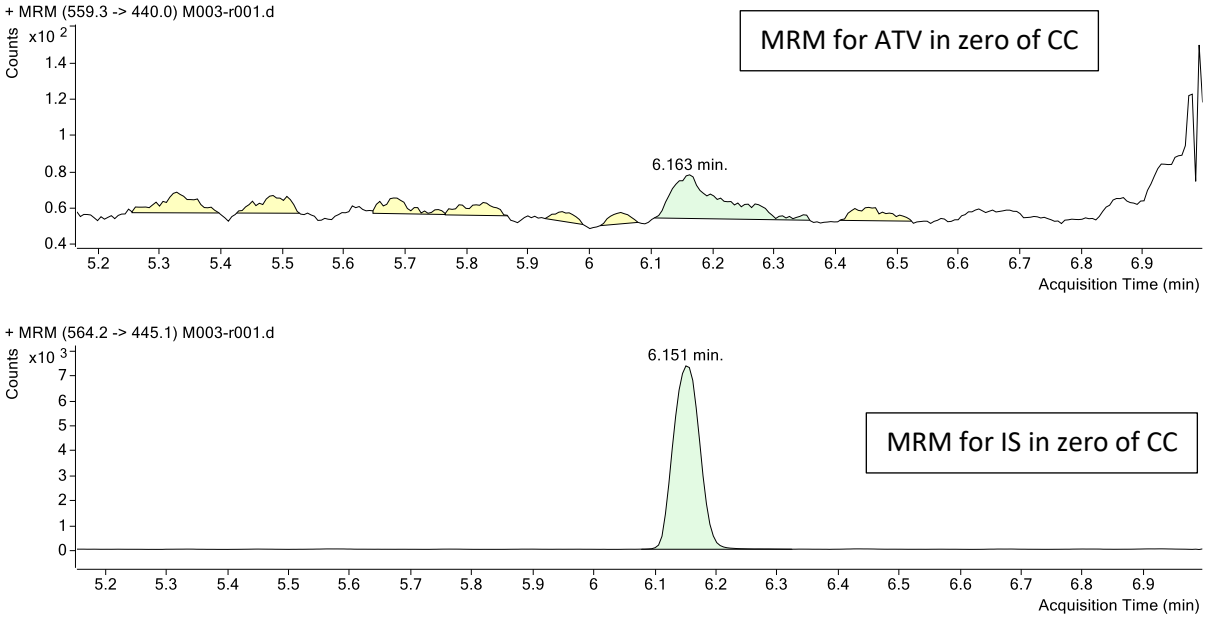

Figure 10: MRM chromatogram for Atorvastatin (upper) and Internal Standard (down) from analysis of zero (in calibration curve-drug free)

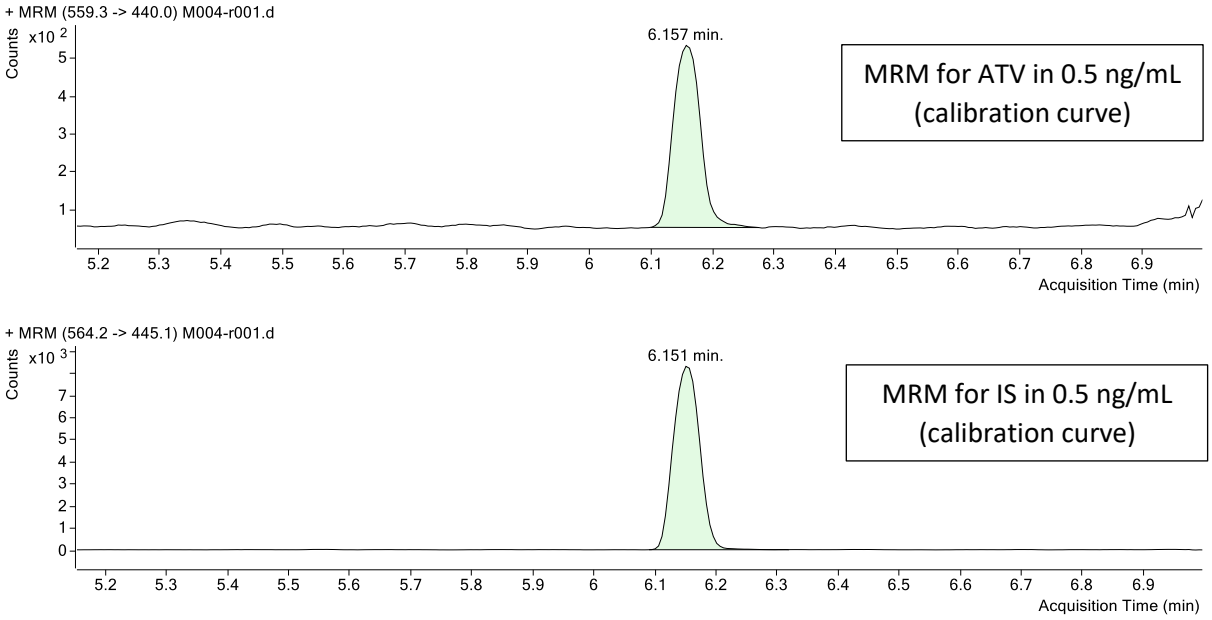

Figure 11: MRM chromatogram for Atorvastatin (upper) and Internal Standard (down) from analysis of LLOQ (0.5 ng/mL)

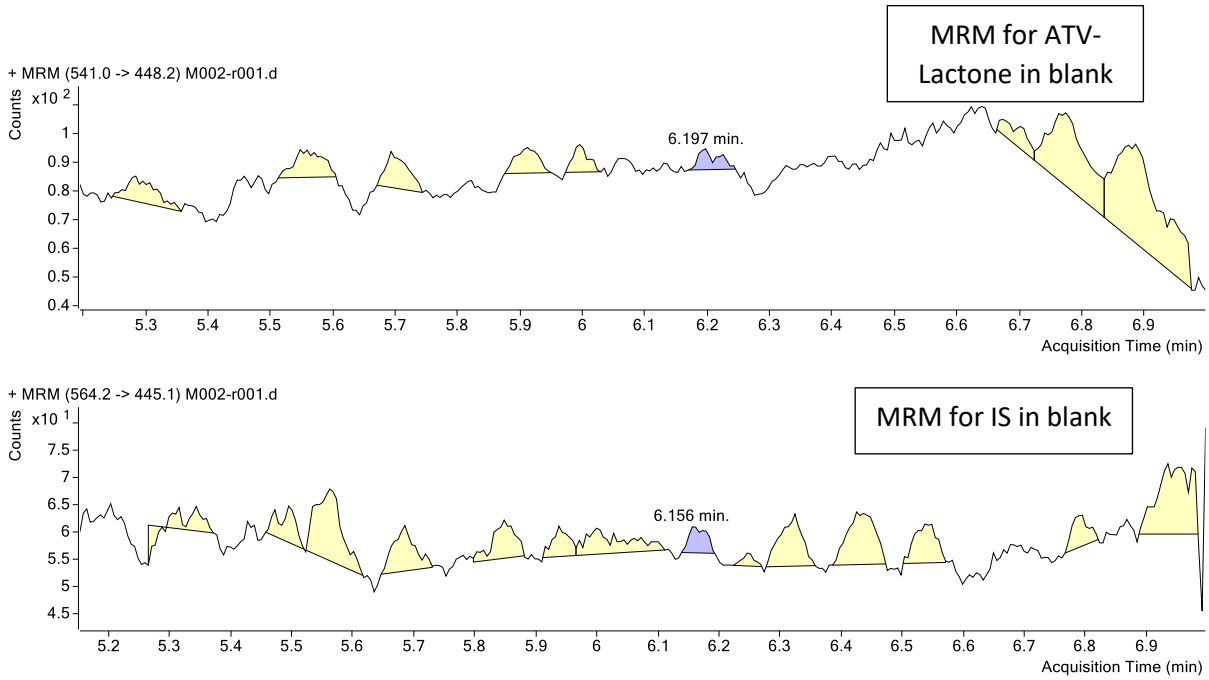

Figure 12: MRM chromatogram for Atorvastatin- Lactone (upper) and Internal Standard (down) from analysis of blank human plasma (drug and IS free)

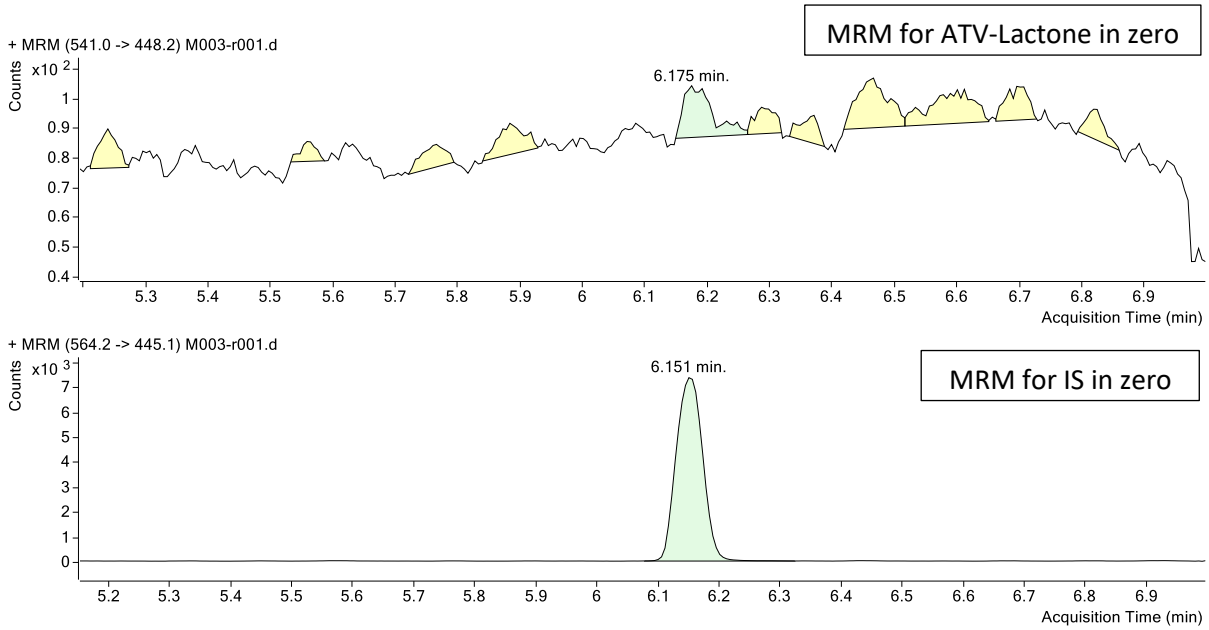

Figure 13: MRM chromatogram for Atorvastatin-Lactone (upper) and Internal Standard (down) from analysis of zero (in calibration curve-drug free)

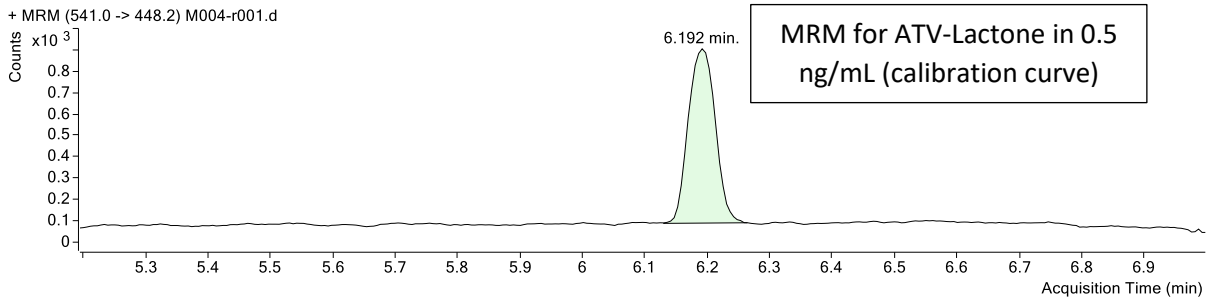

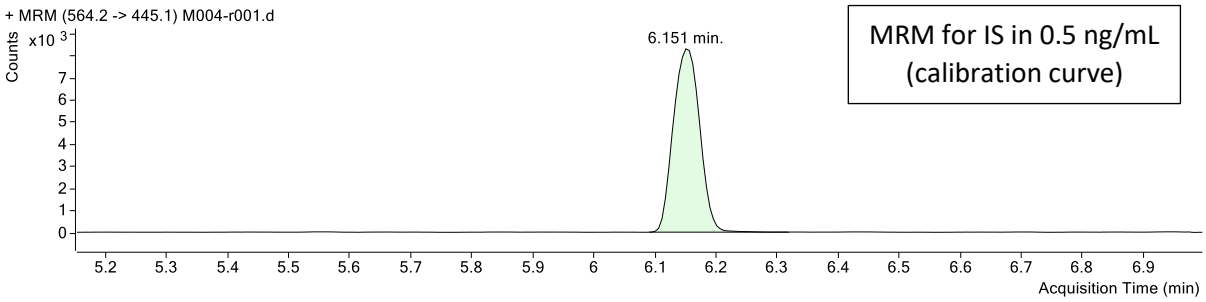

Figure 14: MRM chromatogram for Atorvastatin-Lactone (upper) and Internal Standard (down) from analysis of LLOQ (0.5 ng/mL)

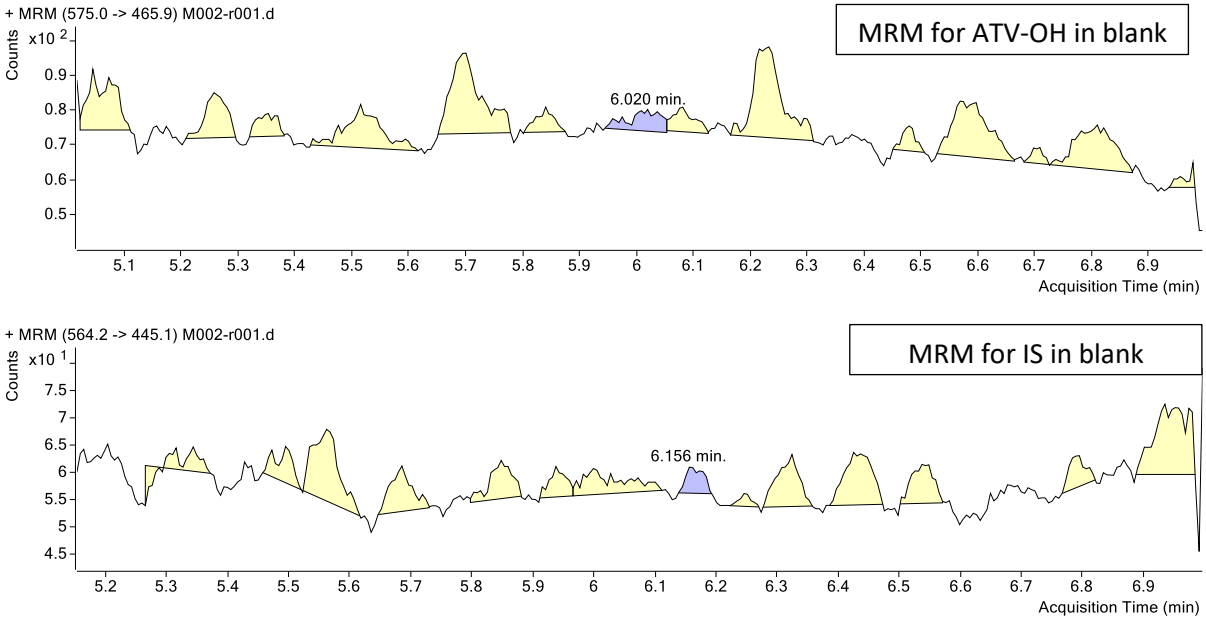

Figure 15: MRM chromatogram for Atorvastatin-OH (upper) and Internal Standard (down) from analysis of blank human plasma (drug and IS free)

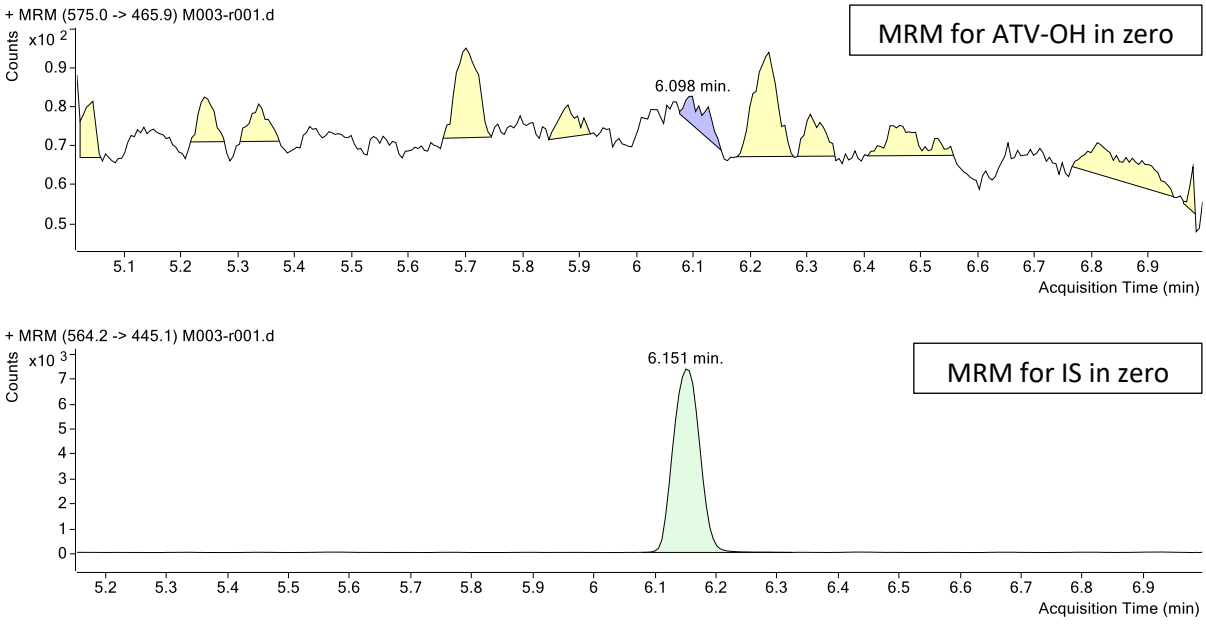

Figure 16: MRM chromatogram for Atorvastatin-OH (upper) and Internal Standard (down) from analysis of zero (in calibration curve-drug free)

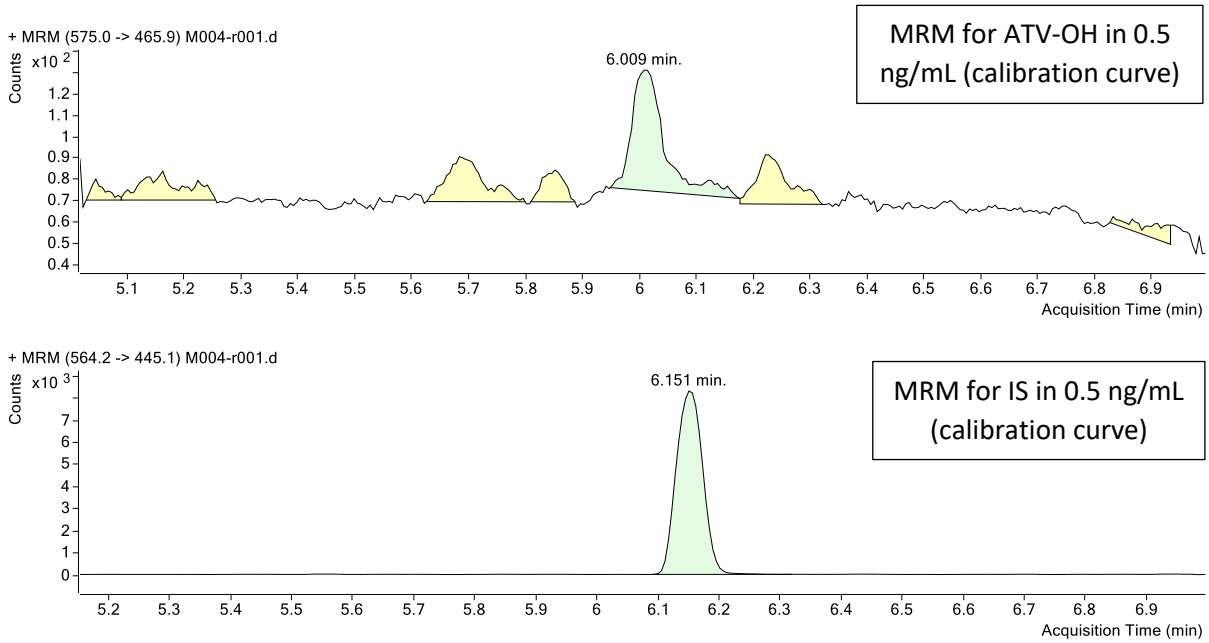

Figure 17: MRM chromatogram for Atorvastatin-OH (upper) and Internal Standard (down) from analysis of LLOQ (0.5 ng/mL)

For each compound (ATV, ATV-lactone and ATV-OH), the peaks are predictable and expected: in the blank, there is no signal for the respective retention times; in zero of calibration curve there is only signal for the internal standard once the drug is free (which peak and retention time is always the same- 6.151 minutes) and, finally, in the 0.5 ng/mL concentration both peaks (IS and the compound) are clearly visible and defined

4.3. Linearity from QQQ Quantitative Analysis

The linear regression curves were fitted to the concentration ranges of 0.5-100 ng/ml for ATV and its metabolites in human plasma. The mean equations of the calibration curves generated for each analyte were as follows:

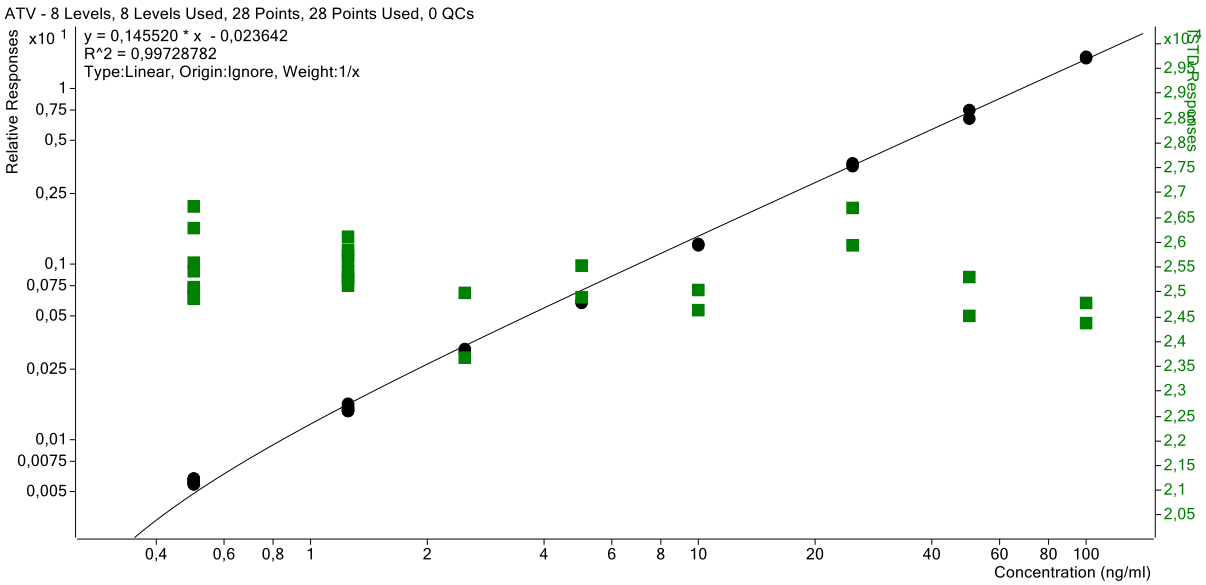

Figure 18: Calibration curve for ATV in human plasma

The calibration curve and respectively r^2 obtained were:

y= 0.145520*x – 0.023642
R^2= 0.9973

The green squares represent the Internal Standard from different runs.

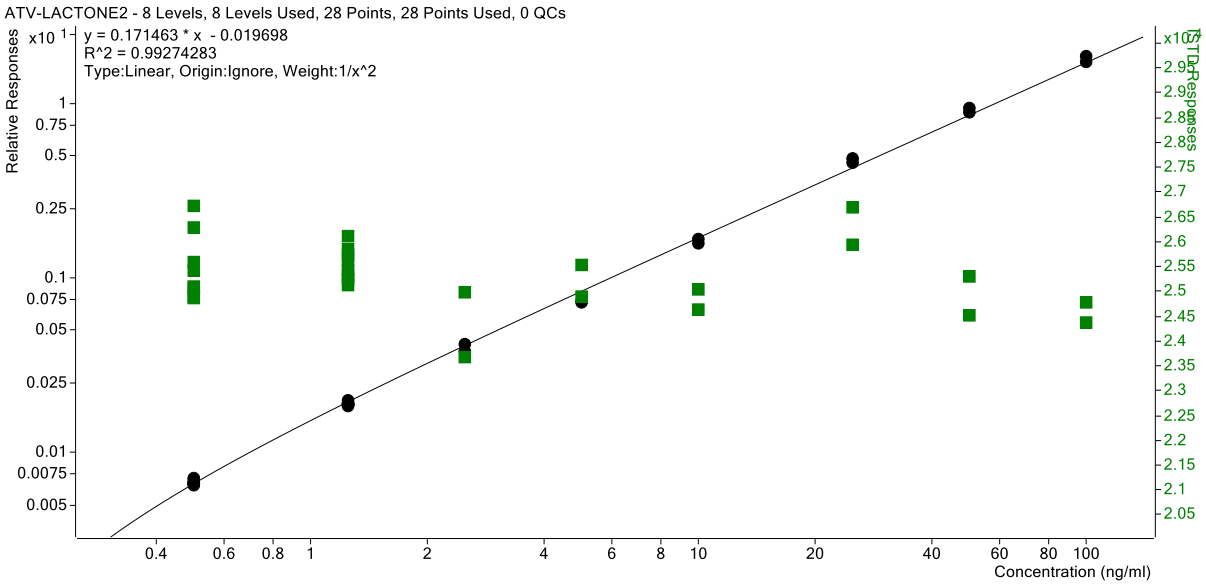

Figure 19: Calibration curve for ATV-Lactone in human plasma

The calibration curve and respectively r^2 obtained were:

y= 0.171463*x – 0.019698
R^2= 0.9927

The green squares represent the Internal Standard from different runs.

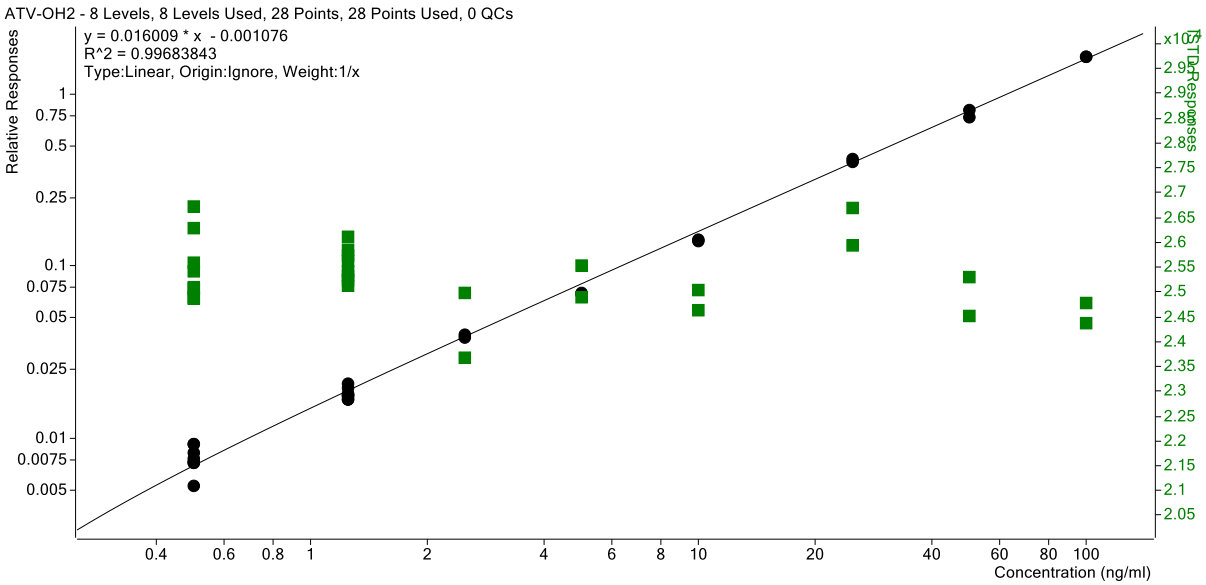

Figure 20: Calibration curve for ATV-OH in human plasma

The calibration curve and respectively r^2 obtained were:

y= 0.016009*x – 0.001076
R^2= 0.9968

The green squares are representing the internal standard which response is relatively constant for all the concentrations.

Analyte	STD (ng/mL)	STD 1 0.5	STD 2 1.25	STD 3 2.5	STD 4 5	STD 5 10	STD 6 25	STD 7 50	STD 8 100	R^2
ATV	% Accuracy % CV	111.8 2.3	94.3 1.05	94.4 1.15	86.2 0.65	89.6 1.3	101.3 1.6	98 5.4	102.6 0.25	0,9973
ATV-Lactone	% Accuracy % CV	101.1 1.56	98.4 1.8	97.4 2.85	89.6 1.65	92.9 0.3	109.5 0.5	107 3.7	106.3 0.75	0,9927
ATV- OH	% Accuracy % CV	102 7.25	90.1 0.85	98.3 4.8	89.7 1.8	99.5 0.91	110.8 0.16	104.2 5.15	112.1 1.15	0,9968

Table 6: Summary of standard and calibration curve parameters.
n=2 (two replicates for each validation run)
% Accuracy= [(determined value/true value)]*100%
%CV calculated as (SD/mean)*100
STD: Standard

The calibration curves obtained from analyte/IS peak area vs. nominal concentration were linear using weighted (1/x) linear regression over the concentration range, with correlation coefficients (R^2)≥0.9927. According to FDA guidelines, the accuracy of calibration standards and quality control samples should be between 80-120% and imprecision below 20%. For the current assay, the measured mean values were within 86.2-111.8 % of their nominal values for calibrators (Table 6) and 95-110.2% for intra run QC´s (Table 7), which indicates acceptable accuracy of the proposed method.

Analyte	QC (ng/mL)	0.5	1.25
ATV	% Accuracy % CV	110.2 2.6	96 3.3
ATV-Lactone	% Accuracy % CV	101.4 4.6	98.2 2.6
ATV- OH	% Accuracy % CV	103.2 7.9	95 3.2

Table 7: Summary of quality control samples
n= 6 (six replicates for each validation run)
% Accuracy= [(determined value/true value)]*100
%CV calculated as (SD/mean)*100
QC: Quality Control

4.4. Results of matrix effect

Sample					ATV-OH2 Results					ATV-OH Results					ATV Results					ATV-LACTONE2 Results				
Name	Data File	Type	Level	Acq. Date-Time	RT	Final Conc.	Accuracy	Sample RSD	Area	RT	Final Conc.	Accuracy	Sample RSD	Area	RT	Final Conc.	Accuracy	Sample RSD	Area	RT	Final Conc.	Accuracy	Sample RSD	Area
MeOH 1.25	M016-r002.d	Sample		9.3.2017 7:55	6,020	1,5461			623	6,014	1,3364			1094	6,163	1,3726			5517	6,192	1,2625			6164
TISSUE	M017-r001.d	Sample		9.3.2017 8:05	6,014	1,2497			286	6,014	1,1436			565	6,163	1,3324			3237	6,192	1,3245			3944
TISSUE	M017-r002.d	Sample		9.3.2017 8:15	6,020	1,4253			329	6,014	1,4169			681	6,163	1,4183			3357	6,192	1,4105			4081
TISSUE	M018-r001.d	Sample		9.3.2017 8:25	6,014	1,4212			359	6,014	1,3739			722	6,163	1,2465			3168	6,192	1,3154			4134
TISSUE	M018-r002.d	Sample		9.3.2017 8:34	6,014	1,6713			434	6,014	1,2254			632	6,163	1,3551			3436	6,192	1,3417			4165
TISSUE	M019-r001.d	Sample		9.3.2017 8:44	6,014	1,3978			371	6,014	1,4596			813	6,157	1,4473			3973	6,192	1,3616			4543
TISSUE	M019-r002.d	Sample		9.3.2017 8:54	6,014	1,5097			411	6,014	1,3532			754	6,163	1,4788			4082	6,192	1,3757			4607
TISSUE	M020-r001.d	Sample		9.3.2017 9:04	6,014	1,5434			485	6,014	1,4905			955	6,163	1,4107			4440	6,192	1,3341			5110
TISSUE	M020-r002.d	Sample		9.3.2017 9:13	6,014	1,7874			576	6,014	1,4721			932	6,163	1,4689			4593	6,192	1,4358			5471
TISSUE	M021-r001.d	Sample		9.3.2017 9:23	6,020	1,3853			372	6,014	1,2044			675	6,157	1,1887			3213	6,192	1,2612			4229
TISSUE	M021-r002.d	Sample		9.3.2017 9:33	6,014	1,4718			397	6,014	1,2694			703	6,163	1,2749			3436	6,192	1,3349			4440
PLASMA 1.25	M022-r001.d	Sample		9.3.2017 11:12	6,009	1,5704			554	6,014	1,3757			983	6,157	1,1631			3977	6,192	0,7885			3155
PLASMA 1.25	M022-r002.d	Sample		9.3.2017 11:22	6,014	1,6679			631	6,014	1,2508			941	6,157	1,2274			4470	6,192	1,0027			4391
PLASMA 1.25	M023-r001.d	Sample		9.3.2017 11:31	6,014	1,1838			417	6,014	1,0126			781	6,157	0,9911			3594	6,192	0,8776			3898
PLASMA 1.25	M023-r002.d	Sample		9.3.2017 11:41	6,014	1,2737			458	6,014	0,8259			627	6,157	0,9997			3607	6,192	0,8953			3961
PLASMA 1.25	M024-r001.d	Sample		9.3.2017 11:51	6,014	1,6672			665	6,014	1,4112			1123	6,157	1,3504			5254	6,192	1,2275			5798
PLASMA 1.25	M024-r002.d	Sample		9.3.2017 12:01	6,014	1,7603			717	6,014	1,4544			1169	6,157	1,3069			5108	6,192	1,3198			6337
PLASMA 1.25	M025-r001.d	Sample		9.3.2017 12:10	6,014	1,6042			640	6,014	1,2846			1030	6,157	1,3150			5152	6,192	1,2443			5949
PLASMA 1.25	M025-r002.d	Sample		9.3.2017 12:20	6,014	1,5872			609	6,014	1,4808			1149	6,157	1,3842			5262	6,192	1,2498			5759
PLASMA 1.25	M026-r001.d	Sample		9.3.2017 12:30	6,014	1,9076			789	6,014	1,4832			1189	6,163	1,4143			5571	6,192	1,3824			6646
PLASMA 1.25	M026-r002.d	Sample		9.3.2017 12:40	6,014	1,5993			674	6,014	1,4699			1250	6,157	1,2990			5363	6,192	1,2201			6151

Sample					ATV-OH Results					ATV Results					ATV-LACTONE2 Results					ATV-LACTONE Results				
Name	Data File	Type	Level	Acq. Date-Time	RT	Final Conc.	Accuracy	Sample RSD	Area	RT	Final Conc.	Accuracy	Sample RSD	Area	RT	Final Conc.	Accuracy	Sample RSD	Area	RT	Final Conc.	Accuracy	Sample RSD	Area
25	M009-r002.d	Cal	L6	9.3.2017 5:39	6..	27,7139	110,9		19306	6,157	25,7263	102,9		96443	6..	28,3547	113,4		125531	6..	27,5072	110,0		173865
5	M007-r001.d	Cal	L4	9.3.2017 4:50	6..	4,5746	91,5		3116	6,157	4,2767	85,5		15284	6..	4,4049	88,1		18778	6..	4,3940	87,9		26806
5	M007-r002.d	Cal	L4	9.3.2017 5:00	6..	4,3951	87,9		2917	6,157	4,3410	86,8		15129	6..	4,3641	87,3		18128	6..	4,5601	91,2		27137
50	M010-r001.d	Cal	L7	9.3.2017 5:48	6..	49,5167	99,0		33671	6,157	46,2916	92,6		169777	6..	51,7692	103,5		224005	6..	51,6555	103,3		319087
50	M010-r002.d	Cal	L7	9.3.2017 5:58	6..	54,6351	109,3		36005	6,157	51,7207	103,4		183886	6..	55,0847	110,2		231006	6..	55,3305	110,7		331254
BLANK	M002-r001.d	Blank		9.3.2017 3:13	6..	80,9967			21	6,141	25,9920			36	6..	34,0710			56	6..	6,9002			16
BLANK	M002-r002.d	Blank		9.3.2017 3:22	6..	143,3350			48	6,180	33,9192			62	6..	16,8089			36	6..	19,7621			60
MeOH	M001-r001.d	DoubleBla..		9.3.2017 2:53	6..	69,7721			14	6,174	36,0622			38	6..	27,5137			34	6..	50,4481			89
MeOH	M001-r002.d	DoubleBla..		9.3.2017 3:03	5..	30,3767			13	6,174	6,2338			14	6..	14,6921			39	6..	9,9777			37
MeOH 1.25	M015-r001.d	Sample		9.3.2017 7:26	6..	1,4483			1073	6,163	1,3888			5047	6..	1,3804			6136	6..	1,4089			9035
MeOH 1.25	M012-r001.d	Sample		9.3.2017 6:28	6..	1,3373			972	6,163	1,3907			4963	6..	1,3062			5679	6..	1,3478			8466
MeOH 1.25	M012-r002.d	Sample		9.3.2017 6:37	6..	1,3161			937	6,163	1,3311			4634	6..	1,2797			5443	6..	1,2661			7754
MeOH 1.25	M013-r001.d	Sample		9.3.2017 6:47	6..	1,4001			1019	6,157	1,3259			4705	6..	1,3981			6120	6..	1,3644			8583
MeOH 1.25	M013-r002.d	Sample		9.3.2017 6:57	6..	1,5559			1108	6,157	1,4306			5003	6..	1,3946			5953	6..	1,3966			8586
MeOH 1.25	M014-r001.d	Sample		9.3.2017 7:07	6..	1,3647			982	6,163	1,3384			4708	6..	1,3426			5792	6..	1,3451			8361
MeOH 1.25	M014-r002.d	Sample		9.3.2017 7:16	6..	1,3418			991	6,163	1,3979			5081	6..	1,3638			6053	6..	1,2787			8129
MeOH 1.25	M015-r002.d	Sample		9.3.2017 7:36	6..	1,5554			1164	6,163	1,4190			5215	6..	1,3850			6211	6..	1,4103			9122
MeOH 1.25	M016-r001.d	Sample		9.3.2017 7:46	6..	1,3574			1080	6,163	1,3183			5121	6..	1,2495			5922	6..	1,3294			9134
MeOH 1.25	M016-r002.d	Sample		9.3.2017 7:55	6..	1,3364			1094	6,163	1,3726			5513	6..	1,2625			6164	6..	1,2609			8874

Figure 21: Specific areas of each solution for ATV, obtained from the Agilent MassHunter Quantitative Analysis (for QQQ), to evaluate the matrix effect, overall recovery and extraction yield

Matrix effect was determined by comparing the peak area of each analyte in methanol solution to the signal obtained in whole blood after the extraction step. Experiments showed positive matrix effect for all analytes, which ranged 80.6% to 94.71% for plasma and 71.3% to 74.9% for tissue. Extraction yield after the protein precipitation step ranged from 76 % to 101.5% and was greater for ATV-Lactone. The peak areas of analytes spiked in methanol and in blood samples after protein precipitation showed good overall recoveries that ranged between 74.7% and 81.8%.

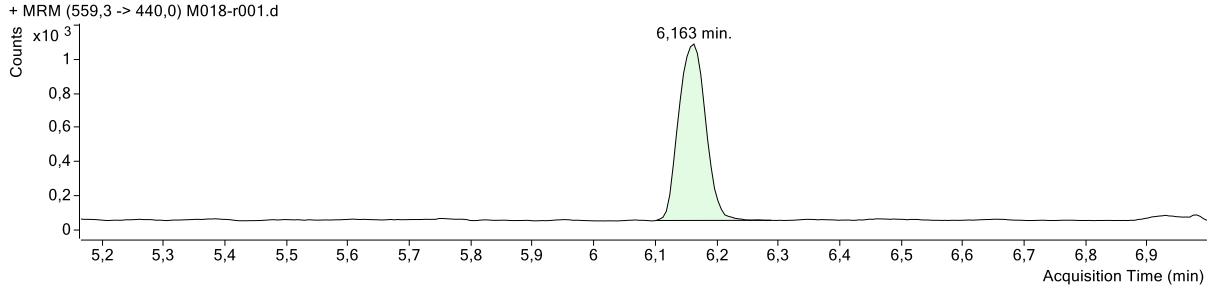

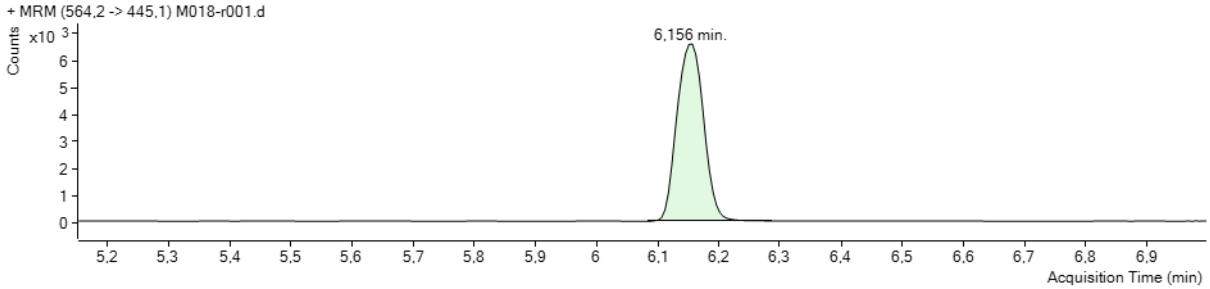

Figure 22: MRM Chromatogram of drug 1.25 ng/ml level (upper) and of IS (down) in the tissue

As shown in figure 22, the signal is very reliable. If it works for liver tissue (a heavy and with high concentrations), we can conclude that the method fits in other tissues too, like prostate (suitable in this experimental).

That being proved, the measurement of atorvastatin (ATV) and atorvastatin lactone (ATV-lactone) in prostate tissue homogenate with HPLC-MS using atorvastatin D_5 (ATV-D_5) as internal standard, was initiated in the same chromatogram conditions.

5. Experimental of samples assay

5.1. Plasma samples

Firstly, the plasma samples that have matching ATV treated tissue samples were selected and melted in ice.

5.2. Tissue homogenate samples

Tissue homogenates were made in liquid nitrogen. The samples were selected from ATV treated patients.

After taking the sample for analysis, the material was kept straight to dry ice and freezer (-80ºC).

5.3. Standards preparation for sample analysis

The calibration curve was obtained in the end for plasma and tissue samples with the same procedure, obtaining two different calibration curves for ATV and ATV-lactone, done in different days.

5.3.1. Dilution of Internal standard

100 μL of IS (ATV-D_5) 1 mg/mL were diluted to 10 mL with 50% MeOH in flask, with a concentration of 10 μg/mL.

100 μL of the previous solution (10 μg/mL) were diluted to 10 mL with 50% MeOH, with a final concentration of 100 ng/mL, in 50% MeOH.

5.3.2. Stock solutions (in freezer)

- Atorvastatin (ATV) in DMSO, with a concentration of 1 mg/mL.
- Atorvastatin lactone (ATV-Lactone) in DMSO, with a concentration of 1 mg/mL.

5.3.3. Working solutions in 50% MeOH for plasma analysis in samples assay

100 µL of ATV and ATV-lactone solutions (1mg/mL) were diluted to 10 mL with 50% MeOH in the same volumetric flask, with a concentration of 10 µg/mL (ATV and ATV-lactone).

Drug Concentration (µg/ml)	Add	Add 50%MeOH
5	0,5 mL of sol 10 µg /mL	0,5 mL
2.5	0,5 mL of sol 5 µg /mL	0,5 mL
1	0,4 mL of sol 2.5 µg /mL	0,6 mL
0.5	0,5 mL of sol 1 µg/mL	0,5 mL
0.25	0,5 mL of sol 0.5 µg/mL	0,5 mL
0.1	0,4 mL of sol 0.25 µg/mL	0,5 mL
0,05	0,5 mL of sol 0.1 µg/mL	0,5mL
0,025	0,5mL of sol 0.05 µg/mL	0,5 mL
0,01	0,4 mL of sol 0.025 µg/mL	0,6 mL
0,005	0,5 mL of sol 0.0125 µg/mL	0,5mL

Table 8: Working solutions for plasma analysis in samples assay

5.3.4. Working solutions in 50% MeOH for tissue analysis in samples assay

100 µL of ATV and 50 µL of ATV-lactone solutions (1mg/mL) were diluted to 10 mL with 50% MeOH in the same volumetric flask, with a concentration of 10 µg/mL (for ATV) and 5 µg/mL (for ATV-lactone).

Drug Concentration (µg/ml)	Add	Add 50%MeOH
2.5	0,5 mL of sol 10 µg /mL	0,5 mL
1.25	0,5 mL of sol 2.5 µg /mL	0,5 mL
0.5	0,4 mL of sol 1.25 µg /mL	0,6 mL
0.25	0,5 mL of sol 0.5 µg/mL	0,5 mL
0.125	0,5 mL of sol 0.25 µg/mL	0,5 mL
0.05	0,4 mL of sol 0.125 µg/mL	0,6 mL
0,025	0,5 mL of sol 0.05 µg/mL	0,5mL
0,0125	0,5mL of sol 0.025 µg/mL	0,5 mL
0,005	0,4 mL of sol 0.0125 µg/mL	0,6 mL
0,0025	0,5 mL of sol 0.005 µg/mL	0,5mL

Table 9: Working solutions for tissue analysis in samples assay

5.4. Calibration curve for plasma in samples assay

The next phase was to elaborate the calibration curve and respective concentrations, using the working solutions. For plasma samples, nine calibrators were used that covered the range of 0.5-500 ng/mL for ATV and its metabolite (ATV-lactose). Calibration standards and QC's were made in human plasma.

Plasma	Drug concentration in plasma (ng/mL)	Add Working solution	IS (ATV-d5) 100ng/mL
100 µL	500	10 µL solution of 5 µg/mL	10 µL
100 µL	100	10 µL solution of 1 µg/mL	10 µL
100 µL	50	10 µL solution of 0,5 µg/mL	10 µL
100 µL	25	10 µL solution of 0,25 µg/mL	10 µL
100 µL	10	10 µL solution of 0,1 µg/mL	10 µL
100 µL	5	10 µL solution of 0,05 µg/mL	10 µL
100 µL	2,5	10 µL solution of 0,025 µg/mL	10 µL
100 µL	1	10 µL solution of 0,01µg/mL	10 µL
100 µL	0,5	10 µL solution of 0,005 µg/mL	10 µL
100 µL	0	10 µL solution of 50% MeOH	10 µL

Table 10: Calibration curve for plasma analysis in samples assay

For tissue samples, nine calibrators were used that covered the range of 0.25-250 ng/mL for ATV and its metabolite (ATV-lactose). Calibration standards and QC's were made in human plasma.

Plasma	Drug concentration in plasma (ng/mL)	Add Working solution	IS (ATV-d5) 100ng/mL
100 µL	250	10 µL solution of 5 µg/mL	10 µL
100 µL	125	10 µL solution of 1 µg/mL	10 µL
100 µL	50	10 µL solution of 0,5 µg/mL	10 µL
100 µL	12.5	10 µL solution of 0,25 µg/mL	10 µL
100 µL	5	10 µL solution of 0,1 µg/mL	10 µL
100 µL	2.5	10 µL solution of 0,05 µg/mL	10 µL
100 µL	1.25	10 µL solution of 0,025 µg/mL	10 µL
100 µL	0.5	10 µL solution of 0,01µg/mL	10 µL

100 µL	0.25	10 µL solution of 0,005 µg/mL	10 µL
100 µL	0	10 µL solution of 50% MeOH	10 µL

Table 11: Calibration curve for tissue analysis in samples assay

5.5. Quality controls (QC) for plasma analysis in samples assay

6 replicates of each concentration were used to the quality controls in plasma samples.

Name	Plasma	Drug concentration in plasma (ng/mL)	Add Working solution	IS (ATV-d5) 100ng/mL
QC 100	100 µL	100	10 µL solution of 1 µg/mL	10 µL
QC10	100 µL	10	10 µL solution of 0,1 µg/mL	10 µL
QC 1	100 µL	1	10 µL solution of 0,01 µg/mL	10 µL

Table 12: Summary of quality controls for plasma analysis in samples assay

5.6. Plasma samples preparation

Samples	Plasma	Drug concentration in plasma (ng/mL)	Add Working solution	IS (ATV-d5) 100ng/mL
(57 in total)	100 µL	X	10 µL 50% MeOH	10 µL

Table 13: Preparation of plasma samples

5.7. Quality controls (QC) in tissue homogenate

Tissue homogenate from patients that were not treated with drug was used in quality controls. That homogenate came in solution (1 part of tissue, 10 parts of isotonic NaCl solution). Six replicates were made.

Name	Homogenate	Drug concentration in homogenate (ng/mL)	Add Working solution	IS (ATV-d5) 100 ng/mL
QC T1- 6	100 µL	10	10 µL solution of 0,1 µg/mL	10 µL

Table 14: Quality controls for tissue analysis in samples assay

5.8. Tissue homogenate preparation

All the tissue samples (in solid state) were firstly smashed by mortar and pestle with liquid nitrogen. Homogenate came then in solution (1 part of tissue, 10 parts of isotonic 0,9% NaCl solution).

*If the tissue weight was 27 mg or more, 100 µL were taken for ATV analysis.

*If the tissue weight was 22 mg or more, 50 µL were taken for ATV analysis.

*If the tissue weight was 19 mg or more, 20 µL were taken for ATV analysis.

Name	Homogenate	Drug concentration in homogenate (ng/mL)	Add Working solution	IS (ATV-d5) 100 ng/mL
number	100 µL	X	10 µL 50% MeOH	10 µL
number	50 µl	X	5 µL 50% MeOH	5 µL
number	20 µL	X	2 µL 50% MeOH	2µL

Table 15: Tissue homogenate preparation

5.9. Tissue without drug treatment as Control of 'zero' of Calibration

Tissue homogenate from patients that were not treated with drug (in duplicate) was used as control of 'zero' in the calibration curve.

Name	Homogenate	Drug concentration in homogenate (ng/mL)	Add Working solution	IS (ATV-d5) 100 ng/mL
BT	100 µL	0	10 µL 50% MeOH	10 µL

Table 16: Zero of calibration curve in tissue from patients who were not treated with drug

5.10. Precipitation of proteins

To each sample it was added 400 µL of 0.1% acetic acid in acetonitrile, ice cold, to the calibration standards. If the sample volume had 50 µL, 200 µL of 0.1% formic acid in acetonitrile, ice cold, was the volume to add. Otherwise, if the sample volume was 20 µL, 80 µL of 0.1% formic acid in acetonitrile, ice cold was the volume to add.

The test tubes were vortex-mixed for approximately 10 seconds and thereafter, all precipitated proteins were separated by centrifugation for 15 min at 14000xg and 4 ºC temperature. The supernatant was recovered (100 µL or 40 µL If total volume was 100 µL) and transferred into HPLC vials.

5.11. Qualitative Analysis B.06.00 for plasma samples

The following MRM's show the retention time for each analyte (atorvastatin, internal standard and atorvastatin-lactone) in blank human plasma (drug and internal standard free-figure 23) in 'zero' of calibration curve (only drug-free- figure 24) and in 10 ng/mL of calibration curve (figure 25).

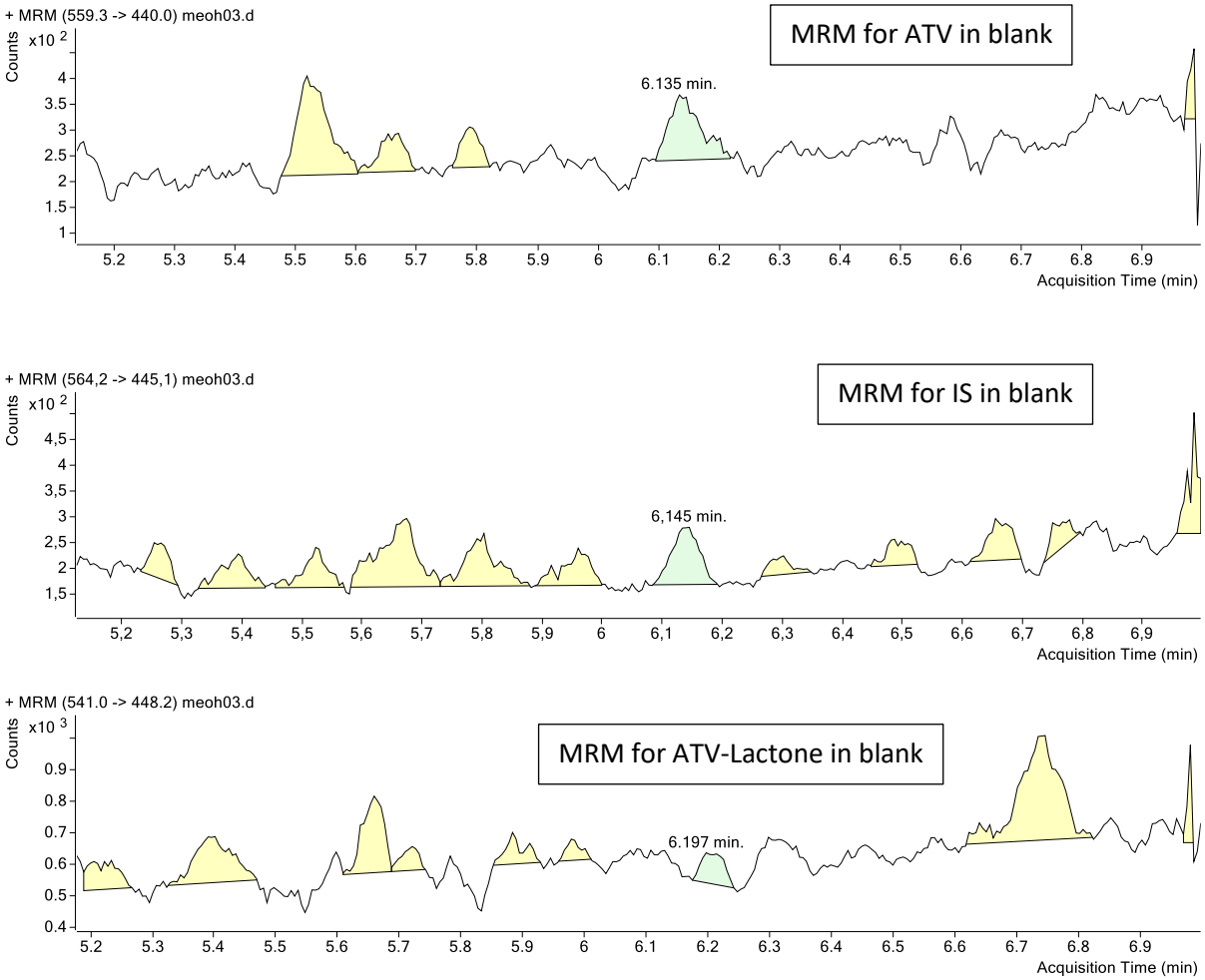

Figure 23: MRM chromatogram for ATV (upper) and IS (in the middle) and ATV-Lactone (down) from analysis of blank human plasma (drug and IS free) in plasma analysis

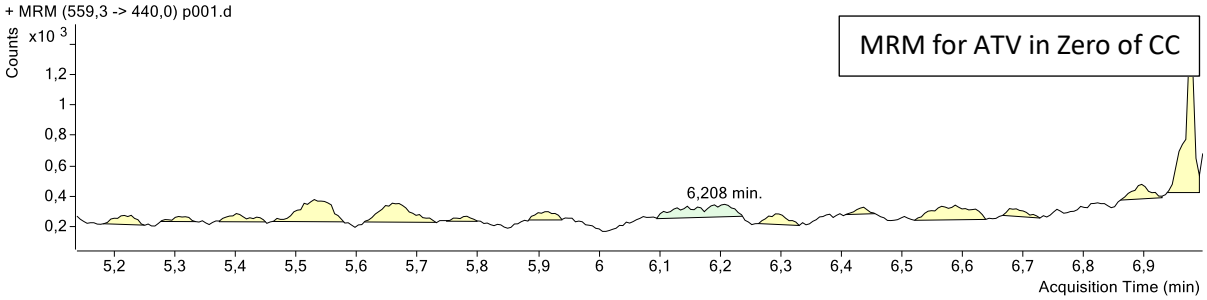

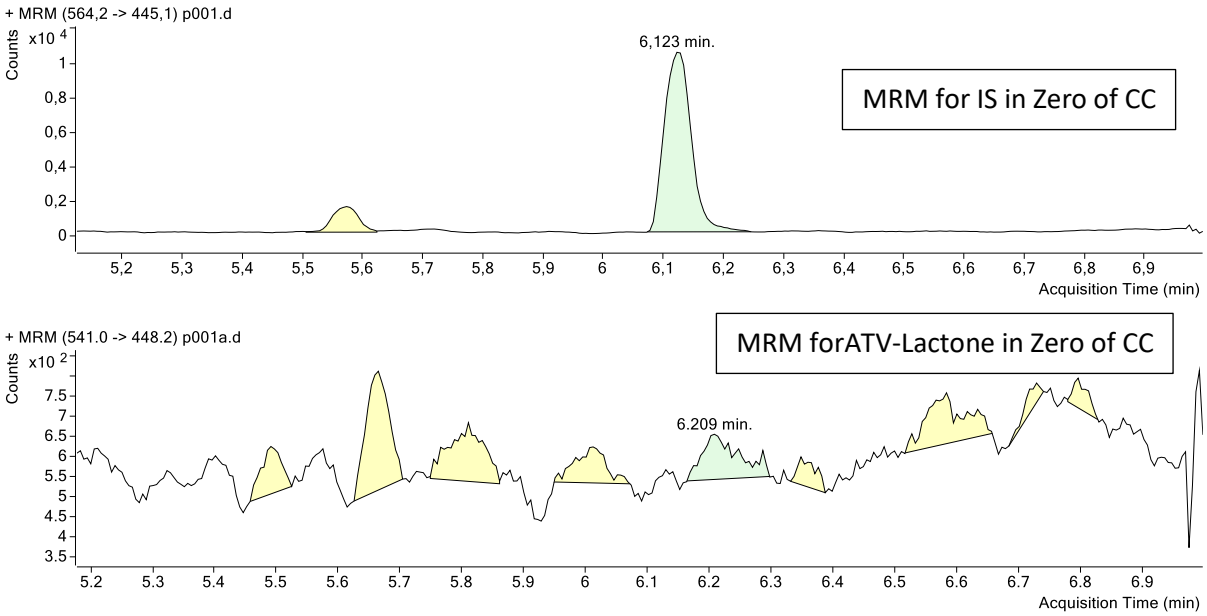

Figure 24: MRM chromatogram for ATV (upper) and IS (in the middle) and ATV-Lactone (down) from analysis of zero (in calibration curve-drug free) in plasma analysis

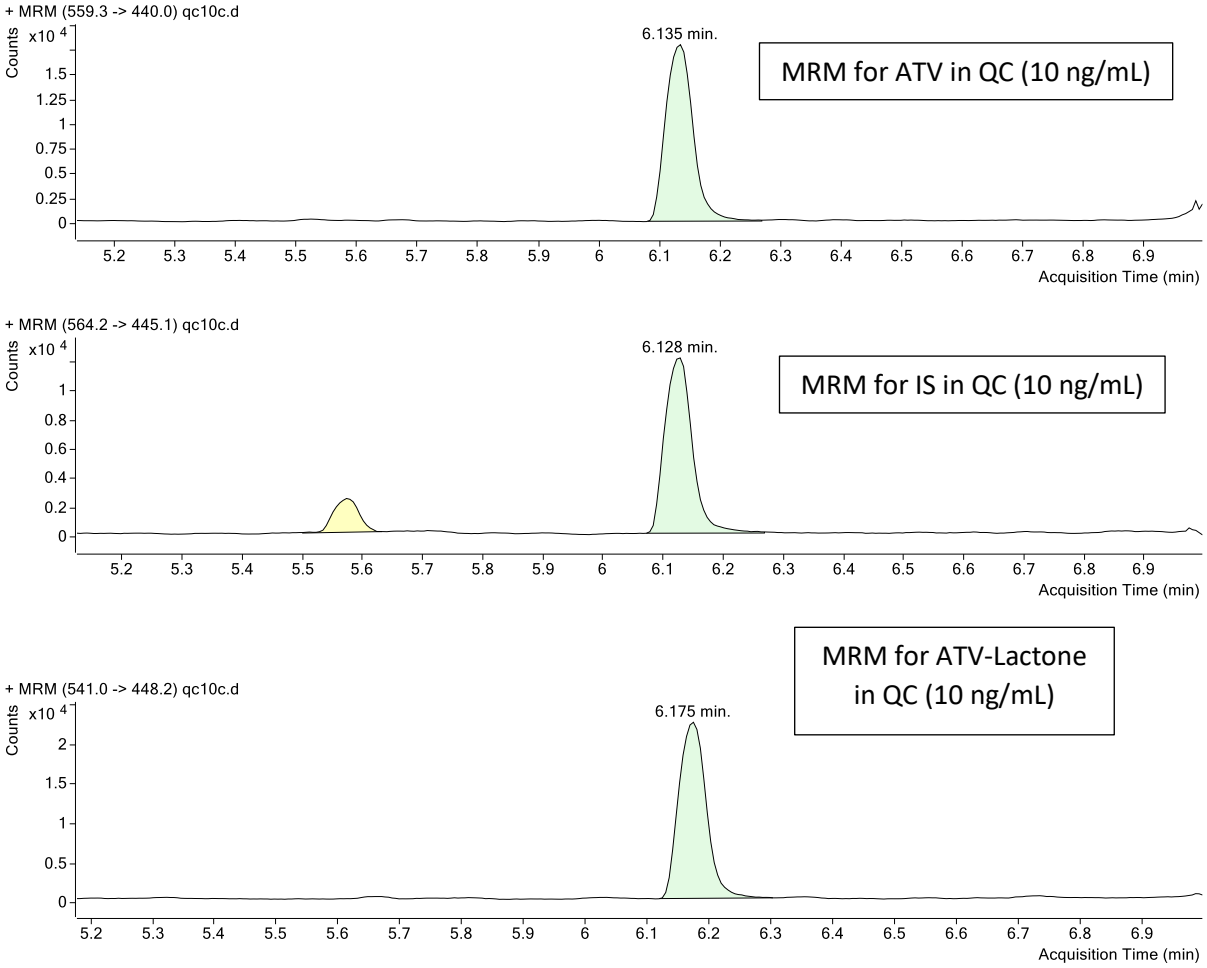

Figure 25: MRM chromatogram for ATV (upper) and IS (in the middle) and ATV-Lactone (down) from analysis of QC (10 ng/mL) in plasma analysis

For each compound (ATV, ATV-lactone and IS), the peaks are predictable and expected: in the blank, there is no signal for the respective retention times; in zero there is only signal for the IS, once the drug is free and, finally, in the 10 ng/mL concentration both peaks (IS and compounds) are clearly visible and defined.

5.12. Linearity from QQQ Quantitative Analysis for plasma samples

The linear regression curves were fitted to the concentration ranges of 0.5-500 ng/mL for ATV and its metabolites in human plasma. The mean equations of the calibration curves generated for each analyte were as follows:

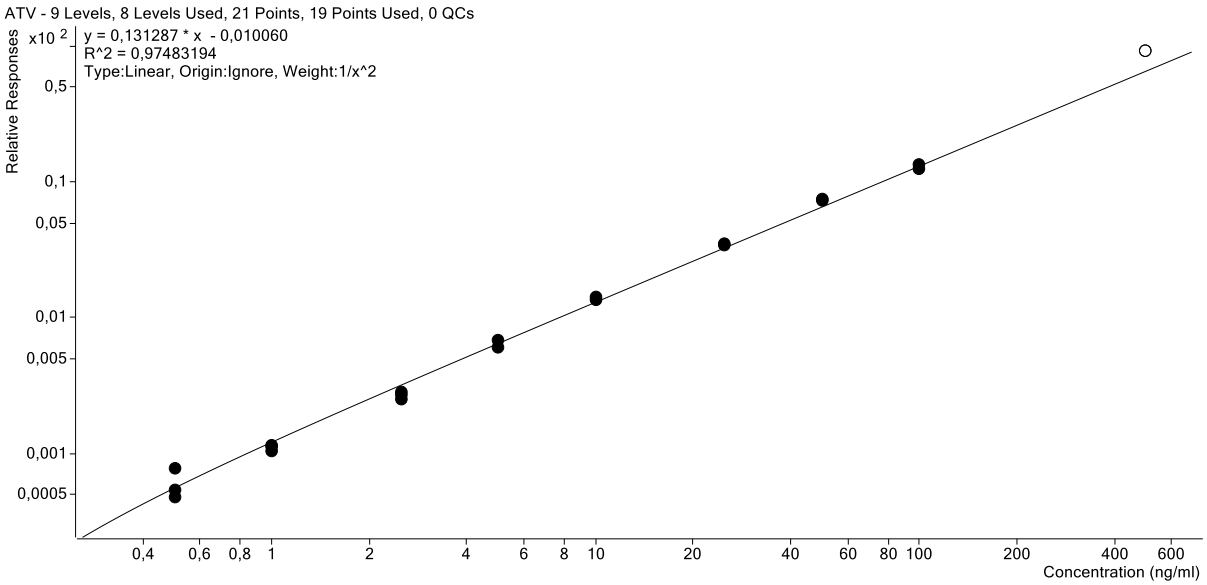

Figure 26: Calibration curve for ATV for plasma samples

The calibration curve and respectively r^2 obtained were:

$y = 0.131287*x - 0.010060$

$R^2 = 0.9748$

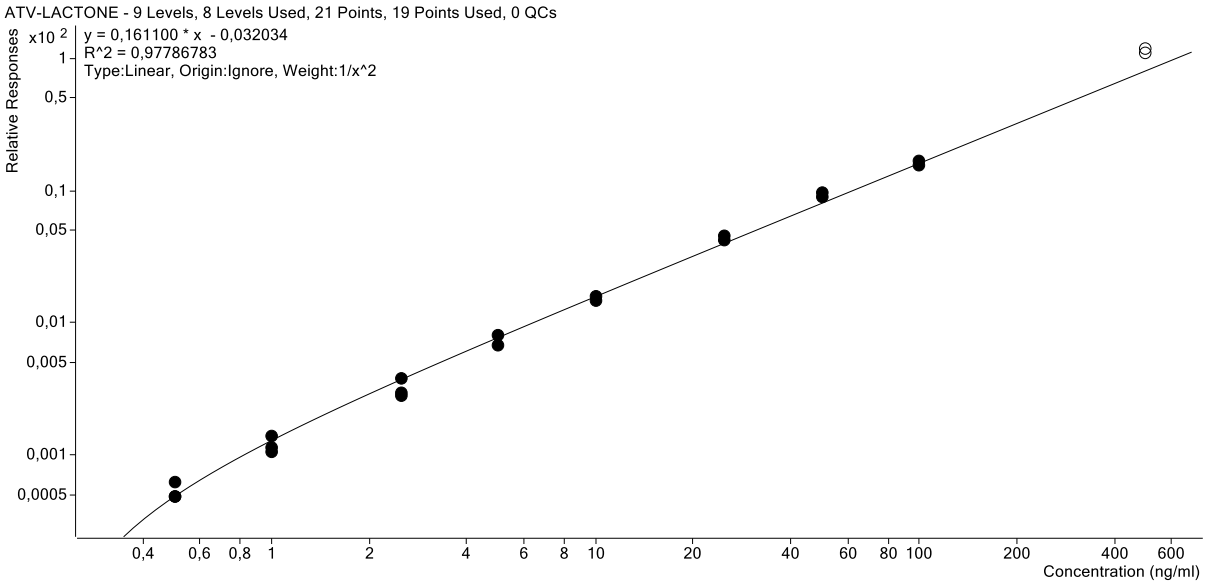

Figure 27: Calibration curve for ATV-Lactone for plasma samples

The calibration curve and respectively r^2 obtained were:

y= 0.161100*x + 0.032034
R^2= 0.9779

The calibration curves obtained from analyte/IS peak area vs. nominal concentration were linear using weighted (1/x) linear regression over the concentration range, with correlation coefficients (R^2)≥0.9748.

5.13. Qualitative Analysis B.06.00 for tissue samples

The following MRM's show the retention time for each analyte (atorvastatin, internal standard and atorvastatin-lactone) in blank human plasma (drug and internal standard free-figure 28), in 'zero' of the tissue from samples not treated with drug (figure 29) and another one of calibration curve (only drug-free- figure 30) and in 10 ng/mL of calibration curve (figure 31).

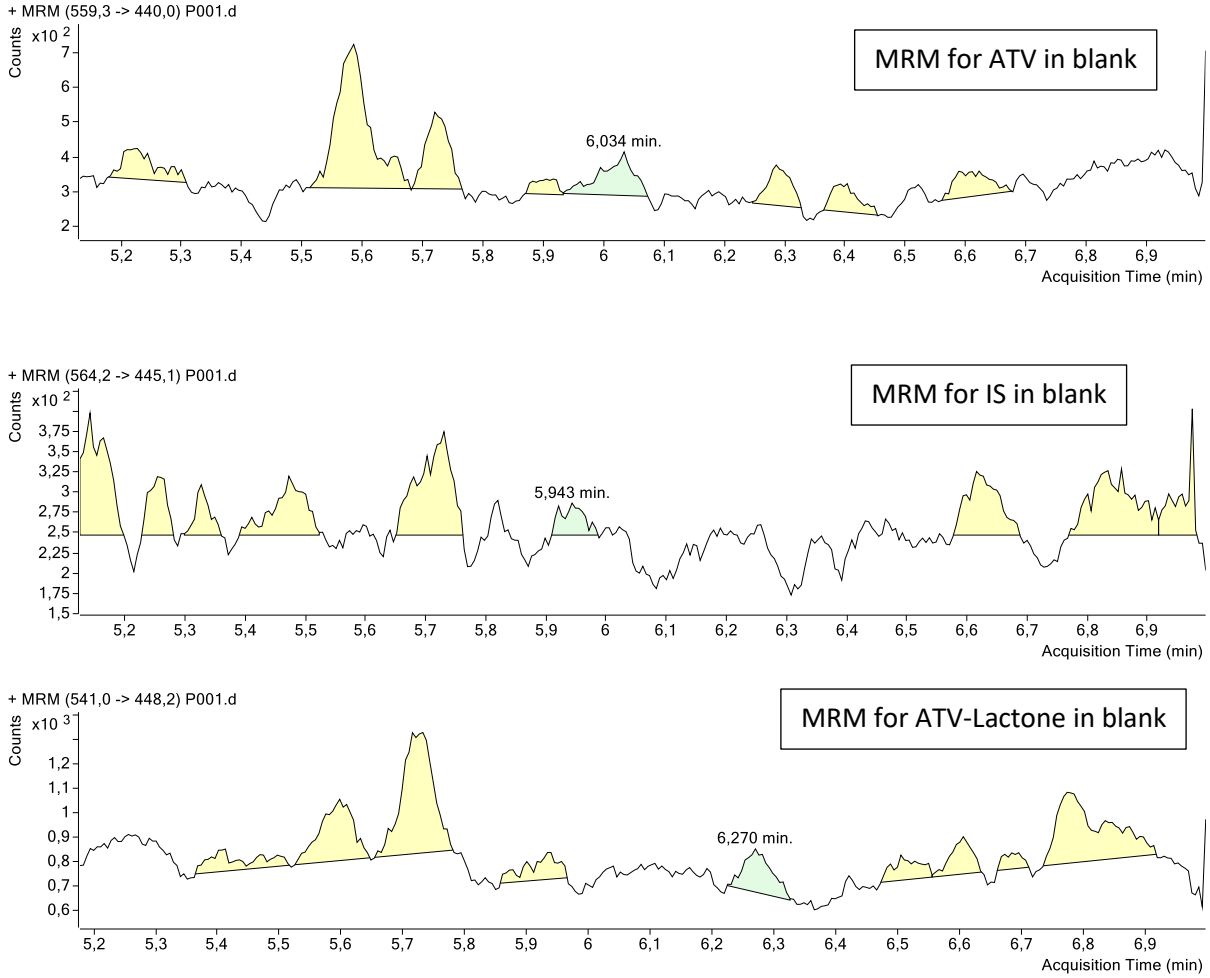

Figure 28: MRM chromatogram for ATV (upper) and IS (in the middle) and ATV-Lactone (down) from analysis of blank human plasma (drug and IS free) in tissue analysis

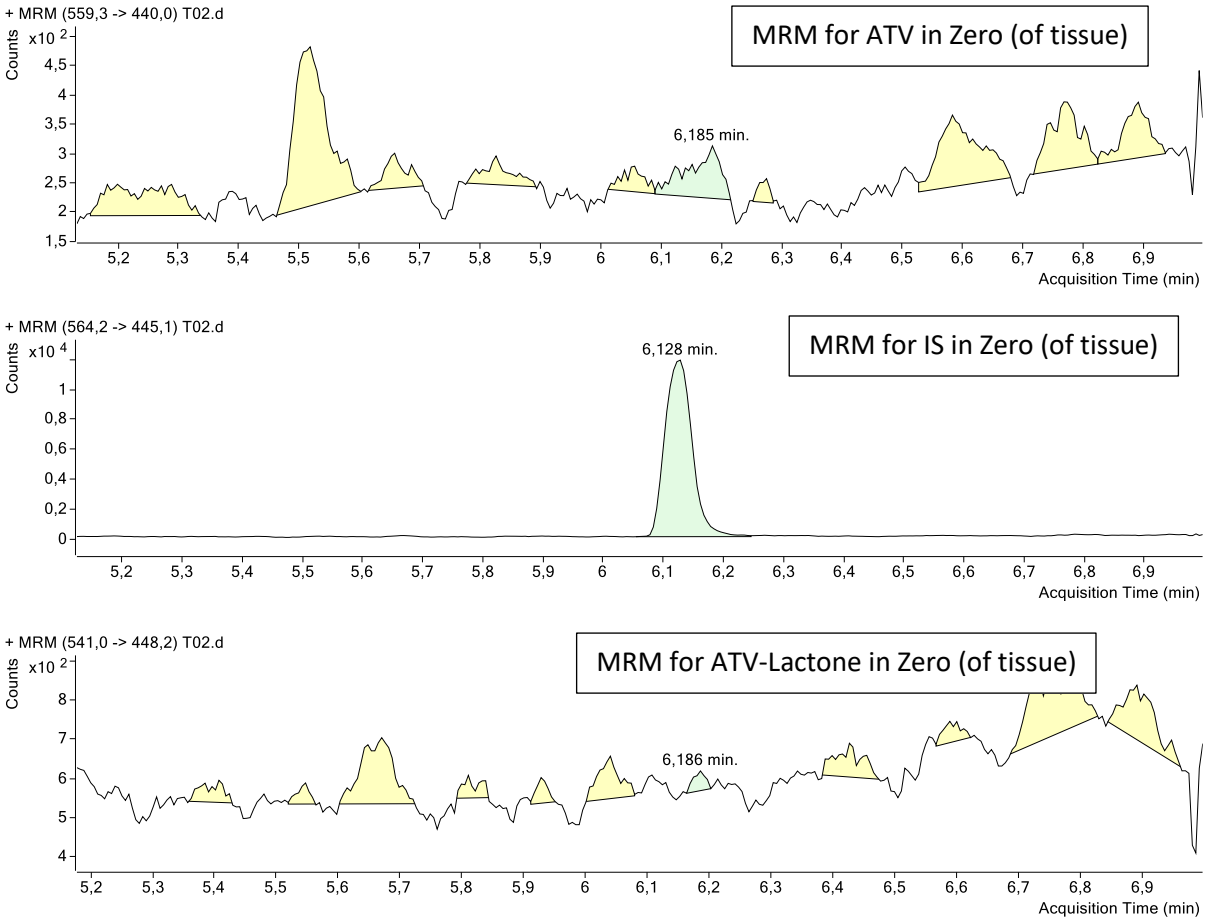

***Figure 29: MRM chromatogram for ATV (upper) and IS (*in the middle) and ATV-Lactone (down) from analysis of zero in tissue samples not treated with drug**

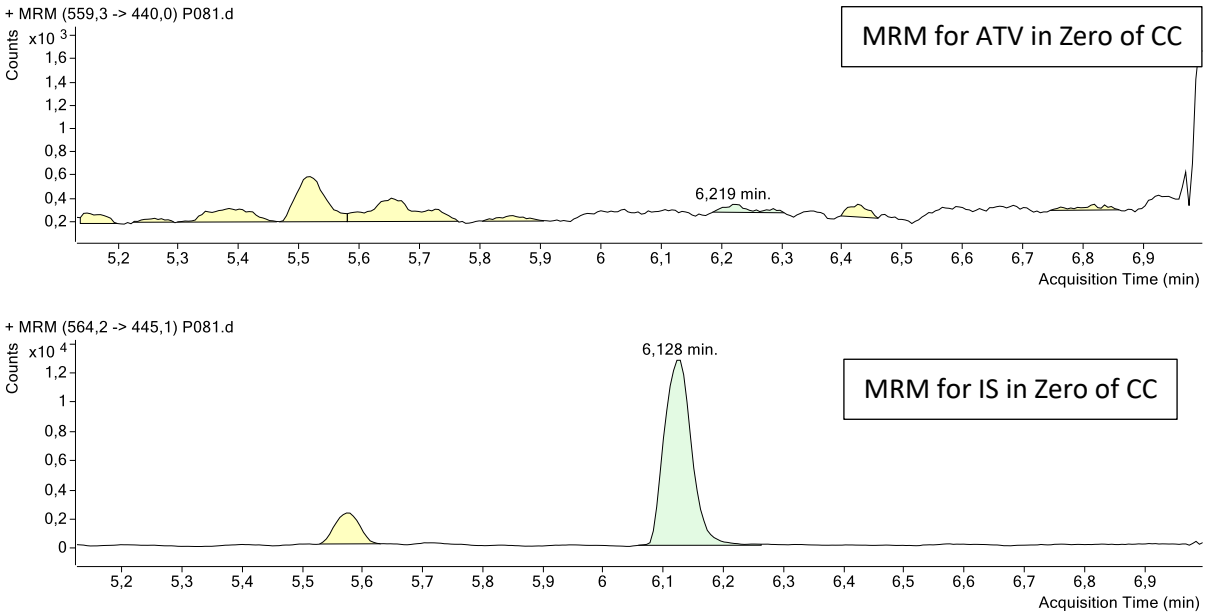

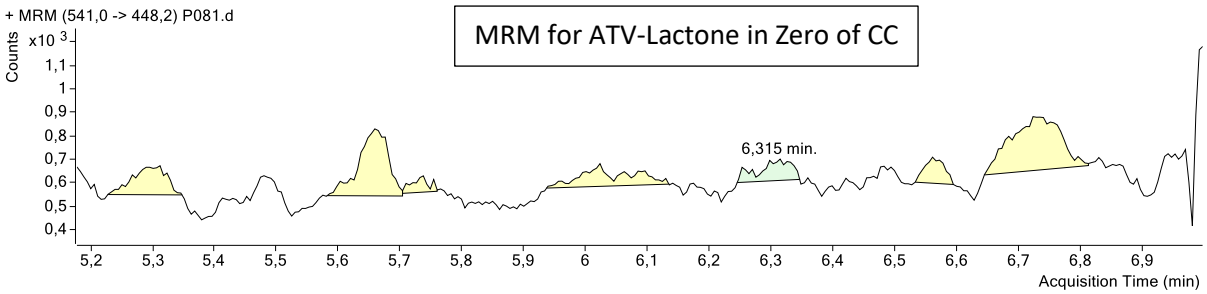

Figure 30: MRM chromatogram for ATV (upper) and IS (in the middle) and ATV-Lactone (down) from analysis of zero (CC-drug free) in tissue analysis

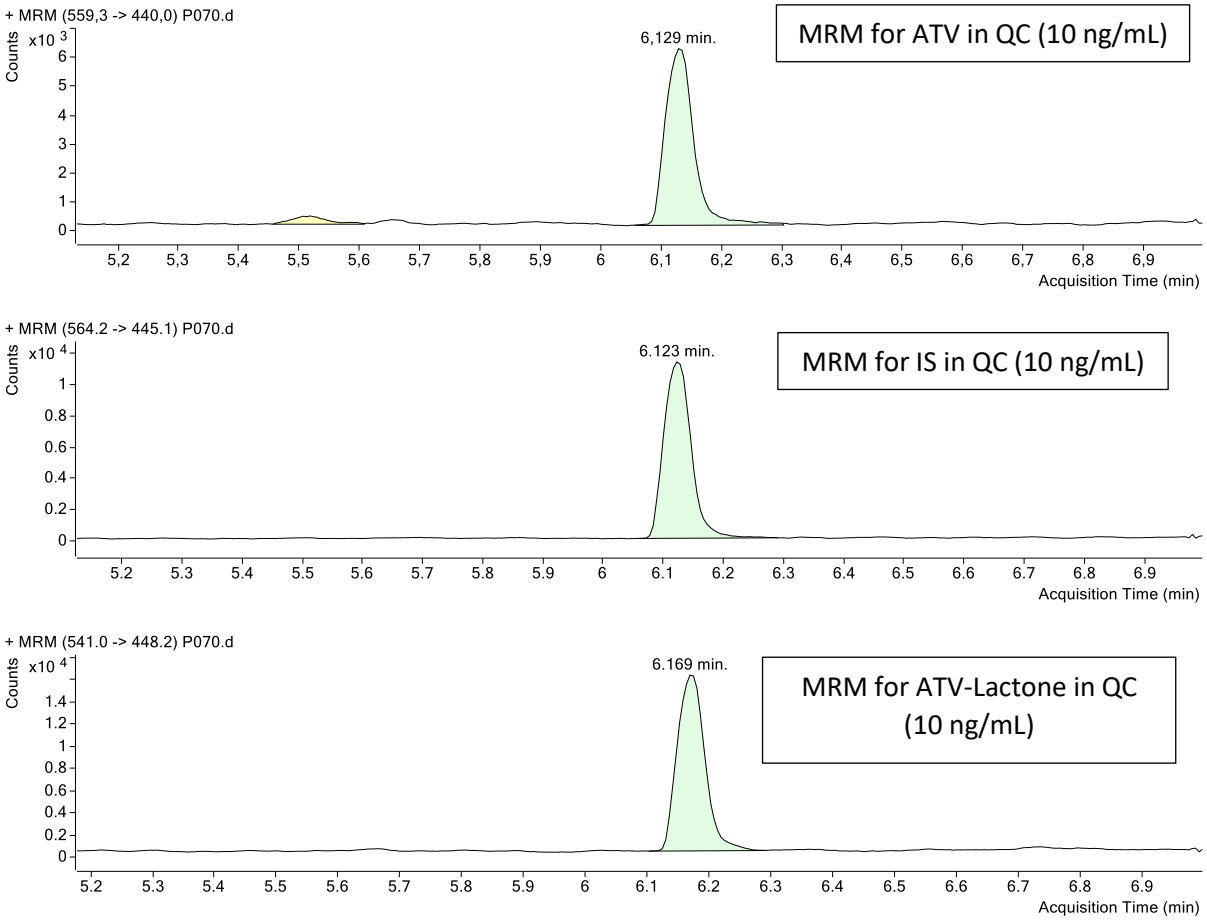

Figure 31: MRM chromatogram for ATV (upper) and IS (in the middle) and ATV-Lactone (down) from analysis of QC (10 ng/mL) in tissue analysis

For each compound (ATV, ATV-lactone and IS), the peaks are predictable and expected: in the blank, there is no signal for the respective retention times; in zero there is only signal for the IS, once the drug is free and, finally, in the 10 ng/mL concentration both peaks (IS and compounds) are clearly visible and defined.

5.14. Linearity from QQQ Quantitative Analysis for tissue samples

The linear regression curves were fitted to the concentration ranges of 0.25-250 ng/mL for ATV and its metabolites in human plasma. The mean equations of the calibration curves generated for each analyte were as follows:

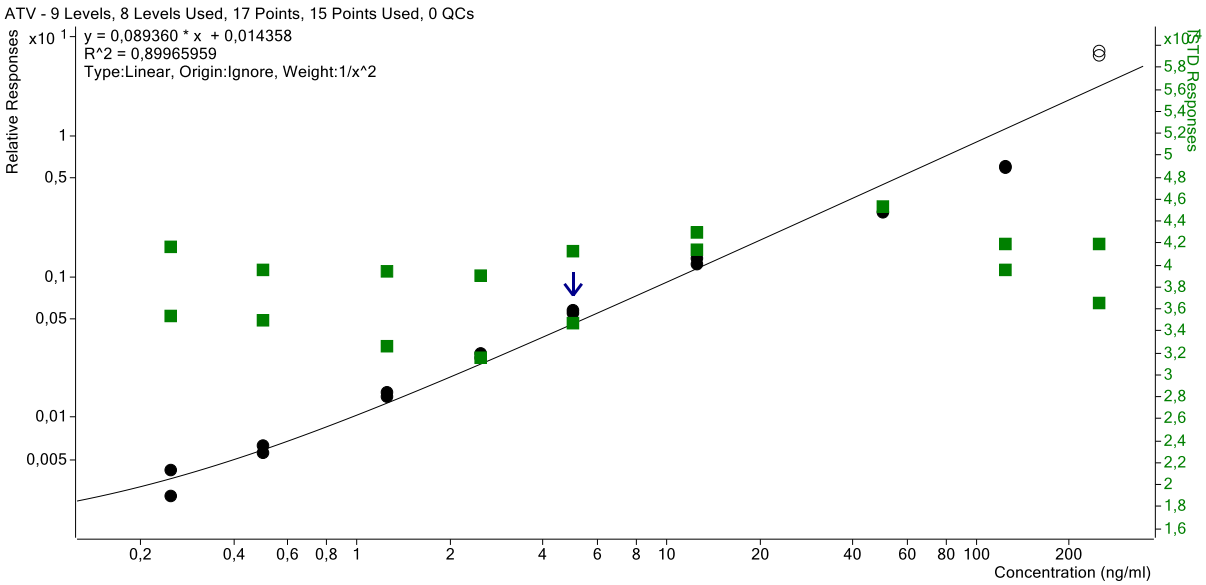

Figure 32: Calibration curve for ATV for tissue samples

The calibration curve and respectively r^2 obtained were:

y= 0.089360*x + 0.014358
R^2= 0.8997

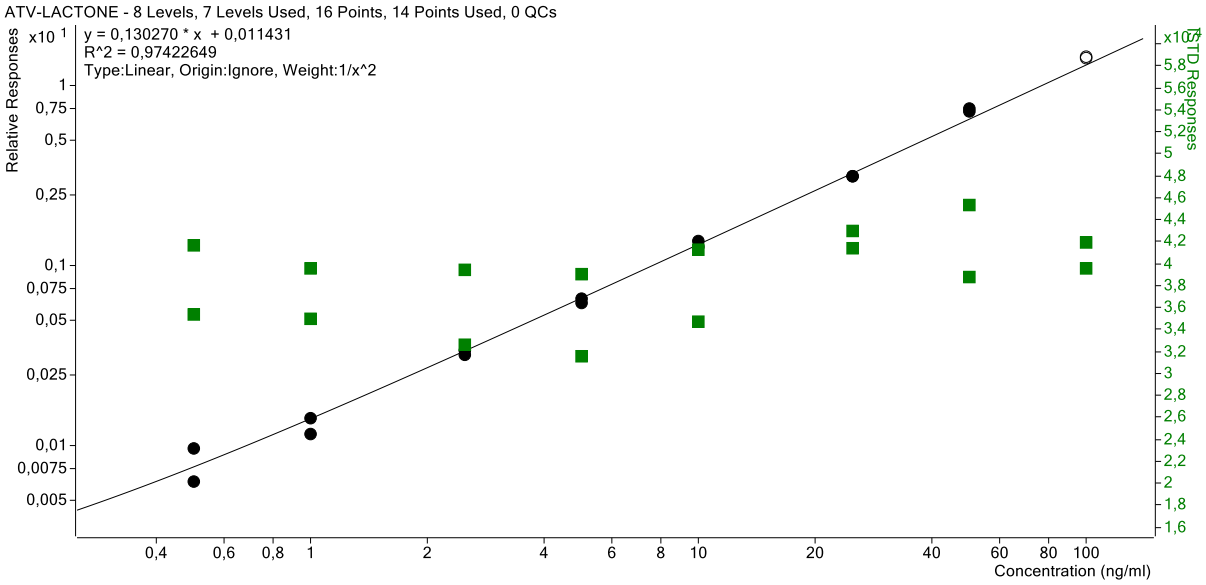

Figure 33: Calibration curve for ATV-Lactone for tissue samples

The calibration curve and respectively r^2 obtained were:

y= 0.130270*x + 0.011431
R^2= 0.9742

The green squares are representing the internal standard which response is relatively constant for all the concentrations.

The calibration curves obtained from analyte/IS peak area vs. nominal concentration were linear using weighted (1/x) linear regression over the concentration range, with correlation coefficients (R^2)≥0.8997.

The following table shows the results of the ratio of ATV and ATV-Lactone in tissue/plasma from the samples previously prepared, according through the obtained calibration curves (see table 17).

A	B	C	D	E	F	G	H	I	J	K
E-003	56,2	562	0	0	0	0	0,3147	0,4438	0	0
E-005	67,3	673	0,1024	0,0216	1,1264	0,2376	0,2528	0,2930	4,455696	0,810922
E-008	28,3	283	0	0,1997	0	2,1967	0,3840	0,2531	0	8,679178
E-013	93,6	936	0,0451	0	0,4961	0	110,3325	48,8222	0,004496	0
E-017	49,3	493	0	0,0041	0	0,0451	0,7637	0,6801	0	0,066314
E-018	89,9	899	0	0,0099	0	0,1089	0,6862	0,8640	0	0,126042
E-022	31,3	313	0	0,0556	0	0,6116	36,6123	32,4678	0	0,018837
E-026	51,3	513	0	0,0261	0	0,2871	0,6805	0,7792	0	0,368455
E-029	33,4	334	0	0,0858	0	0,9438	0,7955	1,2213	0	0,772783
E-031	30	300	0	0,0800	0	0,88	20,5164	19,5384	0	0,04504
E-033	71,2	712	0	0,0119	0	0,1309	1,4935	2,0500	0	0,063854
E-035	53,5	535	0	0,0231	0	0,2541	1,7109	1,7394	0	0,146085
E-038	15,2	152	0	0,0068	0	0,0748	1,8387	3,7403	0	0,019998
E-040	15,6	156	0	0,0385	0	0,4235	8,0257	13,4316	0	0,03153
E-041	187,7	1877	0,2897	0,2547	3,1867	2,8017	0,4698	0,7100	6,783099	3,946056
E-042	15,6	156	0,3424	0,3140	3,7664	3,454	0,8251	0,7323	4,56478	4,716646
E-051	64,9	649	0,5005	0,3439	5,5055	3,7829	4,9812	4,2273	1,105256	0,894874
E-054	15,8	158	2,1088	0,4065	23,1968	4,4715	0,9467	1,0360	24,5028	4,31612
E-055	60	600	0,6562	0,5288	7,2182	5,8168	0,8634	0,9435	8,360204	6,16513
E-058	57	570	0,0518	0,0151	0,5698	0,1661	1,5041	1,4810	0,378831	0,112154
E-061	18,2	182	0	0,0347	0	0,3817	0,7065	1,0858	0	0,351538
E-064	32,1	321	1,3499	0,4450	14,8489	4,895	48,7692	14,3550	0,304473	0,340996
E-066	5,9	59	0	0,0373	0	0,4103	1,0515	1,1803	0	0,347623
E-068	168,2	1682	0	0,0451	0	0,4961	46,7151	60,2850	0	0,008229
E-074	16,1	161	0	0,0316	0	0,3476	131,5541	125,5866	0	0,002768
E-077	270,3	2703	0,2090	0,3224	2,299	3,5464	19,4239	37,7836	0,118359	0,093861
E-091	80,1	801	0	0,0574	0	0,6314	1,0365	1,2030	0	0,524855
E-096	8,2	82	0,0552	0	0,6072	0	37,8954	30,6213	0,016023	0
E-097	257,8	2578	0,2796	0,4531	3,0756	4,9841	19,4149	22,5591	0,158414	0,220935
E-098	81,9	819	1,8497	0,7326	20,3467	8,0586	28,0275	13,5945	0,725955	0,592784
E-102	150,4	1504	1,4741	1,6570	16,2151	18,227	0,6943	0,7522	23,3546	24,23159
E-104	20	200	0	0,0638	0	0,7018	0,1551	0,2993	0	2,344805
E-105	15,3	153	0	0,0502	0	0,5522	0,2432	0,4119	0	1,340617
E-108	20,1	201	0,2183	0,3413	2,4013	3,7543	12,3312	13,2555	0,194734	0,283226
E-109	21,8	218	0,9280	0,1346	10,208	1,4806	3,0786	2,3662	3,315793	0,625729
E-111*	22,6	226	0,2039	0,4692	2,2429	5,1612	68,5521	73,6137	0,032718	0,070112
E-114	101,2	1012	1,8512	1,3813	20,3632	15,1943	0,5466	0,3175	37,2543	47,85606
E-115	225,6	2256	2,2827	1,9015	25,1097	20,9165	110,9934	34,8018	0,226227	0,601018
E-120	75,3	753	1,0026	1,0095	11,0286	11,1045	9,6380	11,7744	1,144283	0,943105
E-124	92,3	923	0,0185	0,0105	0,2035	0,1155	0,3822	0,3333	0,532444	0,346535
E-125	38,5	385	2,0452	1,0228	22,4972	11,2508	0,7723	0,7150	29,13013	15,73538
E-126*	24,9	249	20,5115	11,8617	225,626	130,478	104,1626	53,3765	2,166099	2,444497
E-130	44,4	444	1,1643	0,8622	12,8073	9,4842	1,6532	1,6241	7,746976	5,839665
E-132	72,3	723	2,4848	0,7936	27,3328	8,7296	65,0111	19,1863	0,420433	0,454991
E-133	57,7	577	0	0	0	0	0,6315	0,3972	0	0
E-135	20,6	206	0,7005	0,1944	7,7055	2,1384	72,9233	32,1777	0,105666	0,066456
E-142	23,9	239	0,2966	0,0286	3,2626	0,3146	2,3643	1,3789	1,379943	0,228153
E-145	5,1	51	0	0	0	0	2,4404	2,2428	0	0
E-148	67,1	671	0,0039	0,0483	0,0429	0,5313	0,2006	0,2651	0,213858	2,004149
E-150	34,4	344	0,8703	0,6004	9,5733	6,6044	50,5504	34,6394	0,189381	0,190662
E-159	31,4	314	0,3958	0,1830	4,3538	2,013	1,7464	2,0593	2,493014	0,977517
E-162	54,9	549	11,5637	1,2769	127,2007	14,0459	2,1777	1,6641	58,41057	8,440538
E-164	90,1	901	0,2316	0,2535	2,5476	2,7885	21,9973	26,7933	0,115814	0,104075
E-165*	26,3	263	5,1390	10,6919	56,529	117,6109	0,9850	2,2150	57,38985	53,09747
E-166	92,6	926	1,9284	1,5435	21,2124	16,9785	0,6046	0,6753	35,08501	25,14216
E-170	85,6	856	1,1055	0,8756	12,1605	9,6316	0,8191	1,1437	14,84617	8,421439
E-172	50	500	0,3112	0,3021	3,4232	3,3231	22,7194	23,9788	0,150673	0,138585

Table 17: Results to calculate the ratio of ATV and ATV-Lactone in tissue/plasma A- Samples name; B- Weight (mg); C- Volume added of NaCL (μL) 0,9%; D- Homogenate concentration (ng/mL) of ATV; E- Homogenate concentration (ng/mL) of ATV-lactone; F- Tissue concentration (ng/mL) of ATV; G- Tissue concentration (ng/mL) of ATV-lactone; H- Plasma concentration (ng/mL) of ATV; I- Plasma concentration (ng/mL) of ATV-lactone; J- Ratio Tissue concentration/plasma concentration of ATV; K- Ratio Tissue concentration/plasma concentration of ATV-lactone;

(*) and red, means the peak area of the internal standard is low, as showed in figure 34.

MRM´S of the three samples are showed below.

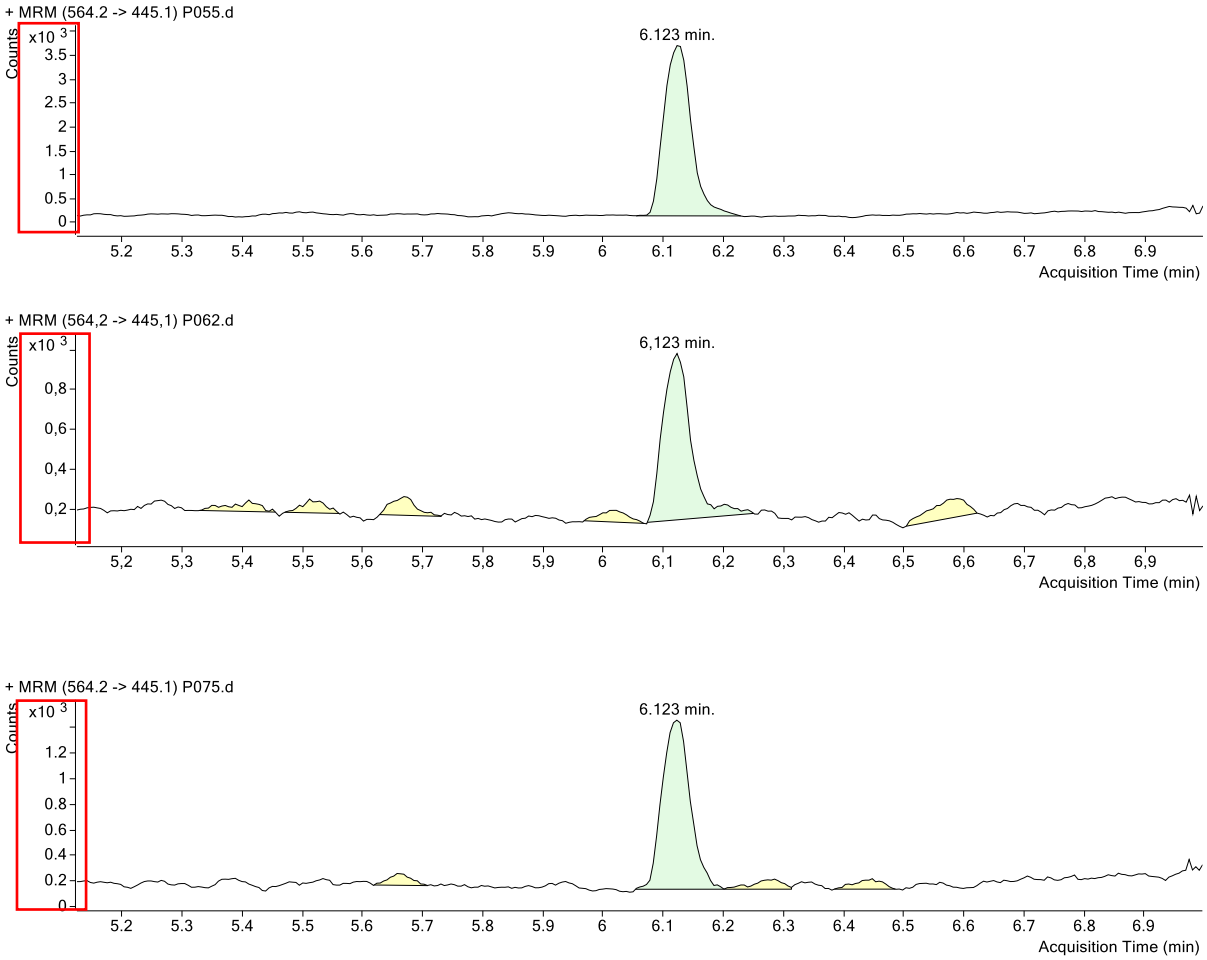

Figure 34: MRM chromatogram of IS in the samples E111, E126 and E165

In the tissue, ATV concentration is found with more difficulty, being zero in some samples. Otherwise, ATV-lactone concentration is easier to detect and therefore with better results. The concentration of both (ATV and ATV-Lactone) seems to be in some cases/samples greater in tissue than in blood, with a huge difference.

6. Conclusion

It was reported in several studies that atorvastatin inhibited cancer growth and induced cancer cell death, decreasing endogenous levels of cholesterol that may aid the prevention of heart disease and atherosclerosis, conditions which potentially lead to heart attack, stroke and/or vascular diseases.

The proposed validated bioanalytical technique accomplishes the required selectivity, sensitivity, accuracy to be applied to studies involving pharmacokinetics, drug metabolism, clinical pharmacology and bioavailability for accurate quantitative analysis of ATV and its metabolite (ATV-lactone) in prostate tissue.

The major advantages of the present method, as compared with previous reports are 100 μL plasma volume, dilution integrity up to fold of the homogenate with 90% of NaCl.

The ability to mix and change isocratic mobile phase composition in-line gives the user flexibility to quickly optimize the separation and obtain the required resolution for analytes of interest. The use of in-line mixing also enables the use of gradient elution methods – giving rise the advantages already established.

Our main conclusion is that ATV levels in tissue can be higher than in plasma. However further studies are still required to investigate the relation between ATV and prostate cancer and the processes how this drug can reach the tissue (prostate).

7. Bibliography

1. Sc G, Rb N, Mb H, At W, Pv M. Incidence of prostate cancer at a single tertiary care center in North Karnataka.
2. Lee CH, Akin-Olugbade O, Kirschenbaum A. Overview of Prostate Anatomy, Histology, and Pathology. Endocrinol Metab Clin North Am. 2011;40(3):565–75.
3. Murtola TJ, Visakorpi T, Lahtela J, Syvälä H, Tammela TL. Statins and prostate cancer prevention: where we are now, and future directions.
4. Sakr WA, Haas GP, Cassin BF, Pontes JE, Crissman JD. The Frequency of Carcinoma and Intraepithelial Neoplasia of the Prostate in Young Male Patients. J Urol. 1993;
5. Ferlay J, Shin HR, Bray F, Forman D, Mathers C, Parkin DM. Estimates of worldwide burden of cancer in 2008: GLOBOCAN 2008. Int J Cancer. 2010;127(12):2893–917.
6. Cózar JM, Miñana B, Gómez-Veiga F, Rodríguez-Antolín A, Villavicencio H, Cantalapiedra A, et al. Prostate cancer incidence and newly diagnosed patient profile in Spain in 2010. BJU Int. 2012;110(11 B):1–6.
7. Curran MP. Amlodipine atorvastatin: A Review of its use in the treatment of hypertension and dyslipidaemia and the prevention of cardiovascular disease. Drugs. 2010.
8. Lennernäs H. Clinical Pharmacokinetics of Atorvastatin. Clin Pharmacokinet. 2003;42(13):1141–60.
9. Nováková L, Šatínský D, Solich P. HPLC methods for the determination of simvastatin and atorvastatin. TrAC - Trends Anal Chem. 2008;
10. Jirásko R, Mikysek T, Chagovets V, Vokřál I, Holčapek M. Structural characterization of electrochemically and in vitro biologically generated oxidation products of atorvastatin using UHPLC/MS/MS ABC Highlights: Authored by Rising Stars and Top Experts. Anal Bioanal Chem. 2013;
11. Ishigami M, Honda T, Takasaki W, Ikeda T, Komai T, Ito K, et al. A comparison of the effects of 3-hydroxy-3-methylglutaryl-coenzyme a (HMG-CoA) reductase inhibitors on the CYP3A4-dependent oxidation of mexazolam in vitro. Drug Metab Dispos. 2001;29(3):282–8.
12. Lennernas H, Fager G. Pharmacodynamics and pharmacokinetics of the HMG-CoA reductase inhibitors. Similarities and differences. Clin Pharmacokinet. 1997;32(0312–5963 (Print)):403–25.
13. Stern RH, Yang BB, Hounslow NJ, MacMahon M, Abel RB, Olson SC. Pharmacodynamics and pharmacokinetic-pharmacodynamic relationships of atorvastatin, an HMG-CoA reductase inhibitor. J Clin Pharmacol. 2000;40(6):616–23.
14. Al-Jenoobi FI. Effect of itraconazole on the pharmacokinetics of diclofenac in beagle dogs. Sci Pharm. 2010;78(3):465–71.
15. Benet LZ, Cummins CL. The drug efflux-metabolism alliance: Biochemical aspects. Adv Drug Deliv Rev. 2001;50(SUPPL. 1):3–11.
16. Lennernäs H. Human jejunal effective permeability and its correlation with preclinical drug absorption models. J Pharm Pharmacol. 1997;49(7):627–38.
17. Winiwarter S, Bonham NM, Ax F, Hallberg A, Lennernäs H, Karlén A. Correlation of human jejunal permeability (in vivo) of drugs with experimentally and theoretically derived

parameters. A multivariate data analysis approach. J Med Chem. 1998;41(25):4939–49.

18. Black ANNE, Hayes RN, Roth BD, Woo P, Woolf TF, Pharmacokinetics D, et al. Metabolism and Excretion of Atorvastatin in Rats and Dogs Abstract : Pharmacology. 1999;27(8):916–23.

19. Lilja JJ, Kivisto KT, Neuvonen PJ. Grapefruit juice increases serum concentrations of atorvastatin and has no effect on pravastatin. Clin Pharmacol Ther. 1999;66(2):118–27.

20. Black AE, Sinz MW, Hayes RN, Woolf TF. METABOLISM AND EXCRETION STUDIES IN MOUSE AFTER SINGLE AND MULTIPLE ORAL DOSES OF THE 3-HYDROXY-3-METHYLGLUTARYL-COA REDUCTASE INHIBITOR ATORVASTATIN. Available from: http://www.dmd.org

21. Radulovic LL, Cilla DD, Posvar EL, Sedman AJ, Whitfield LR. Effect of Food on the Bioavailability of Atorvastatin, an HMG-CoA Reductase Inhibitor. J Clin Pharmacol. 1995;35(10):990–4.

22. Nordström T, Clements M, Karlsson R, Adolfsson J, Grönberg H. The risk of prostate cancer for men on aspirin, statin or antidiabetic medications. Eur J Cancer. 2015;51(6):725–33.

23. Wierzbicki AS, Poston R, Ferro A. The lipid and non-lipid effects of statins16. Pharmacol Ther. 2003;99(1):95–112.

24. Vivanco I, Sawyers CL. The phosphatidylinositol 3-Kinase–AKT pathway in human cancer. Nat Rev Cancer [Internet]. 2002;2(7):489–501. Available from: http://www.nature.com/doifinder/10.1038/nrc839

25. Zheng X, Cui XX, Gao Z, Zhao Y, Lin Y, Shih WJ, et al. Atorvastatin and celecoxib in combination inhibits the progression of androgen-dependent LNCaP xenograft prostate tumors to androgen independence. Cancer Prev Res. 2010;3(1):114–24.

26. Zheng X, Cui XX, Avila GE, Huang MT, Liu Y, Patel J, et al. Atorvastatin and celecoxib inhibit prostate PC-3 tumors in immunodeficient mice. Clin Cancer Res. 2007;13(18):5480–7.

27. Lu J, Monardo L, Bryskin I, Hou Z, Trachtenberg J, Wilson B, et al. Androgens induce oxidative stress and radiation resistance in prostate cancer cells though NADPH oxidase. Prostate Cancer Prostatic Dis. 2009;13:39–46.

28. Stein DG, Halks-Miller M, Hoffman SW. Intracerebral Administration of Alpha-Tocopherol-Containing Liposomes Facilitates Behavioral Recovery in Rats with Bilateral Lesions of the Frontal Cortex. J Neurotrauma. 1991;8(4):281–92.

29. HE ZJYPQZW. Effects of Atorvastatin and Docetaxel. 2015;

30. Montero A, Fossella F, Hortobagyi G, Valero V. Docetaxel for treatment of solid tumours: a systematic review of clinical data. Lancet Oncol [Internet]. 2005;6(4):229–39. Available from: http://www.sciencedirect.com/science/article/pii/S1470204505700942

31. Sassano A, Platanias LC. Statins in tumor suppression. Cancer Lett. 2008;260(1–2):11–9.

32. Parikh A, Childress C, Deitrick K, Lin Q, Rukstalis D, Yang W. Statin-induced autophagy by inhibition of geranylgeranyl biosynthesis in prostate cancer PC3 cells. Prostate. 2010;70(9):971–81.

33. He Z, Yuan J, Qi P, Zhang L, Wang Z. Atorvastatin induces autophagic cell death in prostate cancer cells in vitro. Mol Med Rep [Internet]. 2015;11(6):4403–8. Available from: http://www.ncbi.nlm.nih.gov/pubmed/25672364

34. MacWan JS, Ionita IA, Dostalek M, Akhlaghi F. Development and validation of a sensitive, simple, and rapid method for simultaneous quantitation of atorvastatin and its acid and lactone

metabolites by liquid chromatography-tandem mass spectrometry (LC-MS/MS). Anal Bioanal Chem. 2011;400(2):423–33.

35. Nirogi RVS, Kandikere VN, Shukla M, Mudigonda K, Maurya S, Boosi R, et al. Simultaneous quantification of atorvastatin and active metabolites in human plasma by liquid chromatography-tandem mass spectrometry using rosuvastatin as internal standard. Biomed Chromatogr. 2006;20(9):924–36.

36. Jirásko R, Holčapek M, Kuneš M, Svatoš A. Distribution study of atorvastatin and its metabolites in rat tissues using combined information from UHPLC/MS and MALDI-Orbitrap-MS imaging. Anal Bioanal Chem. 2014;

37. Vogeser M, Parhofer KG. Liquid chromatography tandem-mass spectrometry (LC-MS/MS) - Technique and applications in endocrinology. Exp Clin Endocrinol Diabetes. 2007;115(9):559–70.

38. Matuszewski BK, Constanzer ML, Chavez-Eng CM. Strategies for the assessment of matrix effect in quantitative bioanalytical methods based on HPLC-MS/MS. Anal Chem. 2003;75(13):3019–30.

39. Vogeser M. Liquid chromatography-tandem mass spectrometry - Application in the clinical laboratory. 2003;41(2):117–26. Available from: http://apps.isiknowledge.com/full_record.do?product=UA&search_mode=Refine&qid=88&SID=Y2t3PWxndO4r1XoDPpG&page=1&doc=41

40. Majumdar TK. Chapter 3 Commonly encountered analytical problems and Their Solutions in Liquid Chromatography / Used in Drug Development. 2005;

8. Appendix

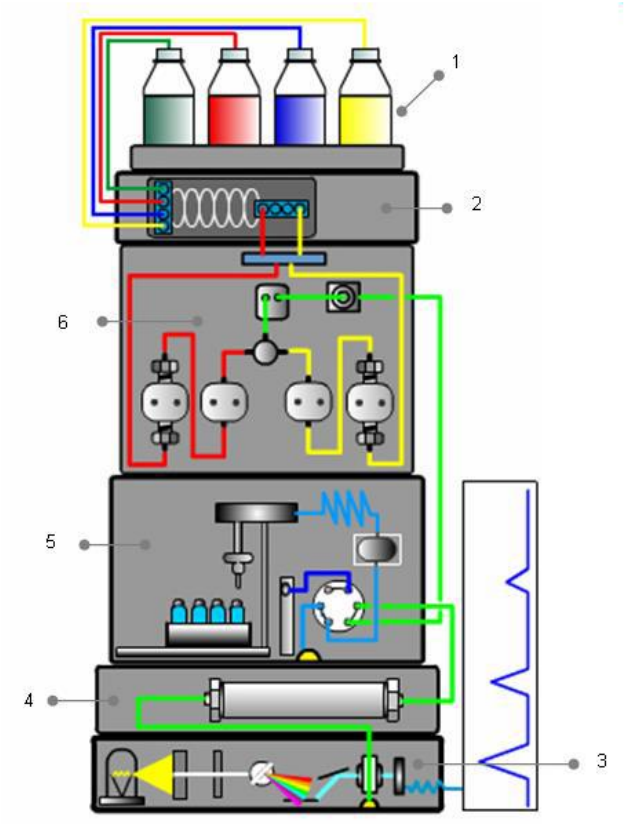

Figure 1- HPLC scheme

1: The mobile phase composition (usually water and an organic solvent plus other additives) needs to be optimized in order to gain good separation.

2: Degassers are often used to remove air from the mobile phase, leading to better chromatographic baselines.

3: The detector conditions are chosen to give the best response to the analytes of interest and to achieve good sensitivity.

4: The column dimensions and stationary phase chemistry are chosen and optimized to give separations of the quality required.

5: The autosampler introduces a plug of sample into the mobile phase flow which is then swept onto the column.

6: Dual reciprocating pumps are used to deliver the mobile phase at back pressures of up to 400 bar. A steady stream of liquid delivered at a constant flow rate is important.

Types of compounds	Mode	Stationary phase	Mobile phase
Neutrals Weak acids Weak bases	Reversed phase	C18, C8, C4, cyano, amino	Water/Organic Modifiers
Ionics, Bases, Acids	Ion Pair	C18, C8	Water/Organic Ion-Pair reagent
Compounds not soluble in water	Normal Phase	Silica, Amino, Cyano, Diol	Organics
Ionics/Inorganic ions	Ion Exchange	Anion or Cation Exchange Resin	Aqueous/Buffer Counter Ion

High Molecular Weight Compounds, Polymers	Size Exclusion	Polystyrene Silica	Gel Filtration – Aqueous Gel Permeation – Organic

Figure 2. The Main Modes of Liquid Chromatography

For ATV:
Average of peak area of methanol: 5000.8 (Set A)

Average of peak area of plasma: 4736.4 (Set B_1)

Average of peak area of tissue: 3693.5 (Set B_2)

Average of peak area of 1.25 ng/mL: 3856.7 (Set C)

Overall recovery $= \frac{3856.7}{5000.8}$ x 100 = 77.1%

Extraction yield $= \frac{3856.7}{4736.4}$ x 100 = 81.4%

Matrix effect for plasma$= \frac{4736.4}{5000.8}$ x 100 = 94.71%

Matrix effect for tissue$= \frac{3693.5}{5000.8}$ x 100 = 73.86%

For ATV-Lactone:
Average of peak area of methanol: 8604.4 (Set A)

Average of peak area of plasma: 6931.9 (Set B_1)

Average of peak area of tissue: 6443.9 (Set B_2)

Average of peak area of 1.25 ng/mL: 7034.1 (Set C)

Overall recovery $= \frac{7034.1}{8604.4}$ x 100 = 81.8%

Extraction yield $= \frac{7034.1}{6931.9}$ x 100 = 101.5%

Matrix effect for plasma$= \frac{6931.9}{8604.4}$ x 100 = 80.6%

Matrix effect for tissue$= \frac{6443.9}{8604.4}$ x 100 = 74.9%

For ATV-OH:
Average of peak area of methanol: 1042 (Set A)

Average of peak area of plasma: 1024.2 (Set B_1)

Average of peak area of tissue: 743.2 (Set B_2)

Average of peak area of 1.25 ng/mL: 777.9 (Set C)

Overall recovery $= \frac{777.9}{1042}$ x 100 = 74.7%

Extraction yield $= \frac{777.9}{1024.2}$ x 100 = 76%

Matrix effect for plasma= $\frac{1024.2}{1042}$ x 100 = 98.3%

Matrix effect for tissue= $\frac{743.2}{1042}$ x 100 = 71.3%

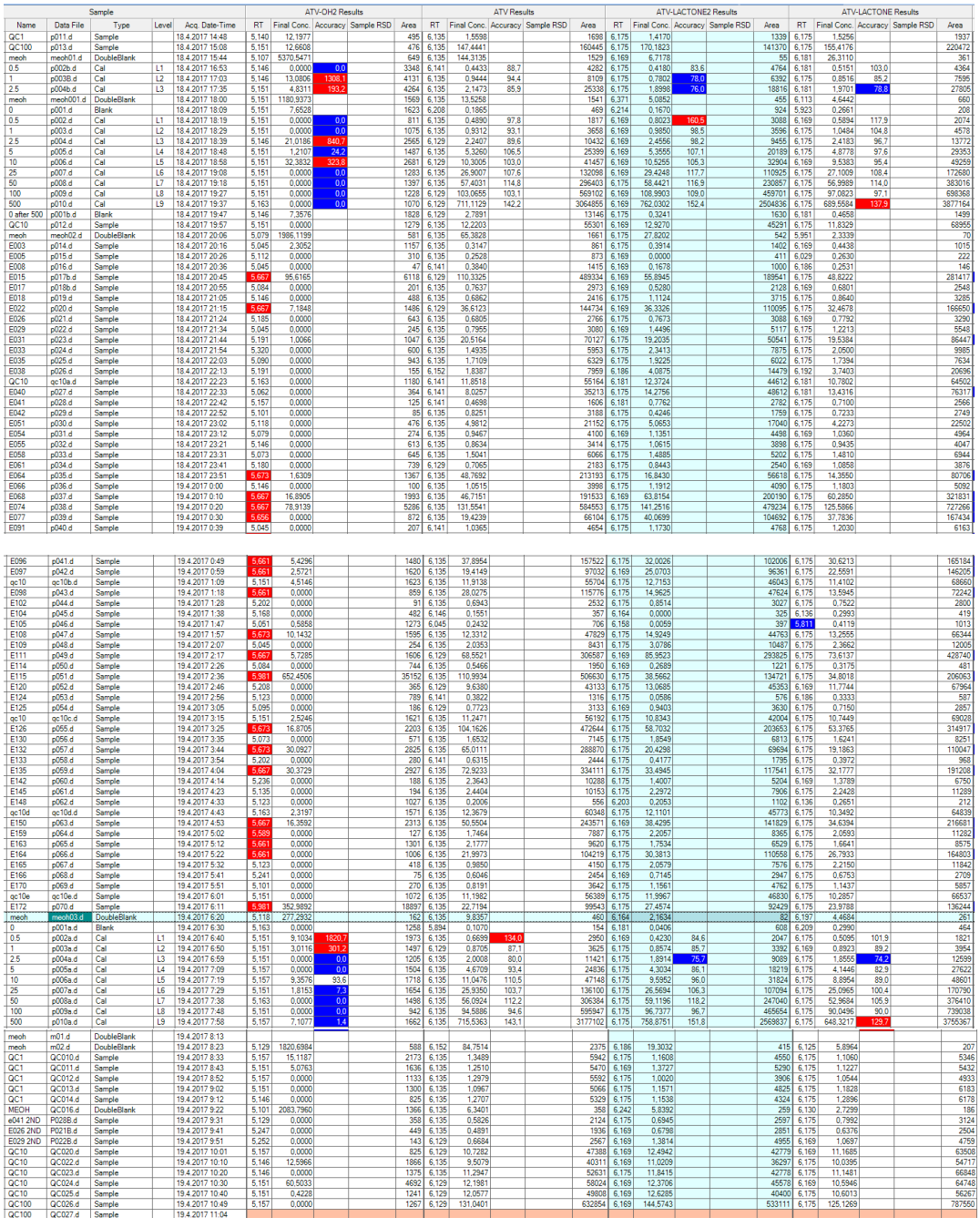

Sample					ATV-OH2 Results					ATV Results					ATV-LACTONE2 Results					ATV-LACTONE Results				
Name	Data File	Type	Level	Acq. Date-Time	RT	Final Conc.	Accuracy	Sample RSD	Area	RT	Final Conc.	Accuracy	Sample RSD	Area	RT	Final Conc.	Accuracy	Sample RSD	Area	RT	Final Conc.	Accuracy	Sample RSD	Area
QC1	p011.d	Sample		18.4.2017 14:48	5,140	12,1977			495	6,135	1,5598			1698	6,175	1,4170			1339	6,175	1,5256			1937
QC100	p013.d	Sample		18.4.2017 15:08	5,151	12,6608			476	6,135	147,4441			160445	6,175	170,1823			141370	6,175	155,4176			220472
meoh	meoh01.d	DoubleBlank		18.4.2017 15:44	5,107	5370,5471			649	6,135	144,3135			1529	6,169	6,7178			55	6,181	26,3110			361
0.5	p002b.d	Cal	L1	18.4.2017 16:53	5,146	0,0000	0,0		3348	6,141	0,4433	88,7		4282	6,175	0,4180	83,6		4764	6,181	0,5151	103,0		4364
1	p003B.d	Cal	L2	18.4.2017 17:03	5,146	13,0806	1308,1		4131	6,135	0,9444	94,4		8109	6,175	0,7802	78,0		6392	6,175	0,8516	85,2		7595
2,5	p004b.d	Cal	L3	18.4.2017 17:35	5,151	4,8311	193,2		4264	6,135	2,1473	85,9		25338	6,175	1,8998	76,0		18816	6,181	1,9701	78,8		27805
meoh	meoh001.d	DoubleBlank		18.4.2017 18:00	5,151	1180,9373			1569	6,135	13,5258			1541	6,371	5,0852			455	6,113	4,6442			660
0	p001.d	Blank		18.4.2017 18:09	5,151	7,6528			1623	6,208	0,1865			469	6,214	0,1670			924	5,923	0,2661			208
0.5	p002.d	Cal	L1	18.4.2017 18:19	5,151	0,0000	0,0		811	6,135	0,4890	97,8		1817	6,169	0,8023	160,5		3088	6,169	0,5894	117,9		2074
1	p003.d	Cal	L2	18.4.2017 18:29	5,151	0,0000	0,0		1075	6,135	0,9312	93,1		3658	6,169	0,9850	98,5		3596	6,175	1,0484	104,8		4578
2,5	p004.d	Cal	L3	18.4.2017 18:39	5,146	21,0186	840,7		2565	6,129	2,2407	89,6		10432	6,169	2,4556	98,2		9455	6,175	2,4183	96,7		13772
5	p005.d	Cal	L4	18.4.2017 18:48	5,151	1,2107	24,2		1487	6,135	5,3260	106,5		25399	6,169	5,3555	107,1		20189	6,175	4,8778	97,6		29353
10	p006.d	Cal	L5	18.4.2017 18:58	5,151	32,3832	323,8		2681	6,129	10,3005	103,0		41457	6,169	10,5255	105,3		32904	6,169	9,5383	95,4		49259
25	p007.d	Cal	L6	18.4.2017 19:08	5,151	0,0000	0,0		1283	6,135	26,9007	107,6		132098	6,169	29,4248	117,7		110925	6,175	27,1009	108,4		172680
50	p008.d	Cal	L7	18.4.2017 19:18	5,151	0,0000	0,0		1397	6,135	57,4031	114,8		296403	6,175	58,4421	116,9		230857	6,175	56,9989	114,0		383016
100	p009.d	Cal	L8	18.4.2017 19:27	5,151	0,0000	0,0		1228	6,129	103,0655	103,1		569102	6,169	108,9903	109,0		459701	6,175	97,0823	97,1		698368
500	p010.d	Cal	L9	18.4.2017 19:37	5,163	0,0000	0,0		1070	6,129	711,1129	142,2		3064855	6,169	762,0302	152,4		2504836	6,175	689,5584	137,9		3877164
0 after 500	p001b.d	Blank		18.4.2017 19:47	5,146	7,3576			1828	6,129	2,7891			13146	6,175	0,3241			1630	6,181	0,4658			1499
QC10	p012.d	Sample		18.4.2017 19:57	5,151	0,0000			1279	6,135	12,2203			55301	6,169	12,9270			45291	6,175	11,8329			68955
meoh	meoh02.d	DoubleBlank		18.4.2017 20:06	5,079	1986,1199			581	6,135	65,3828			1661	6,175	27,8202			542	5,951	2,3339			70
E003	p014.d	Sample		18.4.2017 20:16	5,045	2,3052			1157	6,135	0,3147			861	6,175	0,3914			1402	6,169	0,4438			1015
E005	p015.d	Sample		18.4.2017 20:26	5,112	0,0000			310	6,135	0,2528			873	6,169	0,0000			411	6,029	0,2630			222
E008	p016.d	Sample		18.4.2017 20:36	5,045	0,0000			47	6,141	0,3840			1415	6,169	0,1678			1000	6,186	0,2531			146
E015	p017b.d	Sample		18.4.2017 20:45	5,667	95,6165			6118	6,129	110,3325			489334	6,169	55,8945			189541	6,175	48,8222			281417
E017	p018b.d	Sample		18.4.2017 20:55	5,084	0,0000			201	6,135	0,7637			2973	6,169	0,5280			2128	6,169	0,6801			2548
E018	p019.d	Sample		18.4.2017 21:05	5,146	0,0000			488	6,135	0,6862			2416	6,175	1,1124			3715	6,175	0,8640			3285
E022	p020.d	Sample		18.4.2017 21:15	5,667	7,1848			1486	6,129	36,6123			144734	6,169	36,3326			110095	6,175	32,4578			166650
E026	p021.d	Sample		18.4.2017 21:24	5,185	0,0000			643	6,135	0,6805			2766	6,175	0,7673			3088	6,169	0,7792			3290
E029	p022.d	Sample		18.4.2017 21:34	5,045	0,0000			245	6,135	0,7955			3080	6,169	1,4496			5117	6,175	1,2213			5548
E031	p023.d	Sample		18.4.2017 21:44	5,191	1,0066			1047	6,135	20,5164			70127	6,175	19,2035			50541	6,175	19,5384			86447
E033	p024.d	Sample		18.4.2017 21:54	5,320	0,0000			600	6,135	1,4935			5953	6,175	2,3413			7875	6,175	2,0500			9985
E035	p025.d	Sample		18.4.2017 22:03	5,090	0,0000			943	6,135	1,7109			6329	6,175	1,9225			6022	6,175	1,7394			7634
E038	p026.d	Sample		18.4.2017 22:13	5,191	0,0000			155	6,152	1,8387			7959	6,186	4,0875			14479	6,192	3,7403			20696
QC10	qc10a.d	Sample		18.4.2017 22:23	5,163	0,0000			1180	6,141	11,8518			55164	6,181	12,3724			44612	6,181	10,7802			64502
E040	p027.d	Sample		18.4.2017 22:33	5,062	0,0000			364	6,141	8,0257			35213	6,175	14,2756			48612	6,181	13,4316			76317
E041	p028.d	Sample		18.4.2017 22:42	5,157	0,0000			125	6,141	0,4698			1606	6,181	0,7762			2782	6,175	0,7100			2566
E042	p029.d	Sample		18.4.2017 22:52	5,101	0,0000			85	6,135	0,8251			3188	6,175	0,4246			1759	6,175	0,7233			2749
E051	p030.d	Sample		18.4.2017 23:02	5,118	0,0000			476	6,135	4,9812			21152	6,175	5,0653			17040	6,175	4,2273			22502
E054	p031.d	Sample		18.4.2017 23:12	5,079	0,0000			274	6,135	0,9467			4100	6,169	1,1351			4498	6,169	1,0360			4964
E055	p032.d	Sample		18.4.2017 23:21	5,146	0,0000			613	6,135	0,8634			3414	6,175	1,0615			3898	6,175	0,9435			4047
E058	p033.d	Sample		18.4.2017 23:31	5,073	0,0000			645	6,135	1,5041			6066	6,175	1,4885			5202	6,175	1,4810			6944
E061	p034.d	Sample		18.4.2017 23:41	5,180	0,0000			739	6,129	0,7065			2183	6,175	0,8443			2540	6,169	1,0858			3876
E064	p035.d	Sample		18.4.2017 23:51	5,673	1,6309			1367	6,135	48,7692			213193	6,175	16,8430			56618	6,175	14,3550			80706
E066	p036.d	Sample		19.4.2017 0:00	5,146	0,0000			100	6,135	1,0515			3998	6,175	1,1912			4090	6,175	1,1803			5092
E068	p037.d	Sample		19.4.2017 0:10	5,667	16,8905			1993	6,135	46,7151			191533	6,169	63,8154			200190	6,175	60,2850			321831
E074	p038.d	Sample		19.4.2017 0:20	5,667	78,9139			5286	6,135	131,5541			584553	6,175	141,2516			479234	6,175	125,5866			727266
E077	p039.d	Sample		19.4.2017 0:30	5,656	0,0000			872	6,135	19,4239			66104	6,175	40,0699			104692	6,175	37,7836			167434
E091	p040.d	Sample		19.4.2017 0:39	5,045	0,0000			207	6,141	1,0365			4654	6,175	1,1730			4768	6,175	1,2030			6163
E096	p041.d	Sample		19.4.2017 0:49	5,661	5,4296			1480	6,135	37,8954			157522	6,175	32,0026			102006	6,175	30,6213			165184
E097	p042.d	Sample		19.4.2017 0:59	5,661	2,5721			1620	6,135	19,4149			97032	6,169	25,0703			96361	6,175	22,5591			146205
qc10	qc10b.d	Sample		19.4.2017 1:09	5,151	4,5146			1623	6,135	11,9138			55704	6,175	12,7153			46043	6,175	11,4102			68660
E098	p043.d	Sample		19.4.2017 1:18	5,661	0,0000			859	6,135	28,0275			115776	6,175	14,9625			47624	6,175	13,5945			72242
E102	p044.d	Sample		19.4.2017 1:28	5,202	0,0000			91	6,135	0,6943			2532	6,175	0,8514			3027	6,175	0,7522			2800
E104	p045.d	Sample		19.4.2017 1:38	5,168	0,0000			482	6,146	0,1551			357	6,164	0,0000			325	6,136	0,2993			419
E105	p046.d	Sample		19.4.2017 1:47	5,051	0,5858			1273	6,045	0,2432			706	6,158	0,0059			397	6,811	0,4119			1013
E108	p047.d	Sample		19.4.2017 1:57	5,673	10,1432			1595	6,135	12,3312			47829	6,175	14,3249			44763	6,175	13,2555			66344
E109	p048.d	Sample		19.4.2017 2:07	5,045	0,0000			254	6,135	2,0353			8431	6,175	3,0786			10487	6,175	2,3662			12005
E111	p049.d	Sample		19.4.2017 2:17	5,667	5,7285			1606	6,129	68,5521			306587	6,169	85,9523			293825	6,175	73,6137			428740
E114	p050.d	Sample		19.4.2017 2:26	5,084	0,0000			744	6,135	0,5466			1950	6,169	0,2689			1221	6,175	0,3175			481
E115	p051.d	Sample		19.4.2017 2:36	5,381	652,4506			35152	6,135	110,9934			506630	6,175	38,5662			134721	6,175	34,8018			206063
E120	p052.d	Sample		19.4.2017 2:46	5,208	0,0000			365	6,129	9,6380			43133	6,175	13,0685			45363	6,169	11,7744			67964
E124	p053.d	Sample		19.4.2017 2:56	5,123	0,0000			789	6,141	0,3822			1316	6,175	0,0586			576	6,186	0,3333			587
E125	p054.d	Sample		19.4.2017 3:05	5,095	0,0000			186	6,129	0,7723			3133	6,169	0,9403			3630	6,175	0,7150			2857
qc10	qc10c.d	Sample		19.4.2017 3:15	5,151	2,5246			1621	6,135	11,2471			56192	6,175	10,8343			42004	6,175	10,7449			69028
E126	p055.d	Sample		19.4.2017 3:25	5,673	16,8705			2203	6,135	104,1626			472644	6,175	58,7032			203653	6,175	53,3765			314917
E130	p056.d	Sample		19.4.2017 3:35	5,073	0,0000			571	6,135	1,6532			7145	6,175	1,8549			6813	6,175	1,6241			8251
E132	p057.d	Sample		19.4.2017 3:44	5,673	30,0927			2825	6,135	65,0111			288870	6,175	20,4298			69694	6,175	19,1863			110047
E133	p058.d	Sample		19.4.2017 3:54	5,202	0,0000			280	6,141	0,6315			2444	6,175	0,4177			1795	6,175	0,3972			968
E135	p059.d	Sample		19.4.2017 4:04	5,667	30,3729			2927	6,135	72,9233			334111	6,175	33,4945			117541	6,175	32,1777			191208
E142	p060.d	Sample		19.4.2017 4:14	5,236	0,0000			188	6,135	2,3643			10288	6,175	1,4007			5204	6,169	1,3789			6750
E145	p061.d	Sample		19.4.2017 4:23	5,135	0,0000			194	6,135	2,4404			10153	6,175	2,2972			7906	6,175	2,2428			11289
E148	p062.d	Sample		19.4.2017 4:33	5,123	0,0000			1027	6,135	0,2006			556	6,203	0,2053			1102	6,136	0,2651			212
qc10d	qc10d.d	Sample		19.4.2017 4:43	5,163	2,3197			1571	6,135	12,3679			60348	6,175	12,1101			45773	6,175	10,3492			64839
E150	p063.d	Sample		19.4.2017 4:53	5,667	16,3592			2313	6,135	50,5504			243571	6,169	38,4295			141829	6,175	34,6394			216681
E159	p064.d	Sample		19.4.2017 5:02	5,589	0,0000			127	6,135	1,7464			7887	6,175	2,2057			8365	6,175	2,0593			11282
E163	p065.d	Sample		19.4.2017 5:12	5,661	0,0000			1301	6,135	2,1777			9620	6,175	1,7534			6529	6,175	1,6641			8575
E164	p066.d	Sample		19.4.2017 5:22	5,651	0,0000			1006	6,135	21,9973			104219	6,175	30,3813			110558	6,175	26,7933			164803
E165	p067.d	Sample		19.4.2017 5:32	5,123	0,0000			418	6,135	0,9850			4150	6,175	2,0579			7576	6,175	2,2150			11842
E166	p068.d	Sample		19.4.2017 5:41	5,241	0,0000			75	6,135	0,6046			2454	6,169	0,7145			2947	6,175	0,6753			2709
E170	p069.d	Sample		19.4.2017 5:51	5,101	0,0000			270	6,135	0,8191			3642	6,175	1,1561			4762	6,175	1,1437			5857
qc10e	qc10e.d	Sample		19.4.2017 6:01	5,151	0,0000			1072	6,135	11,1982			56389	6,175	11,9967			46830	6,175	10,2857			66537
E172	p070.d	Sample		19.4.2017 6:11	5,381	352,9892			18897	6,135	22,7194			99543	6,175	27,4574			92429	6,175	23,9788			136244
meoh	meoh03.d	DoubleBlank		19.4.2017 6:20	5,118	277,2932			162	6,135	9,8357			460	6,164	2,1634			88	6,197	4,4684			261
0	p001a.d	Blank		19.4.2017 6:30	5,163	0,0000			1258	5,894	0,1070			154	6,181	0,0406			608	6,209	0,2990			464
0.5	p002a.d	Cal	L1	19.4.2017 6:40	5,151	9,1034	1820,7		1973	6,135	0,6699	134,0		2950	6,169	0,4230	84,6		2047	6,175	0,5095	101,9		1821
1	p003a.d	Cal	L2	19.4.2017 6:50	5,151	3,0116	301,2		1497	6,129	0,8705	87,1		3625	6,175	0,8574	85,7		3392	6,169	0,8923	89,2		3954
2,5	p004a.d	Cal	L3	19.4.2017 6:59	5,151	0,0000	0,0		1205	6,135	2,0008	80,0		11421	6,175	1,8914	75,7		9089	6,175	1,8555	74,2		12599
5	p005a.d	Cal	L4	19.4.2017 7:09	5,157	0,0000	0,0		1504	6,135	4,6709	93,4		24836	6,175	4,3034	86,1		18219	6,175	4,1446	82,9		27622
10	p006a.d	Cal	L5	19.4.2017 7:19	5,157	9,3576	93,6		1718	6,135	11,0476	110,5		47148	6,175	9,5952	96,0		31824	6,175	8,8954	89,0		48601
25	p007a.d	Cal	L6	19.4.2017 7:29	5,151	1,8153	7,3		1654	6,135	25,9350	103,7		136100	6,175	26,5694	106,3		107094	6,175	25,0965	100,4		170790
50	p008a.d	Cal	L7	19.4.2017 7:38	5,163	0,0000	0,0		1498	6,135	56,0924	112,2		306384	6,175	59,1196	118,2		247040	6,175	52,9684	105,9		376410
100	p009a.d	Cal	L8	19.4.2017 7:48	5,151	0,0000	0,0		942	6,135	94,5886	94,6		595947	6,175	96,7377	96,7		465654	6,175	90,0496	90,0		739038
500	p010a.d	Cal	L9	19.4.2017 7:58	5,157	7,1077	1,4		1662	6,135	715,5363	143,1		3177102	6,175	758,8751	151,8		2569837	6,175	648,3217	129,7		3755367
meoh	m01.d	DoubleBlank		19.4.2017 8:13																				
meoh	m02.d	DoubleBlank		19.4.2017 8:23	5,129	1820,6984			588	6,152	84,7514			2375	6,186	19,3032			415	6,125	5,8964			207
QC1	QC010.d	Sample		19.4.2017 8:33	5,157	15,1187			2173	6,135	1,3489			5942	6,175	1,1608			4550	6,175	1,1060			5346
QC1	QC011.d	Sample		19.4.2017 8:43	5,151	5,0763			1636	6,135	1,2510			5470	6,169	1,3727			5290	6,175	1,1227			5432
QC1	QC012.d	Sample		19.4.2017 8:52	5,157	0,0000			1133	6,135	1,2979			5592	6,175	1,0020			3906	6,175	1,0544			4933
QC1	QC013.d	Sample		19.4.2017 9:02	5,151	0,0000			1300	6,135	1,0967			5066	6,175	1,1571			4825	6,175	1,1828			6183
QC1	QC014.d	Sample		19.4.2017 9:12	5,146	0,0000			825	6,135	1,2707			5329	6,175	1,1538			4324	6,175	1,2896			6178
MEOH	QC016.d	DoubleBlank		19.4.2017 9:22	5,101	2083,7960			1366	6,135	6,3401			358	6,242	5,8392			259	6,130	2,7299			186
e041 2ND	P028B.d	Sample		19.4.2017 9:31	5,129	0,0000			358	6,135	0,5826			2124	6,175	0,6945			2597	6,175	0,7982			3124
E026 2ND	P021B.d	Sample		19.4.2017 9:41	5,247	0,0000			449	6,135	0,4891			1936	6,169	0,6798			2851	6,175	0,6376			2504
E029 2ND	P022B.d	Sample		19.4.2017 9:51	5,252	0,0000			143	6,129	0,6684			2567	6,169	1,3814			4955	6,169	1,0697			4759
QC10	QC020.d	Sample		19.4.2017 10:01	5,157	0,0000			825	6,129	10,7282			47388	6,169	12,4942			42779	6,169	11,1685			63508
QC10	QC022.d	Sample		19.4.2017 10:10	5,146	12,5966			1866	6,135	9,5079			40311	6,169	11,0209			36297	6,175	10,0395			54717
QC10	QC023.d	Sample		19.4.2017 10:20	5,146	0,0000			1375	6,135	11,2947			52631	6,175	11,8415			42778	6,175	11,1481			66848
QC10	QC024.d	Sample		19.4.2017 10:30	5,151	60,5033			4692	6,129	12,1981			58024	6,169	12,3706			45578	6,169	10,5946			54748
QC10	QC025.d	Sample		19.4.2017 10:40	5,151	0,4228			1241	6,129	12,0577			49808	6,169	12,6285			40400	6,175	10,6013			56267
QC100	QC026.d	Sample		19.4.2017 10:49	5,157	0,0000			1267	6,129	131,0401			632854	6,169	144,5743			533111	6,175	125,1269			787550
QC100	QC027.d	Sample		19.4.2017 11:04																				

Figure 3. Specific areas of each compound obtained from the Agilent MassHunter Quantitative Analysis (for QQQ) in plasma samples

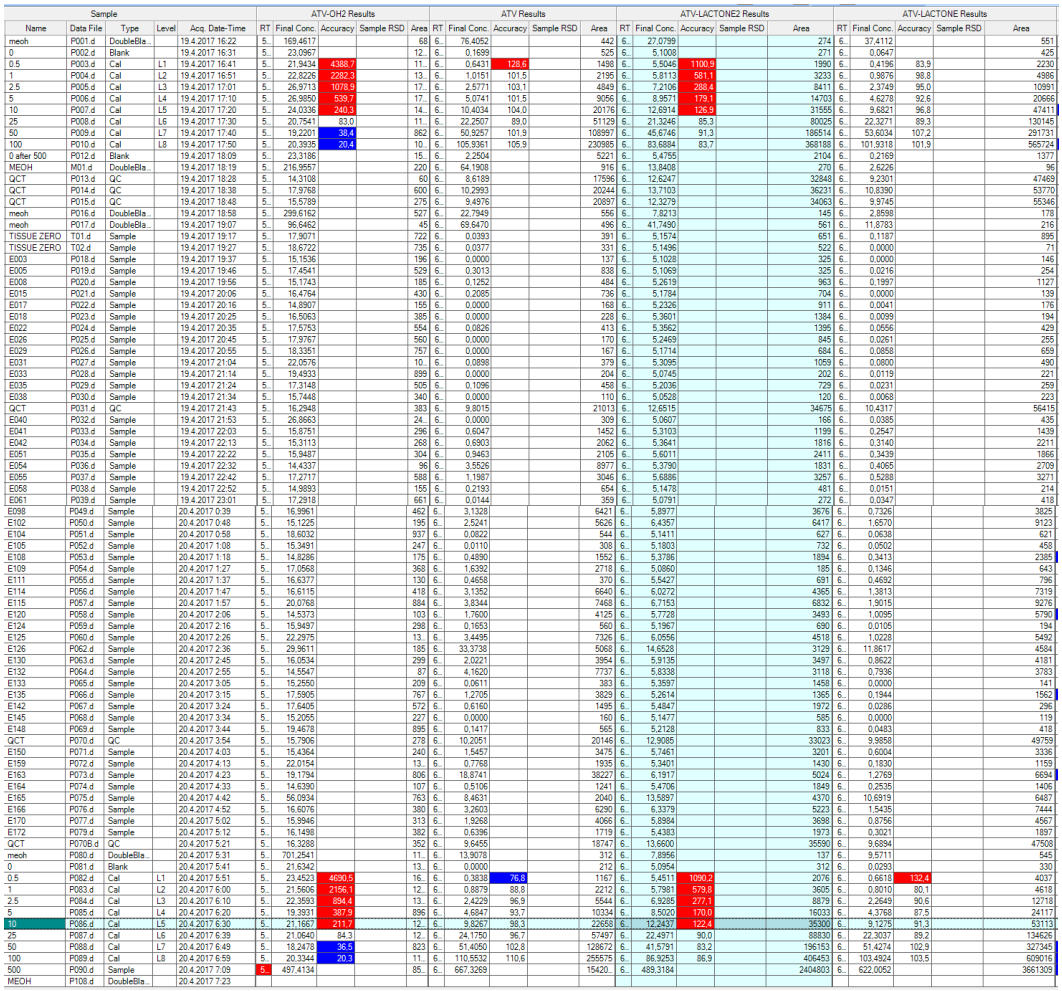

Sample					ATV-OH2 Results					ATV Results					ATV-LACTONE2 Results					ATV-LACTONE Results				
Name	Data File	Type	Level	Acq. Date-Time	RT	Final Conc.	Accuracy	Sample RSD	Area	RT	Final Conc.	Accuracy	Sample RSD	Area	RT	Final Conc.	Accuracy	Sample RSD	Area	RT	Final Conc.	Accuracy	Sample RSD	Area
meoh	P001.d	DoubleBla...		19.4.2017 16:22	5...	169,4617			68	6...	76,4052			442	6...	27,0799			274	6...	37,4112			551
0	P002.d	Blank		19.4.2017 16:31	5...	23,0967			12...	6...	0,1699			525	6...	5,1008			271	6...	0,0647			425
0.5	P003.d	Cal	L1	19.4.2017 16:41	5...	21,9434	4388,7		11...	6...	0,6431	128,6		1498	6...	5,5046	1100,9		1990	6...	0,4196	83,9		2230
1	P004.d	Cal	L2	19.4.2017 16:51	5...	22,8226	2282,3		13...	6...	1,0151	101,5		2195	6...	5,8113	581,1		3233	6...	0,9876	98,8		4986
2.5	P005.d	Cal	L3	19.4.2017 17:01	5...	26,9713	1078,9		17...	6...	2,5771	103,1		4849	6...	7,2106	288,4		8411	6...	2,3749	95,0		10991
5	P006.d	Cal	L4	19.4.2017 17:10	5...	26,9850	539,7		17...	6...	5,0741	101,5		9056	6...	8,9571	179,1		14703	6...	4,6278	92,6		20666
10	P007.d	Cal	L5	19.4.2017 17:20	5...	24,0336	240,3		14...	6...	10,4034	104,0		20176	6...	12,6914	126,9		31555	6...	9,6821	96,8		47411
25	P008.d	Cal	L6	19.4.2017 17:30	5...	20,7541	83,0		11...	6...	22,2507	89,0		51129	6...	21,3246	85,3		80025	6...	22,3271	89,3		130145
50	P009.d	Cal	L7	19.4.2017 17:40	5...	19,2201	38,4		862	6...	50,9257	101,9		108997	6...	45,6746	91,3		186514	6...	53,6034	107,2		291731
100	P010.d	Cal	L8	19.4.2017 17:50	5...	20,3935	20,4		10...	6...	105,9361	105,9		230985	6...	83,6884	83,7		368188	6...	101,9318	101,9		565724
0 after 500	P012.d	Blank		19.4.2017 18:09	5...	23,3186			15...	6...	2,2504			5221	6...	5,4755			2104	6...	0,2169			1377
MEOH	M01.d	DoubleBla...		19.4.2017 18:19	5...	216,9557			220	6...	64,1908			916	6...	13,8408			270	6...	2,6226			96
QCT	P013.d	QC		19.4.2017 18:28	5...	14,3108			60	6...	8,6189			17596	6...	12,6247			32848	6...	9,2301			47469
QCT	P014.d	QC		19.4.2017 18:38	5...	17,9768			600	6...	10,2993			20244	6...	13,7103			36231	6...	10,8390			53770
QCT	P015.d	QC		19.4.2017 18:48	5...	15,5789			275	6...	9,4976			20897	6...	12,3279			34063	6...	9,9745			55346
meoh	P016.d	DoubleBla...		19.4.2017 18:58	5...	299,6162			527	6...	22,7949			556	6...	7,8213			145	6...	2,8598			178
meoh	P017.d	DoubleBla...		19.4.2017 19:07	5...	96,6462			45	6...	69,6470			496	6...	41,7490			561	6...	11,8783			216
TISSUE ZERO	T01.d	Sample		19.4.2017 19:17	5...	17,9071			722	6...	0,0393			391	6...	5,1574			651	6...	0,1187			895
TISSUE ZERO	T02.d	Sample		19.4.2017 19:27	5...	18,6722			735	6...	0,0377			331	6...	5,1496			522	6...	0,0000			71
E003	P018.d	Sample		19.4.2017 19:37	5...	15,1536			196	6...	0,0000			137	6...	5,1028			325	6...	0,0000			146
E005	P019.d	Sample		19.4.2017 19:46	5...	17,4541			529	6...	0,3013			838	6...	5,1069			325	6...	0,0216			254
E008	P020.d	Sample		19.4.2017 19:56	5...	15,1743			185	6...	0,1252			484	6...	5,2619			963	6...	0,1997			1127
E015	P021.d	Sample		19.4.2017 20:06	5...	16,4764			430	6...	0,2085			736	6...	5,1784			704	6...	0,0000			139
E017	P022.d	Sample		19.4.2017 20:16	5...	14,8907			155	6...	0,0000			168	6...	5,2326			911	6...	0,0041			176
E018	P023.d	Sample		19.4.2017 20:25	5...	16,5063			385	6...	0,0000			228	6...	5,3601			1384	6...	0,0099			194
E022	P024.d	Sample		19.4.2017 20:35	5...	17,5753			554	6...	0,0826			413	6...	5,3562			1395	6...	0,0656			429
E026	P025.d	Sample		19.4.2017 20:45	5...	17,9767			560	6...	0,0000			170	6...	5,2469			845	6...	0,0261			255
E029	P026.d	Sample		19.4.2017 20:55	5...	18,3351			757	6...	0,0000			167	6...	5,1714			684	6...	0,0858			659
E031	P027.d	Sample		19.4.2017 21:04	5...	22,0576			10...	6...	0,0898			379	6...	5,3095			1059	6...	0,0800			490
E033	P028.d	Sample		19.4.2017 21:14	5...	19,4933			899	6...	0,0000			204	6...	5,0745			202	6...	0,0119			221
E035	P029.d	Sample		19.4.2017 21:24	5...	17,3148			505	6...	0,1096			458	6...	5,2036			729	6...	0,0231			259
E038	P030.d	Sample		19.4.2017 21:34	5...	15,7448			340	6...	0,0000			110	6...	5,0528			120	6...	0,0068			223
QCT	P031.d	QC		19.4.2017 21:43	5...	16,2948			383	6...	9,8015			21013	6...	12,6515			34675	6...	10,4317			56415
E040	P032.d	Sample		19.4.2017 21:53	5...	26,8663			24...	6...	0,0000			309	6...	5,0607			166	6...	0,0385			435
E041	P033.d	Sample		19.4.2017 22:03	5...	15,8751			296	6...	0,6047			1452	6...	5,3103			1199	6...	0,2547			1439
E042	P034.d	Sample		19.4.2017 22:13	5...	15,3113			268	6...	0,6903			2062	6...	5,3641			1816	6...	0,3140			2211
E051	P035.d	Sample		19.4.2017 22:22	5...	15,9487			304	6...	0,9463			2105	6...	5,6011			2411	6...	0,3439			1866
E054	P036.d	Sample		19.4.2017 22:32	5...	14,4337			96	6...	3,5526			8977	6...	5,3790			1831	6...	0,4065			2709
E055	P037.d	Sample		19.4.2017 22:42	5...	17,2717			588	6...	1,1987			3046	6...	5,6886			3257	6...	0,5288			3271
E058	P038.d	Sample		19.4.2017 22:52	5...	14,9893			155	6...	0,2193			654	6...	5,1478			481	6...	0,0151			214
E061	P039.d	Sample		19.4.2017 23:01	5...	17,2918			661	6...	0,0144			359	6...	5,0791			272	6...	0,0347			418
E098	P049.d	Sample		20.4.2017 0:39	5...	16,9961			462	6...	3,1328			6421	6...	5,8977			3676	6...	0,7326			3825
E102	P050.d	Sample		20.4.2017 0:48	5...	15,1225			195	6...	2,5241			5626	6...	6,4357			6417	6...	1,6570			9123
E104	P051.d	Sample		20.4.2017 0:58	5...	18,6032			937	6...	0,0822			544	6...	5,1411			627	6...	0,0638			621
E105	P052.d	Sample		20.4.2017 1:08	5...	15,3491			247	6...	0,0110			308	6...	5,1803			732	6...	0,0502			458
E108	P053.d	Sample		20.4.2017 1:18	5...	14,8286			175	6...	0,4890			1552	6...	5,3786			1894	6...	0,3413			2385
E109	P054.d	Sample		20.4.2017 1:27	5...	17,0568			368	6...	1,6392			2718	6...	5,0860			185	6...	0,1346			643
E111	P055.d	Sample		20.4.2017 1:37	5...	16,6377			130	6...	0,4658			370	6...	5,5427			691	6...	0,4692			796
E114	P056.d	Sample		20.4.2017 1:47	5...	16,6115			418	6...	3,1352			6640	6...	6,0272			4365	6...	1,3813			7319
E115	P057.d	Sample		20.4.2017 1:57	5...	20,0768			884	6...	3,8344			7468	6...	6,7153			6832	6...	1,9015			9276
E120	P058.d	Sample		20.4.2017 2:06	5...	14,5373			103	6...	1,7600			4125	6...	5,7728			3493	6...	1,0095			5790
E124	P059.d	Sample		20.4.2017 2:16	5...	15,9497			298	6...	0,1653			560	6...	5,1967			690	6...	0,0105			194
E125	P060.d	Sample		20.4.2017 2:26	5...	22,2975			13...	6...	3,4495			7326	6...	6,0556			4518	6...	1,0228			5492
E126	P062.d	Sample		20.4.2017 2:36	5...	29,9611			185	6...	33,3738			5068	6...	14,6528			3129	6...	11,8617			4584
E130	P063.d	Sample		20.4.2017 2:45	5...	16,0534			299	6...	2,0221			3954	6...	5,9135			3497	6...	0,8622			4181
E132	P064.d	Sample		20.4.2017 2:55	5...	14,5547			87	6...	4,1620			7737	6...	5,8338			3118	6...	0,7936			3783
E133	P065.d	Sample		20.4.2017 3:05	5...	15,2550			209	6...	0,0611			383	6...	5,3597			1458	6...	0,0000			141
E135	P066.d	Sample		20.4.2017 3:15	5...	17,5905			767	6...	1,2705			3829	6...	5,2614			1365	6...	0,1944			1562
E142	P067.d	Sample		20.4.2017 3:24	5...	17,6405			572	6...	0,6160			1495	6...	5,4847			1972	6...	0,0286			296
E145	P068.d	Sample		20.4.2017 3:34	5...	15,2055			227	6...	0,0000			160	6...	5,1477			585	6...	0,0000			119
E148	P069.d	Sample		20.4.2017 3:44	5...	19,4678			895	6...	0,1417			565	6...	5,2128			833	6...	0,0483			418
QCT	P070.d	QC		20.4.2017 3:54	5...	15,7906			278	6...	10,2051			20146	6...	12,9085			33023	6...	9,9858			49759
E150	P071.d	Sample		20.4.2017 4:03	5...	15,4364			240	6...	1,5457			3475	6...	5,7461			3201	6...	0,6004			3336
E159	P072.d	Sample		20.4.2017 4:13	5...	22,0154			13...	6...	0,7768			1935	6...	5,3401			1430	6...	0,1830			1159
E163	P073.d	Sample		20.4.2017 4:23	5...	19,1794			806	6...	18,8741			38227	6...	6,1917			5024	6...	1,2769			6694
E164	P074.d	Sample		20.4.2017 4:33	5...	14,6390			107	6...	0,5106			1241	6...	5,4706			1849	6...	0,2535			1406
E165	P075.d	Sample		20.4.2017 4:42	5...	56,0934			763	6...	8,4631			2040	6...	13,5897			4370	6...	10,6919			6487
E166	P076.d	Sample		20.4.2017 4:52	5...	16,6076			380	6...	3,2603			6290	6...	6,3379			5223	6...	1,5435			7444
E170	P077.d	Sample		20.4.2017 5:02	5...	15,9946			313	6...	1,9268			4066	6...	5,8984			3698	6...	0,8756			4567
E172	P079.d	Sample		20.4.2017 5:12	5...	16,1498			382	6...	0,6396			1719	6...	5,4383			1973	6...	0,3021			1897
QCT	P070B.d	QC		20.4.2017 5:21	5...	16,3288			352	6...	9,6455			18747	6...	13,6600			35590	6...	9,6894			47508
meoh	P080.d	DoubleBla...		20.4.2017 5:31	5...	701,2541			11...	6...	13,9078			312	6...	7,8956			137	6...	9,5711			545
0	P081.d	Blank		20.4.2017 5:41	5...	21,6342			13...	6...	0,0000			212	6...	5,0954			312	6...	0,0293			330
0.5	P082.d	Cal	L1	20.4.2017 5:51	5...	23,4523	4690,5		16...	6...	0,3838	76,8		1167	6...	5,4511	1090,2		2076	6...	0,6618	132,4		4037
1	P083.d	Cal	L2	20.4.2017 6:00	5...	21,5606	2156,1		12...	6...	0,8879	88,8		2212	6...	5,7981	579,8		3605	6...	0,8010	80,1		4618
2.5	P084.d	Cal	L3	20.4.2017 6:10	5...	22,3593	894,4		13...	6...	2,4229	96,9		5544	6...	6,9235	277,1		8879	6...	2,2649	90,6		12718
5	P085.d	Cal	L4	20.4.2017 6:20	5...	19,3931	387,9		896	6...	4,6847	93,7		10334	6...	8,5020	170,0		16033	6...	4,3768	87,5		24117
10	P086.d	Cal	L5	20.4.2017 6:30	5...	21,1667	211,7		12...	6...	9,8267	98,3		22658	6...	12,2437	122,4		35300	6...	9,1275	91,3		53113
25	P087.d	Cal	L6	20.4.2017 6:39	5...	21,0640	84,3		12...	6...	24,1750	96,7		57497	6...	22,4971	90,0		88830	6...	22,3037	89,2		134626
50	P088.d	Cal	L7	20.4.2017 6:49	5...	18,2478	36,5		823	6...	51,4060	102,8		128672	6...	41,5791	83,2		196153	6...	51,4274	102,9		327345
100	P089.d	Cal	L8	20.4.2017 6:59	5...	20,3344	20,3		11...	6...	110,5532	110,6		255575	6...	86,9253	86,9		405453	6...	103,4924	103,5		609016
500	P090.d	Sample		20.4.2017 7:09	5...	497,4134			85...	6...	667,3269			15420...	6...	489,3184			2404803	6...	622,0052			3661309
MEOH	P108.d	DoubleBla...		20.4.2017 7:23																				

Figure 4. Specific areas of each compound, obtained from the Agilent MassHunter Quantitative Analysis (for QQQ) in tissue samples